

**NEURAL NETWORK REORGANIZATION  
FOLLOWING EARLY-LIFE SEIZURES:  
NEUROPROTECTIVE ROLE OF ACTH IN  
PRESERVING COGNITIVE FUNCTION**

by

Mohamed Rabieh Khalife

A dissertation submitted to the Faculty of the University of Delaware in partial fulfillment of the requirements for the degree of Doctor of Philosophy in Interdisciplinary Neuroscience

Spring 2025

© 2025 Mohamed Rabieh Khalife  
All Rights Reserved

**NEURAL NETWORK REORGANIZATION  
FOLLOWING EARLY-LIFE SEIZURES:  
NEUROPROTECTIVE ROLE OF ACTH IN  
PRESERVING COGNITIVE FUNCTION**

by

Mohamed Rabieh Khalife

Approved: \_\_\_\_\_  
Philip Gable, Ph.D.  
Graduate Director, Interdisciplinary Neuroscience Program

Approved: \_\_\_\_\_  
Louis F. Rossi, Ph.D.  
Dean of the Graduate College, Interdisciplinary Programs

Approved: \_\_\_\_\_  
Louis F. Rossi, Ph.D.  
Vice Provost for Graduate and Professional Education and  
Dean of the Graduate College

I certify that I have read this dissertation and that in my opinion it meets the academic and professional standard required by the University as a dissertation for the degree of Doctor of Philosophy.

Signed:

---

Amanda E. Hernan, Ph.D.  
Professor in charge of dissertation

I certify that I have read this dissertation and that in my opinion it meets the academic and professional standard required by the University as a dissertation for the degree of Doctor of Philosophy.

Signed:

---

Amy Griffin, Ph.D.  
Member of dissertation committee

I certify that I have read this dissertation and that in my opinion it meets the academic and professional standard required by the University as a dissertation for the degree of Doctor of Philosophy.

Signed:

---

Matthew J. Mahoney, Ph.D.  
Member of dissertation committee

I certify that I have read this dissertation and that in my opinion it meets the academic and professional standard required by the University as a dissertation for the degree of Doctor of Philosophy.

Signed:

---

Rodney C. Scott, MD, Ph.D.  
Member of dissertation committee

I certify that I have read this dissertation and that in my opinion it meets the academic and professional standard required by the University as a dissertation for the degree of Doctor of Philosophy.

Signed:

---

William Kenkel, Ph.D.

Member of dissertation committee

## ACKNOWLEDGMENTS

I am incredibly grateful to my advisor, Dr. Amanda Hernan, whose mentorship, patience, and unwavering support have been instrumental throughout my PhD journey. Her insightful discussions, guidance, and genuine care for my development as a scientist have significantly shaped my research and academic growth. I truly appreciate her endless enthusiasm and dedication, which made my doctoral studies both productive and enjoyable. Amanda always pushed me to explore my data, come up with novel ideas and secretly threw hints about analysis directions by sending papers my way without any comment.

I also extend my heartfelt gratitude to my co-mentors, Dr. Rod Scott and Dr. Matt Mahoney. Their valuable insights, constructive feedback, and collaborative spirit have immensely enhanced my scientific understanding and contributed greatly to my research. I am thankful for their generosity with their time, expertise, and encouragement. I will always remember Rod's comments on my statistical analysis like "do you really think this is the right way to analyze data" or "that is a crappy analysis". Of course, I can't forget Matt's "no no do not tell me this is the magic of deep learning".

Special thanks to my dissertation committee members, Dr. Amy Griffin and Dr. Will Kenkel, for their thoughtful critiques, invaluable suggestions, and support. Their perspectives and expert advice have been essential in refining and improving the quality of this dissertation.

To my wife, Dr. Dyala, whose endless patience, love, and support have kept me grounded and motivated, I offer my deepest appreciation. Her belief in me and constant encouragement have carried me through the toughest moments.

Finally, I am thankful to my family and friends, especially Remy, Vanessa and Rita, for their continuous support, understanding, and encouragement. My friendship with each of them was a truly amazing experience that I really can't explain in words. Their steadfast presence and unwavering belief in my abilities have made this academic journey possible and fulfilling. I am truly fortunate to have such wonderful people by my side.

## TABLE OF CONTENTS

LIST OF TABLES .....	xi
LIST OF FIGURES .....	xii
ABSTRACT .....	xiv

### Chapter

1	INTRODUCTION .....	1
1.1	Dissertation Overview .....	5
2	BACKGROUND & OVERVIEW .....	8
2.1	Early Life Insults and Long-Term Cognitive/Behavioral Deficits .....	8
2.1.1	Hypoxic–Ischemic Injury .....	8
2.1.2	Maternal Immune Activation .....	9
2.1.3	Traumatic Brain Injury (TBI) .....	10
2.1.4	Early Life Seizures (ELS) .....	10
2.2	Brain Network Dynamics: Rate, Population and Temporal Coding .....	12
2.2.1	Rate Coding .....	16
2.2.2	Population Coding .....	19
2.2.3	Temporal Coding .....	24
2.2.4	Firing Dynamics Support Plasticity .....	31
2.3	Network Disruption as a Central Mechanism in Cognitive Impairment .....	33
2.3.1	Evidence from Epilepsy and Early Life Insults .....	34
2.3.2	Network Disruptions in Diverse Neurological Disorders .....	43
2.3.2.1	Alzheimer’s Disease (AD) .....	43
2.3.2.2	Network Disruptions in Fragile X Syndrome .....	47
2.3.2.3	Traumatic Brain Injury and Post-Traumatic Epilepsy .....	50
2.4	The Neuroprotective Effects of ACTH Across Neurological Disorders .....	53
2.5	The Melanocortin System and MC4R in Cognitive Function .....	58

2.5.1	Overview of the Melanocortin Receptors (MCRs) .....	58
2.5.2	MC4R and Diseases .....	59
2.6	Astrocytes Function and Alteration in Neurological Disorders .....	62
2.6.1	Astrocytic Function in the Brain .....	62
2.6.2	Astrocytes in Diseases.....	63
2.6.2.1	Alzheimer’s Disease (AD) .....	63
2.6.2.2	Parkinson’s Disease (PD).....	66
2.6.2.3	Schizophrenia .....	68
2.6.2.4	Epilepsy .....	69
2.6.3	MC4R Expression in Astrocytes .....	71
3	COMMON METHODOLOGIES .....	74
3.1	Animals.....	74
3.2	Animal Handling and Habituation.....	75
3.3	Early Life Seizure Mouse Model .....	75
3.4	Flurothyl Induction.....	76
3.5	Drug Administration.....	76
3.6	Open Field Task .....	76
3.7	Seizure Latency and Duration .....	77
3.8	Software Validation.....	77
3.9	Statistical Analysis .....	78
4	MELANOCORTIN 4 RECEPTOR-DEPENDENT MECHANISM OF ACTH IN PREVENTING ANXIETY-LIKE BEHAVIORS AND NORMALIZING ASTROCYTE PROTEINS AFTER EARLY LIFE SEIZURES <sup>448</sup> .....	79
4.1	Introduction .....	79
4.2	Methods .....	81
4.2.1	Animals.....	81
4.2.2	Early Life Seizure Animals .....	82
4.2.3	Light/Dark Box Task.....	82
4.2.4	Immunohistochemistry .....	82
4.2.5	Power Analysis.....	83
4.3	Results .....	84

4.3.1	Seizure Latency and Duration Is Unaffected by Treatment or MC4R knockout .....	84
4.3.2	ELS Did Not Affect Exploration and Spontaneous Activity in Open Field Task .....	85
4.3.3	ACTH Ameliorates Anxiety in Light/Dark Box Task .....	86
4.3.4	Acute astrocyte dysfunction in the prefrontal cortex and hippocampus after recurrent early life seizures .....	87
4.3.5	Cell-type specific re-expression of MC4R in neurons and astrocytes .....	89
4.4	Discussion.....	93
5	<b>NETWORK ABNORMALITIES UNDERLYING COGNITIVE IMPAIRMENT AFTER EARLY LIFE SEIZURES ARE NORMALIZED WITH ACTH TREATMENT.....</b>	<b>100</b>
5.1	Introduction .....	100
5.2	Methods .....	103
5.2.1	Animals.....	103
5.2.2	Early Life Seizure Animals .....	104
5.2.3	Electrode Implantation .....	104
5.2.4	Single Neuron Recording .....	104
5.2.5	Generalized Linear Modeling:.....	105
5.2.6	Post-spike filters (PSFs) generation: .....	105
5.2.7	Principal Component Analysis (PCA).....	106
5.2.8	PSTH Construction and Firing Rate Percentage Change Analysis .....	107
5.2.9	Graph Metrics Analysis for Baseline and Fear Extinction .....	108
5.2.10	Graph Neural Network (GNN) Analysis for Predicting Behavioral Outcomes .....	112
5.2.11	Fear Conditioning.....	114
5.2.12	Power Analysis .....	114
5.3	Results .....	115
5.3.1	ACTH Protects Fear Extinction Learning in Mice After ELS ..	115
5.3.2	ACTH Preserves Firing Rates During Baseline .....	117
5.3.3	ACTH Prevents Temporal Coding Deficits During Baseline ...	118
5.3.4	Population Dynamics Do Not Differ Between Groups at Baseline .....	121
5.3.5	ACTH Conserves Rate Dynamics During Learning .....	123
5.3.6	ACTH Preserves Population Dynamics During Learning.....	124
5.3.7	Neuron Features Can Predict Behavior Outcome .....	129

5.4	Discussion.....	135
6	ADDITIONAL BEHAVIORAL AND ELECTROPHYSIOLOGICAL FINDINGS .....	145
6.1	Fear Conditioning Behavior Across WildType, MC4R Knockout, and Knock-In Lines.....	145
6.2	Rate Coding Across Wildtype and MC4R KO Animals .....	147
6.3	Temporal Coding Across MC4R KO Animals .....	149
7	OVERALL DISCUSSION AND FUTURE DIRECTIONS .....	152
	REFERENCES .....	164
Appendix		
A	IACUC Approval.....	211
B	PERMISSIONS .....	212

## LIST OF TABLES

Table 2.1: Frequency bands and cognitive processes.....	25
Table 5.1: Summary of Network Metrics and Statistical Comparisons Across Groups .....	128

## LIST OF FIGURES

Figure 2.1: Schematic of neuronal firing mechanisms and information processing ....	15
Figure 4.1: Seizure parameters are not altered by ACTH treatments.....	85
Figure 4.2. No behavioral differences in open field task parameters .....	86
Figure 4.3. ACTH ameliorates the anxiety phenotype in mice with ELS .....	87
Figure 4.4. ACTH mitigates the astrocytic dysfunction in mice with ELS.....	89
Figure 4.5. ACTH-treated KI mice with ELS show less anxiety compared to vehicle-treated mice with no differences in seizure parameters or spontaneous activity. ....	92
Figure 5.1: Average Training and Validation Loss Curves.....	113
Figure 5.2: ACTH Improves Fear Extinction Deficit After ELS .....	116
Figure 5.3: ACTH Normalizes Baseline Firing Rates of Prefrontal Cortex (PFC) Neurons at Baseline.....	117
Figure 5.4: Heatmaps of post-spike filters (PSFs) sorted by PC1 score across groups .....	119
Figure 5.5: ACTH Preserves mPFC Neuron Temporal Coding After ELS .....	120
Figure 5.6: Network Metrics Show No Differences at Baseline After ELS .....	122
Figure 5.7: ACTH Treatment Preserves Neuronal Rate Dynamics During Extinction Learning.....	124
Figure 5.8: ACTH Restores Network Properties During Fear Extinction Learning ..	126
Figure 5.9: Spearman Correlation matrices of network metrics during fear extinction.....	129
Figure 5.10: Predictive Performance of Graph Attention Network vs. Linear Regression Models. ....	133

Figure 5.11: Network Metrics Across Baseline and Fear Extinction Phases .....	134
Figure 5.12: Community Structures in PFC Neural Networks During Fear Extinction .....	135
Figure 6.1: MC4R-Dependent Rescue of Fear Extinction Deficits Following Early Life Seizures .....	147
Figure 6.2: Baseline mPFC Firing Rates and Spike-Timing Variability Across Genotypes .....	149
Figure 6.3: ACTH Fails to Restore Flexible Temporal Coding in MC4R Knockout Mice at Baseline .....	150

## ABSTRACT

Action potentials represent the fundamental mechanism by which neurons transmit and encode signals, governed by complex and interdependent neural coding schemes known as rate, temporal, and population coding. Disruptions to these schemes, particularly during early developmental periods, can lead to profound and enduring cognitive deficits. This thesis investigates how early-life neurological insults, specifically early-life seizures (ELS), disrupt neural dynamics and subsequently impair cognitive functions. We chose the medial prefrontal cortex (mPFC) as our primary region of interest due to its critical but less extensively studied role in cognitive processes compared to regions like the hippocampus. Utilizing electrophysiological, behavioral and computational approaches, including single-unit recordings, fear extinction learning, graph theoretical analysis, and Graph Attention Networks (GATs), we characterized disruptions in neuronal firing rates, neuronal spike-timing, and population connectivity in the mPFC following ELS.

Our findings demonstrate that ELS significantly impairs cognitive function by inducing rigid temporal firing patterns, reducing firing rates, and disrupting population-level network dynamics essential for adaptive cognitive processing. Importantly, implementing a neuroprotective intervention using Adrenocorticotrophic Hormone (ACTH), acting through melanocortin 4 receptor (MC4R) signaling pathways, effectively preserved neural coding dynamics and rescued cognitive performance post-ELS. This therapeutic approach highlights the centrality of

maintaining flexible and dynamic neural network function as a critical determinant of cognitive resilience.

The future direction of this dissertation extend beyond ELS, suggesting a convergent mechanistic model where disrupted neural dynamics underpin cognitive dysfunction across multiple neurological and neurodevelopmental disorders, including Alzheimer's disease (AD), Parkinson's disease (PD), Fragile X syndrome (FMR1), and traumatic brain injury (TBI). By emphasizing the preservation of neural network dynamics, this thesis advocates for a fundamental shift toward network-centric therapeutic strategies aimed at maintaining and restoring cognitive integrity across diverse neurological conditions.

## **Chapter 1**

### **INTRODUCTION**

Early-life seizures (ELS) occur during critical developmental windows and can have long-lasting impacts on cognition and behavior. Although they may appear transient, acute brain early-life insults often coincide with the formation and maturation of neural networks, during which synaptic connections, functional connectivity, and large-scale brain circuits are being established. This process is known as network formation and involves the refinement of structural and functional connectivity across regions critical for higher-order cognitive functions, such as the prefrontal cortex (PFC) and hippocampus. Disruptions in these processes during early life can lead to maladaptive network organization which affects how neural circuits integrate, process information and regulate behavior. As a result, rodents with a history of ELS show significant deficits in spatial learning, memory, sociability, attention, and fear extinction. Current interventions do not address the network-level dysfunctions which include abnormalities in neural connectivity, disrupted functional coordination within and between brain regions, and altered neural coding dynamics driving long-term cognitive and behavioral impairments.

Adrenocorticotrophic hormone (ACTH), a melanocortin family neuropeptide within the hypothalamic-pituitary-adrenal (HPA) axis, plays a critical role in brain function beyond its classical role in regulating the hypothalamic-pituitary-adrenal (HPA) axis. Even though ACTH is primarily known for stimulating glucocorticoid secretion via melanocortin 2 receptor (MC2R) activation in the adrenal glands, it also

binds to other melanocortin receptors (MCRs), including MC3R and MC4R, which are highly expressed in the brain. This dissertation focuses on MC4R specifically due to prior evidence implicating its role in synaptic plasticity and cognitive recovery in different diseases like Alzheimer's disease (AD), Parkinson's disease (PD) and ischemia. Through its engagement with MC4R, ACTH is thought to influence synaptic plasticity, neuroinflammation, and neuronal survival, suggesting a broader neuroprotective role that extends beyond endocrine regulation in different conditions like epilepsy, ELS, multiple sclerosis (MS), PD and ischemia.

Previous research has demonstrated that ACTH exerts direct cognitive benefits even when seizure frequency remains unchanged, indicating a mechanism of action independent of seizure suppression. . In models of epilepsy and ELS, ACTH treatment restores hippocampal synaptic plasticity and improves spatial learning and memory deficits, compared to ELS animals without ACTH treatment. We have previously shown that rodents with a history of early life seizures treated with ACTH exhibited no deficits in fear extinction learning and attention compared to vehicle-treated ELS animals. These effects appear to be mediated by MC4R activation in the prefrontal cortex (PFC), a region critical for executive function and learning. Importantly, these protective benefits were not replicated with in corticosteroid-treated ELS animals, further supporting that ACTH's neuroprotective effects occur independently of its role in adrenal steroidogenesis and might be driven by the direct modulation of brain networks via MC4R signaling.

The objectives of this dissertation are 1) investigate the behavior and cognition after recurrent ELS in vehicle-treated and ACTH-treated ELS mice compared to controls, 2) investigate the effects of ACTH on ameliorating the behavioral and

cognitive deficits through melanocortin 4 receptor (MC4R), 3) understand the specific features of neuronal activity like changes in rate, temporal and population coding, known as neural dynamics, that underlie the cognitive impairments following the early life insult, and 4) elucidate the mechanism of cognitive improvement after treatment with ACTH.

To address these objectives, wildtype (WT), MC4R knock-out (KO), Syn1-cre MC4R knock-in (KI), and GFAP-cre MC4R KI animals were distributed into three groups: control, ELS with vehicle treatment and ELS with ACTH treatment. For the ELS groups, Mice experienced 20 flurothyl-induced generalized seizures between p10 and p14 followed by in vivo single unit recording in the prelimbic prefrontal cortex (PFC) at p50. Recordings were performed at baseline and during a fear extinction learning task.

ACTH treatment ameliorated anxiety-like behavior and learning impairments associated with ELS, without altering seizure parameters, in WT mice but not in MC4R KO mice. We also show that knocking-in MC4R in either neurons or astrocytes rescued the anxiety-like behavior and learning impairment after ACTH treatment. Further, we show that ACTH normalizes important astrocytic proteins like Glial Fibrillary Acidic Protein (GFAP) and Aquaporin-4 (AQP4) after ELS.

To investigate how ACTH modulates neural dynamics underlying behavioral changes, we quantified spiking activity using a generalized linear model that characterizes firing rate, temporal structure, and population-level coordination. Post-spike filters capturing the temporal dynamics showed less flexibility in the firing repertoire of PFC neurons in animals with a history of ELS compared to controls. However, ACTH protected the firing flexibility after ELS. During learning periods,

peri-stimulus histograms showed that animals with a history of ELS exhibited decreased neuron-tone firing rate responsiveness compared to controls, which was preserved by ACTH treatment. Population coding supports the integration of complex inputs across brain regions and is particularly important for coordinating activity during tasks that require dynamic information updating, such as fear extinction. To explore changes in population coding associated with fear extinction learning, we implemented a Graph Neural Network (GNN) analysis to quantify the evolution of cofiring of PFC neurons during the fear extinction task. Cofiring patterns reflect ensemble-level functional connectivity, allowing us to track how population structure changes over time. The GNN revealed that learning is associated with the formation of stronger functional connections over the course of the task. Control animals show a significant edge weight increase from the first to the last third of the session, whereas animals with a history of ELS show no change at all. ACTH treatment significantly preserved the functional connectivity strength during the learning session.

These results suggest that ACTH treatment improves behavioral performance after induced ELS by preserving dynamic coordination within local PFC networks, in a manner that is dependent on MC4R activation in both neuronal and astrocytic populations. Furthermore, these findings offer crucial insights into the underlying mechanisms of fear extinction learning within local PFC networks. Specifically, they show that PFC circuits must maintain timing flexibility and population-level plasticity to support adaptive behavioral learning which are capabilities preserved by ACTH. Additionally, they provide important insight into how these networks may be altered following an early life insult. Notably, the recovery observed with ACTH even in the absence of overt seizure-related changes, implies a potential avenue for mitigating

cognitive impairments in an MC4R-dependent manner by restoring neural network function.

## **1.1 Dissertation Overview**

**Chapter 1** introduces the critical developmental role of neural network formation and how ELS disrupts these processes, leading to cognitive impairments related to higher-order cognition regions such as the PFC. It introduces ACTH as a neuroprotective intervention, highlighting its established endocrine role and expanding upon emerging evidence for its broader neuroprotective effects via MC4R. It sets the stage for the thesis by laying out the rationale for focusing on the neural coding mechanisms to improve cognitive outcomes.

**Chapter 2** introduces how different early life insults lead to a common cognitive outcome. It then introduces the conceptual foundation of the dissertation: that brain networks communicate through a combination of rate, temporal, and population coding. The chapter further explains how disruption of these coding schemes constitutes a central mechanism of cognitive impairment across different disorders by examining the shared patterns of altered functional connectivity, impaired neuronal communication and impaired synaptic integration in epilepsy, Alzheimer's disease, Fragile X syndrome, and traumatic brain injury. It then transitions into introducing the neuroprotective roles of ACTH, the melanocortin system and the role of astrocytes in neurological disorders.

**Chapter 3** details the experimental methods shared across our main studies.

**Chapter 4** presents findings from our study demonstrating that ACTH, via MC4R signaling, prevents anxiety-like behavior and preserves astrocytic protein levels after ELS. Using both MC4R knockout and astrocyte- or neuron-specific knock-

in mice, we show that astrocytes and neurons have different contributions to ACTH's positive effects.

**Chapter 5** examines the electrophysiological and network-level behavior in the mPFC in control and ELS animals with and without ACTH during baseline and fear extinction learning. ELS animals show impaired firing rate, impaired spike-timing, reduced functional connectivity strength, lower graph-based centrality, and diminished global and local efficiency in mPFC networks. ACTH rescues these deficits, restoring firing rates, flexible temporal structure and predictive power of neural networks during behavior. These findings position neural coding and network flexibility as mechanisms underlying cognitive capacity.

**Chapter 6** presents additional behavioral and electrophysiological data that were not central to the main storyline. These include baseline and task-related firing properties in MC4R knockout mice, along with pattern analyses of post-spike filters. Findings suggest that ACTH-mediated anxiety-behavior rescue requires MC4R signaling in either astrocytes or neurons, however fear extinction learning rescue requires MC4R signaling in astrocytes and not neurons.

**Chapter 7** integrates these findings within a unified conceptual framework, emphasizing that cognitive impairments resulting from ELS primarily stem from disruptions in mPFC network coding schemes. ACTH preserves neural network dynamics crucial for cognitive flexibility and adaptation. The chapter expands on what can be understood from the astrocytic and neuronal data and how astrocytic-neuronal connection impact cognitive outcome. The chapter covers the study limitations and advocates for a paradigm shift away from focusing solely on structural damage or seizure frequency toward prioritizing dynamic coding and glial-neuronal interactions

as therapeutic targets. Future directions outlined include using multi-region electrophysiological recordings, astrocyte-specific imaging, and computational modeling approaches to deepen the understanding of neuron-glia interactions and network-level dynamics, ultimately guiding more effective therapeutic interventions across neurological disorders.

Together, this dissertation supports a future direction that advances a new systems-level perspective on neurodevelopmental injury, identifying neural coding, glial modulation, and network flexibility as core aspects of cognitive function and promising targets for therapeutic intervention.

## Chapter 2

### BACKGROUND & OVERVIEW

#### 2.1 Early Life Insults and Long-Term Cognitive/Behavioral Deficits

Early developmental periods represent a high vulnerability phase for the brain, during which various insults, such as hypoxic–ischemic injury, maternal immune activation, traumatic brain injury (TBI), and induced early life seizures (ELS), can disrupt the maturing brain and lead to enduring cognitive and behavioral deficits<sup>1–14</sup>.

These impairments can manifest as long-term deficits in memory, attention, executive function, social behavior, and emotional regulation, severely affecting educational achievement, independence, and overall quality of life. Understanding how early life insults at this stage alter the brain is crucial for mitigating long-term consequences.

While this dissertation focuses on ELS as an early life insult, we briefly review other common early-life insults to highlight the shared outcomes of disrupted neural development. These include impairments in cognition, emotion regulation, attention, and social behavior, which stem from altered connectivity, inflammation, and disrupted plasticity across models.

##### 2.1.1 Hypoxic–Ischemic Injury

Perinatal hypoxic–ischemic events refer to conditions during the perinatal period, where an infant's brain is deprived of adequate oxygen (hypoxia) and blood flow (ischemia). This deprivation can lead to significant brain injury, known as

hypoxic–ischemic encephalopathy (HIE), which can lead to long-term neurological impairments including cerebral palsy, epilepsy, cognitive impairments, sensory deficits, and behavioral disorders<sup>15,16</sup>. One study investigated the long-term effects of neonatal HIE in a mouse model, focusing on cognitive impairments in adult mice with a history of neonatal HIE. They found significant deficits in spatial learning and memory in the Morris Water Maze test and suggest that these cognitive impairments are a result of long-lasting hippocampal dysfunction due to neonatal HIE<sup>17</sup>. Another study found that postnatal HIE was associated with significant developmental delays and motor deficits. Gene expression analyses further revealed activation of inflammatory pathways in monocytes, suggesting a link between systemic inflammation and the observed neurological impairments<sup>18</sup>. Collectively, these studies underscore the profound and lasting impact of neonatal HIE on motor and cognitive functions, highlighting the critical role of inflammatory responses, hippocampal dysfunction, and developmental delays in shaping the trajectory of neurological outcomes.

### **2.1.2 Maternal Immune Activation**

Maternal infection or heightened immune activity during pregnancy can trigger the release of inflammatory cytokines that cross the placenta, impacting fetal brain development. Research indicates that MIA can lead to significant neurodevelopmental alterations, resulting in long-term cognitive and behavioral deficits. For instance, it was shown that MIA leads to significant impairments in spatial discrimination and social interaction, with mice previously exposed to MIA exhibiting significant deficits in adapting to changing task demands, a hallmark of cognitive flexibility impairments<sup>19</sup>. Another study found that animals exposed to MIA exhibited deficits in

spatial learning in addition to altered long-term potentiation and NMDA receptor function in the prefrontal cortex<sup>20</sup>.

### **2.1.3 Traumatic Brain Injury (TBI)**

Although TBI occurs less frequently in children compared with adults, even mild head injuries during critical periods of brain maturation can have pronounced consequences. Research showed that pediatric TBI is associated with observable deficits in memory, attention, and executive function, which may become evident only as children age and cognitive demands grow. Pediatric traumatic brain injury (TBI) has been extensively studied using animal models to understand its impact on cognitive functions. Studies have found that animals with a history of TBI exhibit significant cognitive deficits compared to shams. For instance, rodents subjected to TBI exhibit deficits in spatial learning and memory in the Morris water maze during adulthood<sup>21</sup>. Further studies have shown significant deficits in Barnes Maze, Novel Object Recognition, and Radial Arm Maze in adulthood after early life TBI injury<sup>22-25</sup>. These findings suggest that TBI during development can lead to long-term cognitive challenges.

### **2.1.4 Early Life Seizures (ELS)**

Early Life Seizures (ELS) refer to seizures occurring within the first years of life, a critical period of brain development associated with high incidence of seizures<sup>1-4</sup>. ELS are particularly disruptive because they coincide with developmental windows which are time-sensitive periods when the brain undergoes rapid changes, like synaptic pruning, myelination, and neural network formation<sup>26-28</sup>. ELS-related

disruptions impair the refinement and proper formation of neural connections, leading to long-term neurological and cognitive deficits that persist into adulthood<sup>29–32</sup>.

Research shows that these disruptions impair cognitive flexibility and learning abilities. Longitudinal studies highlight that children with ELS are more likely to be diagnosed with neurodevelopmental disorders, including autism spectrum disorder (ASD), anxiety, and attention-deficit disorders<sup>31,33–35</sup>. Moreover, histological and electrophysiological studies show that ELS is associated with structural abnormalities in the hippocampus. These hippocampal malformations include two major disruptions which are the spreading out of CA1–CA4 pyramidal cell layers and the presence of misplaced clusters of neurons, within the CA1 region<sup>36–38</sup>. In a healthy hippocampus, pyramidal neurons are arranged in tightly organized layers that help ensure efficient communication between cells. After ELS, these layers become disorganized where neurons are no longer compactly arranged but instead are scattered across a wider area. This disrupts how signals are processed and weakens the circuit's ability to send precise information. In addition, the misplaced cells represent neurons that migrated to the wrong place during development, forming abnormal clusters that can interfere with normal signal flow. Together, these abnormalities impair how inputs are integrated and how the hippocampus coordinates with other brain regions, leading to memory and learning problems that persist even when seizures are no longer present<sup>36–38</sup>.

Previous studies have shown that animals with a history of early life seizures exhibit alterations in synaptic transmission and organization in the hippocampal network<sup>39</sup>. However, the hippocampus is not the only region affected by ELS. Animals with a history of ELS also exhibit deficits in the prefrontal cortex (PFC) including increased PFC thickness, particularly in layer V, which may reflect insufficient

synaptic pruning during development<sup>40</sup>. In addition to the morphological abnormalities, the short-term plasticity (STP) of the PFC after ELS is also altered. Specifically, ELS impairs STP across cortical layers particularly from layer II/III to layer V, and within layer V circuits<sup>41</sup>. These impairments affect frequency- and activity-dependent synaptic transmission, which are crucial for dynamic processing of information between superficial and deep layers. These alterations in the hippocampus and PFC caused by ELS are associated with deficits in spatial learning and memory and impaired behavioral flexibility, respectively.

Thus, early life insults, regardless of etiology, share a common outcome which is the disruption of the developing neural network, which predisposes individuals to chronic cognitive and behavioral deficits.

## **2.2 Brain Network Dynamics: Rate, Population and Temporal Coding**

Brain networks rely on precise patterns of neuronal activity to process information, encode memories, and enable cognition. The action potential is the fundamental unit of information processing in the brain, and sequences of action potential firing in neuronal populations over time are therefore considered to be mechanisms of cognition, as cognitive function is explicitly about information processing<sup>42,43</sup>. Three primary coding schemes: rate coding, temporal coding, and population coding, are widely used to describe how neurons transmit and transform information across time and space<sup>44-46</sup>. Figure 2.1 is a representative figure for these coding schemes under physiological conditions (Figure 2.1A) and how they are altered in disease conditions (Figure 2.1B), especially in the hippocampus and neocortex, which are important structures involved in information processing and cognitive function. Each of these coding mechanisms is fundamental to maintaining proper brain

function, and disruptions in any of them can lead to significant cognitive impairments<sup>45,47</sup>. Disruptions in rate, temporal, and population coding have been linked to impaired learning, memory, and plasticity in epilepsy models, particularly through reductions in theta-phase precession, network connectivity, and spike-timing precision<sup>48–52</sup>.

While oscillatory coupling, neuromodulation, or dendritic computation can serve as additional modes of communication, these frameworks ultimately reduce to the foundational principles of rate<sup>53</sup>, temporal<sup>44</sup>, and population coding<sup>46</sup>. Oscillatory coherence, for instance, relies on the alignment of spike timing to ongoing rhythms and is therefore a form of temporal coding<sup>44,54</sup>. Cell assembly theories and engram models describe how groups of neurons coactivate to encode information, which maps onto population coding<sup>46,55</sup>. Neuromodulatory systems like dopamine, acetylcholine, and serotonin influence how neurons fire by adjusting gain, thresholds, or excitability—but even the release of neuromodulators depends on action potential propagation and presynaptic activity, which are governed by rate and timing<sup>53</sup>. Once released, neuromodulators influence spike rate, timing precision, or population engagement, not in isolation but by shaping those core dimensions. Dendritic computation adds complexity through nonlinear integration, but remains dependent on input timing (temporal), frequency (rate), and converging sources (population). Other examples like burst coding or latency-based encoding are refinements of rate and temporal coding, rather than distinct systems.

In short, while neural communication involves multiple levels of regulation and modulation, its informational structure consistently reflects when neurons fire (temporal), how often they fire (rate), and which groups of neurons fire together

(population). These frameworks offer not only descriptive power but mechanistic insight into how distributed neural activity gives rise to cognition.

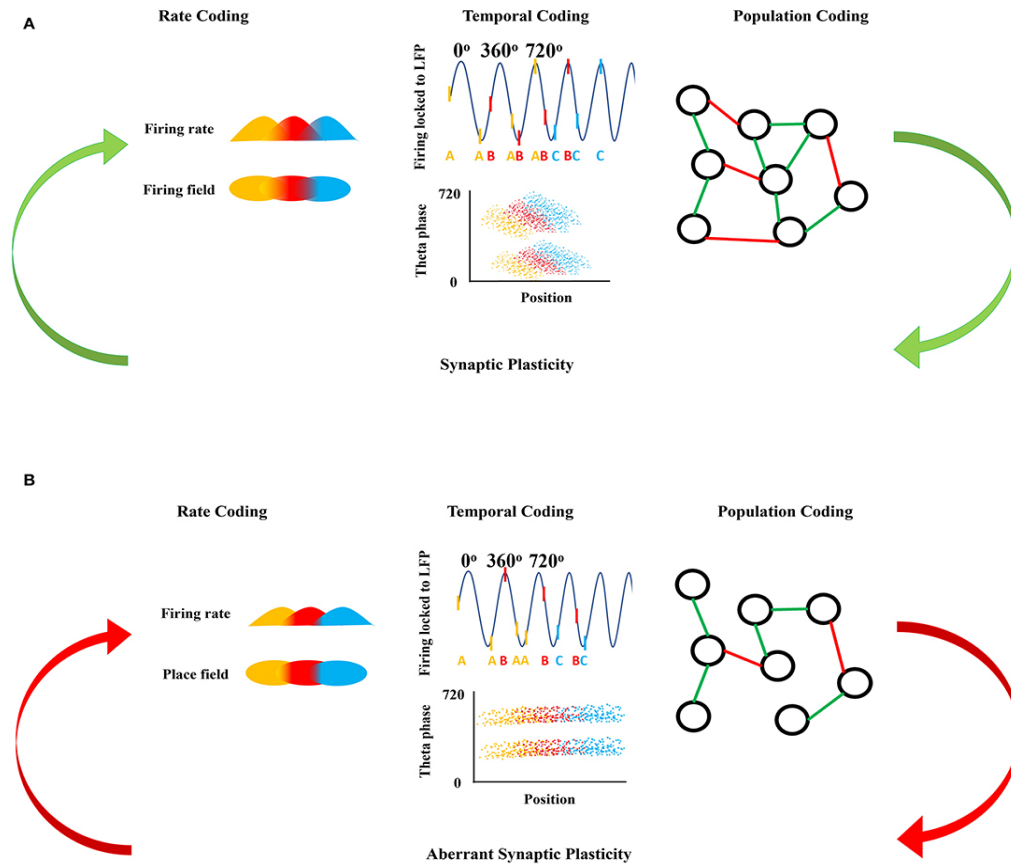


Figure 2.1: Schematic of neuronal firing mechanisms and information processing (A) Shows the normal information processing and synaptic plasticity feedback loop based on the neural coding mechanisms. Rate coding is shown as the firing rate in time (top) with respect to each firing field in space (bottom) coded by the same color. Temporal coding shows the action potentials as raster ticks superimposed on the LFP with respect to theta oscillation indicating theta phase precession with each successive peak of theta, with action potentials also represented as a letter at the bottom of the LFP representing firing from the same neuron over time (top). Over many LFP cycles, theta phase precession can be seen in the downward slope of the clouds of dots in the bottom panel, each representing an action potential from three representative neurons shown in the top panel. Population coding shows the connections between neurons forming a population network, green representing an excitatory connection between two neurons and red representing an inhibitory connection between two neurons. Synaptic plasticity refines and is refined by these firing mechanisms. (B) Shows the disrupted information processing and synaptic plasticity feedback loop based on the neural coding mechanisms in epileptic brain. In epilepsy<sup>56,57</sup>, rate coding is

disrupted shown here as a decreased firing rate in time with respect to each firing field in space, with decreased overlap in the firing and place fields from each of the three color-coded neurons. Temporal coding is also altered; firing of the colored neurons with respect to theta oscillation is disorganized and there is an absence of theta precession as shown by a flat relationship between the clouds of action potentials from each of the three colored neurons. Population coding shows fewer connections between neurons forming a smaller population network, with potentially different proportions of positive (green) and negative (red) connections in the epileptic brain compared to controls in (A), reflecting experimentally observed reductions in functional connectivity and ensemble coherence in epileptic circuits. Aberrant synaptic plasticity emerges from these altered dynamics because disrupted spike timing, reduced rate modulation, and impaired ensemble recruitment limit the coincidence of pre- and postsynaptic activity necessary for effective LTP/LTD mechanisms.

### **2.2.1 Rate Coding**

Rate coding, refers to the frequency at which neurons fire action potentials (spikes/second). This firing rate is thought to convey information about the intensity or salience of sensory inputs, with higher firing rates corresponding to stronger or more important stimuli. In many neural circuits, rate coding is a key mechanism by which sensory information is processed, memories are encoded, and decisions are made<sup>43</sup>. For example, in motor neurons, the degree of muscle flexion depends on the number of action potentials per unit time<sup>42</sup>. Tactile and texture perception in rodents is also, at least in part, a function of rate coding. When rats use their whiskers to discriminate textures, neurons in the somatosensory cortex (S1 and S2) respond with texture-specific firing rates. While spike timing carries more precise information, firing rate still contributes significantly to perceptual accuracy in these tasks<sup>58</sup>.

Although this dissertation focuses on the medial prefrontal cortex (mPFC), foundational insights into rate coding have been most clearly established in spatial and memory circuits, particularly the hippocampus and entorhinal cortex. These studies

have been critical in establishing how neuronal firing rates map onto behavior and cognition, and provide a model framework for interpreting rate-based dynamics in less well-characterized areas such as the PFC.

In the hippocampus and entorhinal cortex, rate coding is exhibited by place, time, and grid cells, respectively<sup>59,60</sup>. Place cells are hippocampal pyramidal cells that fire when an animal visits a specific region of the environment: the cell's “place field”<sup>61,62</sup>. In any given environment, place fields cover the entire space to create a hippocampal cognitive map that is a representation of that space<sup>61,62</sup>. Repeated recordings of place cell populations have shown that the same cells are activated whenever the animal visits the same region in physical space, which suggests that the cells' representation is held in the network once the animal explores that specific field<sup>63</sup>. This representation is thought to allow for the recollection of specific spaces and accurate navigation through the environment. This idea is further supported by the observation that lesioning the hippocampus results in loss of spatial memory<sup>64–67</sup>.

Time cells are hippocampal neurons that fire at successive, specific time points during a delay interval in a temporally structured task which means that they encode the passage of time within a behavioral task. These cells fire at specific and reliable temporal intervals after a triggering event such as a cue, creating “time fields” that span the delay period of a memory or decision-making task<sup>68</sup>. Importantly, these time fields can be anchored to both external cues like a tone or movement onset or emerge internally through circuit dynamics, and has been proposed to support memory of temporal sequences<sup>42,43,68</sup>.

Grid cells, first discovered in layer II of the dorsomedial entorhinal cortex (dMEC), exhibit a periodic spatial firing pattern that forms a triangular pattern across

an environment that provide activity-based maps of speed and direction in a certain environment<sup>69</sup>. These intervals form a repeating triangular pattern that covers the environment, creating an internal coordinate system for navigation. Grid cells recorded at the same cortical location share the same grid orientation and spacing but differ in spatial phase, meaning that their peak activity occurs at different physical locations while preserving the shared geometry<sup>69,70</sup>. The orientation of this grid is influenced by inputs from the hippocampal place cell map, which helps anchor the entorhinal representation to salient features of the environment<sup>62,70,71</sup>. Interestingly, the map formed by the grid cells is based on external cues, however the formed map persists even in the absence of these cues<sup>69</sup>. Together with the place cell map, the grid cell map is believed to be part of the greater hippocampal cognitive map<sup>62</sup>. This integrated map enables vector-based navigation and flexible spatial planning, allowing animals to infer paths and recall spatial contexts even in the absence of cues.

Although grid cells reside in the medial entorhinal cortex (MEC), inputs from the lateral entorhinal cortex (LEC) are also essential. LEC contributes non-spatial contextual information that modulates rate coding in hippocampal place cells. Lesioning the LEC impairs the hippocampus's ability to update firing rates without altering place field locations, a phenomenon known as rate remapping<sup>69,72</sup>. Rate remapping allows the same spatial representation to encode different experiences based on changes in task demands or environmental context<sup>69,72</sup>.

Rate coding is also a crucial principle of activity in the PFC, particularly in tasks involving working memory, attention, and fear regulation. During working memory, PFC neurons increase or decrease their firing rates depending on the content and duration of mnemonic representations<sup>73,74</sup>. For example, dorsolateral PFC neurons

in primates showed sustained elevation of firing rates during delay periods of a spatial working memory task, reflecting active maintenance of information<sup>74</sup>. In the context of fear extinction, mPFC neurons modulate firing rates depending on memory retrieval and extinction progress, and animals that successfully extinguish fear show distinct increases in firing during tone presentations<sup>75</sup>, and these shifts have been linked to behavioral flexibility and outcome prediction. Moreover, attention and decision-making tasks show PFC neurons modulate rate in relation to cue salience and task rules<sup>76,77</sup>. These findings indicate that, even outside spatial domains, rate coding in the PFC plays a critical role in encoding internal states, guiding goal-directed behavior, and supporting executive functions.

Taken together, the examples from both hippocampal-entorhinal and prefrontal circuits demonstrate that firing rate serves as a key mechanism for maintaining representations, guiding behavior, and flexibly updating context-dependent information. Disruptions in this rate coding such as reduced responsiveness, inflexible firing rates, or failure to remap can impair the encoding of stimulus intensity and spatial context, ultimately degrading memory precision, sensory discrimination, and adaptive decision-making<sup>60</sup>. In this dissertation, disruptions in firing rate after ELS are interpreted as impairments in the coding dimension, with downstream consequences for learning and behavioral flexibility.

### **2.2.2 Population Coding**

Neurons are functionally connected into a network and interactions between the neurons is also critically important<sup>43,78</sup>. Population coding refers to the collective and coordinated activity of neuronal ensembles, where each neuron contributes uniquely to the representation of a variable, such as direction, spatial location, or

stimulus identity. Unlike rate or temporal coding, which involve the activity of individual neurons, population coding integrates these dimensions across multiple neurons simultaneously. It is typically analyzed through a population vector which is a vector sum of all constituent neural vectors, where each vector's magnitude is proportional to firing rate and direction reflects that neuron's tuning preference<sup>79</sup>. This method, originally developed in the motor cortex, provided early evidence for the cell assembly hypothesis proposed by Hebb, in which distributed neural groups encode a shared representational state. Population coding increases robustness of network function and minimizes the effects of noise carried by an individual neuron, ensuring that the signal and processing times are not affected<sup>43</sup>, and since information is distributed across the ensemble, damage or silencing of one neuron does not erase the encoded signal. For example, damage to one cell will not have a devastating effect on the information being carried since it is carried by many cells<sup>78</sup>. Population coding is common in the nervous system and is illustrated in mammalian visual pathways<sup>80</sup>, primary motor cortex activity in cats and monkeys<sup>81</sup>, owl auditory cortex, cricket nervous system<sup>82</sup>, and mice visual cortex<sup>83-85</sup>. Neurons in the visual cortex in cats and monkeys and the auditory cortex in owls have shown the ability to synchronize their firing on a few milliseconds time scale through time cells<sup>42,86</sup>. However, population coding does not require synchrony alone as neurons can also contribute via sequential activation for example. Synchrony seen in the visual cortex of cats and monkeys takes place when the neurons are activated by one stimulus<sup>86</sup>, and this synchrony is lost when the neurons are activated by two independent stimuli. Once two neurons synchronize to represent a certain stimulus, these two neurons always synchronize to represent the same stimulus and will desynchronize when representing two

independent stimuli<sup>42</sup>. Sequential activation can be seen during rest or sleep where the hippocampus exhibits replay events. Sequences of place cells activate in the same order as during prior awake experiences, but at a faster timescale. This phenomenon is believed to play a role in memory consolidation and planning<sup>87</sup>.

In the primary visual cortex (V1) of awake mice, population-level dynamics underlie fine-tuned sensory processing. Whole cell recordings in layers 2/3 (L2/3) of awake mice have shown that the excitation/inhibition ratio changes based on the visual stimulus<sup>85</sup>. Different studies revealed that patterns of excitation and inhibition are generated in response to various visual stimuli<sup>88,89</sup>. For example, as the stimulus contrast or size increases, the excitation/inhibition ratio decreases. This change in ratio is important for tuning and sharpening of the information processing in the visual system<sup>90</sup>. The Stabilized Supralinear Network (SSN) model proposes that these population-level cortical dynamics which are interactions between strong recurrent excitation and feedback inhibition, create flexible gain control based on the collective input-output properties of neurons<sup>85,91</sup>. Such gain modulation allows the visual cortex to dynamically scale sensitivity to input strength and context.. This layer-specific dynamic coordination is further supported by optogenetic experiments showing that V1 excitatory populations generate gamma oscillations with specific excitatory/inhibitory timing balances across layers<sup>85</sup>. These rhythms define the direction and strength of interlayer communication which is another example of population-level processing.

Notably, place cells in the hippocampus are an excellent example of not only rate coding, but also population dynamics. We previously mentioned that the place cells fire whenever the animal is in a specific place field and these cells are distributed

within the hippocampus in a way that covers the whole environment the animal occupies. This distribution within the hippocampus will cause a certain degree of overlap between the place fields, thus a population of cells will respond when the animal goes into the field rather than an individual cell since the cells in the hippocampus are receiving multiple sensory inputs to encode a multidimensional map<sup>92</sup>.

Pattern separation is another canonical form of population coding. It depends on forming orthogonal activity patterns across neural ensembles to distinguish between similar stimuli, spatial contexts, or events<sup>93</sup>. Rather than relying on single neuron firing rate shifts, pattern separation emerges from the collective recruitment of distinct neuronal populations to encode overlapping inputs as separable traces. In both rodents and humans, successful memory retrieval is associated with reinstatement of encoding-specific high frequency activity (HFA) in the hippocampus and posterior occipitotemporal cortex<sup>94</sup>. HFA refers to gamma-band power recorded through intracranial EEG or LFPs. When similar stimuli are encoded, dentate gyrus (DG) activity ensures sparse, non-overlapping representations. This is achieved through DG's unique anatomy of low excitability, inhibitory tone, and a high degree of synaptic divergence to CA3<sup>95-100</sup>. Lesion or dysfunction of DG impairs the ability to differentiate similar environments which is a clear demonstration of population-level failure in coding.

A final relevant domain in which population coding has been extensively characterized is working memory in the prefrontal cortex. Working memory is the temporary maintenance of information involving specialized components of cognition that allows retaining immediate past-experience, supporting new knowledge

acquisition, solving problems, reasoning, and planning<sup>101</sup>. Early models of working memory suggested that persistent firing activity of the neurons in the prefrontal cortex (PFC) throughout the delay phase of the working memory task was required to maintain information in working memory, however, due to the heterogeneity of neurons within the PFC, recent work has shown that the persistent activity of PFC can be weak or absent<sup>102–104</sup>. This observation was seen during the delay phase of an image-sequence matching task in monkeys and humans. In this task, spiking activity in the PFC decreased during the delay phase of the task in monkeys, and BOLD signal on fMRI decreased during the delay phase in humans performing the task, thus challenging the persistent firing working memory model<sup>105,106</sup>. However, multiple studies now support the idea that working memory can be maintained in latent network states via changes in synaptic weights or short-term plasticity mechanisms, rather than sustained firing. Electrophysiological work shows that memory content is reactivated through transient, stimulus-specific gamma bursts at the population level, especially in PFC, and that these bursts are temporally structured by beta rhythms<sup>107,108</sup>. In parallel, population-level stability across delay periods despite variable individual neuron firing has been demonstrated in primates<sup>106</sup>, while distributed BOLD activity patterns in humans track item-specific working memory content even in the absence of sustained activation<sup>105</sup>. These converging findings suggest that population coding and not continuous activity preserves task-relevant information until retrieval through dynamic ensemble-level reactivation and synaptic trace maintenance.

### **2.2.3 Temporal Coding**

Oscillatory activity is divided into frequency bands as described in Table 2.1: infra-slow oscillations (0.5–1 Hz), delta (1.5–4 Hz), theta (4–8, 10 Hz), alpha (8, 10–12 Hz), beta (15–30 Hz), gamma (30–80 Hz), in addition to fast (80–200 Hz), and ultra-fast (200–600 Hz) ripples<sup>44</sup>. Each band is thought to be related to specific aspects of cognition. Both in vivo and in vitro experiments suggest that synaptic inhibition plays a role in generating neuronal oscillations through two different mechanisms, either through interneuron network activity or reciprocal excitatory-inhibitory loops<sup>109</sup>. Theta, as previously discussed, and gamma are two important readouts of the hippocampal function and function of connected regions.

Table 2.1: Frequency bands and cognitive processes

Bands	Frequency (Hz)	Cognitive Processes
Infra-slow	0.5-1	Show resting state networks (RSNs) in awake human subjects
Delta	1.5-4	Anticipation and predictive coding
Theta	4-8 (humans) 6-10 (rodents)	Spatial navigation, working memory, and temporal coding
Alpha	8,10-12	Suppression and selection of attention
Beta	15-30	Involved in consciousness, logical/active thinking, focus and stress
Gamma	30-80	Readout of information transfer from CA3 to CA1 for hippocampal memory retrieval. Show the temporal organization of movement sequences, memory encoding and formation, sensory processing and planned trajectories underlying spatial navigation.
Fast ripples	80-200	Show synchronous inhibitory postsynaptic potentials (IPSP) generated by interneuronal cell subpopulations
Ultra-fast ripples	200-600	Show synchronous inhibitory postsynaptic potentials (IPSP) generated by interneuronal cell subpopulations

Temporal coding involves the precise timing of neuronal spikes, particularly in relation to ongoing brain oscillations, such as theta and gamma rhythms. Importantly, this coordination does not involve isolated spikes, but the timing of spikes across neuronal populations. Unlike rate coding, which depends on the frequency of spikes, temporal coding focuses on when spikes occur relative to specific neural events or phases of oscillatory cycles. This timing is critical for the coordination of neural activity across distant brain regions and is especially important for tasks requiring the integration of sensory inputs, memory encoding, and retrieval.

One of the most well-studied examples of temporal coding occurs in the hippocampus, where theta oscillations (4–8 Hz) play a pivotal role in organizing neural spikes during learning and memory tasks<sup>110</sup>. Theta rhythm indicates a network that is actively involved in spatial navigation, working memory, and temporal coding<sup>111,112</sup>. Lesion or inactivation of the medial septum-diagonal band of Broca neurons recognized as the theta rhythm generators eliminates theta oscillation in all connected cortical regions<sup>113</sup> and leads to spatial and working memory deficits<sup>114–116</sup>.

Gamma oscillations are another key timing structure. They are transient rhythms (30-80 Hz) that often nest within theta and reflect coordinated inhibitory-excitatory loops. Gamma oscillations dynamically couple hippocampal networks to specific behavioral demands, especially during memory retrieval tasks<sup>117–119</sup>. For example, during a T-maze alternation task in rats, peak gamma power and coherence between CA3 and CA1 regions increases specifically during decision points suggesting gamma acts as a window for transferring information from CA3 to CA1<sup>117</sup>. As such, gamma oscillations reflect the underlying coordination of region-specific

networks during memory-guided behavior, providing a physiological signature of inter-regional communication.

While oscillations can be viewed as causal mechanisms, here we adopt the view that oscillations serve as readouts of population-level signatures of coordinated firing at specific frequencies. Neurons firing at specific timescales create rhythmic fluctuations and those rhythms allow us to read when and how populations fire. Movement sequences, memory encoding and formation, sensory processing, and planned trajectories during spatial navigation are all associated with temporally structured neural activity that is reflected in gamma oscillations<sup>118,119</sup>. Gamma activity emerges from coordinated spiking within local circuits and between distant regions to reflect the coordinated activation of groups of neurons that work together to represent a cognitive state and create discrete temporal windows during which spikes can be organized into coherent units of information. This activity aligns with behavioral demands, with different gamma frequencies like slow vs. fast gamma corresponding to different information pathways, such as input from CA3 versus entorhinal cortex to CA1<sup>120,121</sup>. In this way, gamma oscillations act as signatures of how the brain segments time and organizes population-level information flow. The recurring structure of gamma rhythms enables temporally precise firing patterns that underlie processes like trajectory planning, sensorimotor integration, and the selective routing of memory-related signals. Importantly, gamma power and coherence have been shown to correlate with memory load, reflecting the amount of information actively held in working memory, and decision epochs which are task phases when subjects evaluate options or initiate responses. This underscores the utility of gamma as a dynamic readout of ongoing cognitive operations<sup>118,119</sup>.

The rate of populations of neuronal firing is also modulated in time in respect to theta frequency. For example, in the hippocampus, temporal modulation is manifested as burst firing with bursts occurring at theta frequency (4-12 Hz). This burst firing has been primarily observed in pyramidal neurons of CA1 and CA3, and is shaped by inhibition from PV+ basket cells, which help constrain the timing of spike output within theta cycles. The fidelity of burst firing within theta, termed theta modulation, is important for phenomena such as phase precession and phase preference, which are believed to allow encoding of space with higher resolution than is possible in the absence of modulation. Phase preference refers to the phenomenon that neuronal firing in the hippocampus is often locked in time with respect to ongoing hippocampal inputs in the theta frequency of the local field potential (LFP). Specific cells fire preferentially at specific phases in the ongoing theta oscillation. For example, directly after the peak of the theta oscillation, PV+ basket cells in CA2/3 area fire at the same phase as pyramidal cells in CA3, but later than basket cells in CA1<sup>122</sup>. Importantly, because there is a known phase shift in theta oscillation along the dorsoventral axis and across laminae, the reference to peak is based on recordings from stratum pyramidale of dorsal CA1. CA1 pyramidal cells preferentially fire at the trough of<sup>123,124</sup>, especially when recorded from the stratum pyramidale.

Phase precession describes the observation that place cells discharge whenever the rodent is crossing a place field and this firing occurs at an earlier phase in the theta cycle with each progressive theta cycle<sup>125,126</sup>. This allows temporally aligned sequences of spatial information to be encoded within single theta cycles. Theta-phase precession could be an indication of item-context associations through spike timing-dependent plasticity<sup>126,127</sup> given that synaptic inputs need to be precisely synchronized

within 5 ms so that EPSPs from different locations will be able to induce postsynaptic firing<sup>43</sup>. This precise temporal ordering strengthens associative links between items and their contexts across space and time.

Beyond spatial mapping, neurons in the hippocampus also encode elapsed time. Time cells first identified by Howard Eichenbaum's lab fire at specific moments within temporally structured tasks. These cells form population-level representations of sequences unfolding over seconds and bridge temporal gaps in experience<sup>128,129</sup>. Studies have shown that time cells, like place cells, can exhibit theta-phase precession during memory encoding, and the activity of these cells correlates with the use of temporal location during the retrieval phase of the task<sup>130</sup> supporting a shared temporal coding mechanism. Neuronal firing coordination with the LFP, like phase-locking and phase precession, offers a key glimpse at the relative timing of inputs in the LFP with outputs of the information processing as the neuronal firing, but neural oscillations are also readouts of synchronized behavior of the network and, as such, are on their own important mesoscale mechanisms of cognition, memory, and behavior.

Coordination between oscillations seen in the LFP or EEG can be an indicator of communication between different brain regions<sup>131,132</sup>. Coherence is a measure of this synchronization with values that range between 0 and 1. The higher the coherence, the more synchronized the regions are<sup>132</sup>. The coherence value differs between different brain regions depending on the task performed, for example, theta coherence between hippocampus and striatum during periods of decision is high (>0.8) which indicate learning<sup>132,133</sup>. In decision-making tasks, this theta coherence has been shown to increase during learning phases, and is positively correlated with behavioral performance. Further, theta coherence between the hippocampus and prefrontal cortex

increases during spatial working memory tasks, and that this increased coherence is associated with accurate decisions and trial performance which suggests that HPC-PFC coherence reflects task-relevant communication during cognitive control<sup>134</sup>.

Changes in gamma coherence have also been observed during attention-demanding tasks. Gamma synchrony increases between parietal and prefrontal areas during focused attention, highlighting that both theta and gamma coherence dynamically respond to cognitive demands<sup>135</sup>. Furthermore, CA1 can become coherent with the entorhinal cortex or CA3 through fast or slow gamma characteristics of the entorhinal cortex or CA3, respectively<sup>121</sup>. Elevation of hippocampal-entorhinal cortex synchrony was shown to be important for declarative memory formation in epileptic patients performing a memorization task<sup>136</sup>. This led to the hypothesis that synchronized brain activity in the gamma range might be an important indicator of controlled flow and routing of information<sup>131,137</sup>, because the rules guiding synaptic plasticity dictate that inputs will be most effective whenever they coincide with peaks of oscillatory network excitability<sup>131</sup>.

Finally, neural coherence alterations especially across key regions such as PFC-HPC, parietal-PFC, and hippocampus-striatum, were associated with different neuropsychiatric and neurological disorders. For example, schizophrenia is associated with reduced HPC-PFC theta coherence, ADHD with altered gamma synchrony between frontoparietal areas, and Alzheimer's disease and temporal lobe epilepsy with disrupted interregional coherence patterns<sup>138-143</sup>. This shows that neural dynamics alterations are present in multiple diseases further supporting investigating neurological diseases from a systems perspective.

#### **2.2.4 Firing Dynamics Support Plasticity**

Temporal, population, and rate coding facilitate plasticity shaped through experiences that enable the brain to adapt to new information. These mechanisms underlie the careful coordination of information between synapses and neurons in the brain that is necessary to promote synaptic plasticity and ensure efficient flow of information between different brain regions required for cognition. In 1949, Donald Hebb postulated that synapse strength can change based on previous activity, which led to what we now know as long-term potentiation (LTP) and long-term depression (LTD), fundamental to network communication. LTP strengthens synaptic transmission through high frequency stimulation of synapses. The first stage of LTP depends on the NMDA and AMPA glutamate receptors<sup>144,145</sup>. The second and third stages of LTP depend on protein synthesis to maintain changes in synaptic strength<sup>144,145</sup>. Maintenance of LTP is essential for place cell stability<sup>146-149</sup>. Even though neural plasticity is not a determinant of place cell spatial specificity, rats with neural plasticity deficits had unstable place fields upon revisiting the same environment<sup>150,151</sup>. This shows that neural plasticity is playing a role in the organization of place cells and long-term maintenance of this representation.

The frequency of action potential timing matters; low frequency firing induces LTD, which decreases synaptic efficacy. LTD is also essential for memory formation as it counteracts the LTP to allow new memories to form. Recent evidence has shown that LTD may be involved in formation and maintenance of place fields<sup>152</sup>, supporting previous experiments showing that a decrease in the expression of LTD impairs spatial memory retention and consolidation<sup>153,154</sup>. It is worth noting that plastic synapses can form positive feedback loops on the rate, temporal, and population coding mechanisms where this positive loop aids the mechanisms in refining and precisely timing the

neuronal firing leading to a more efficient information processing. Another form of plasticity known as short-term plasticity (STP) takes place on a millisecond to minutes timescale and depends on presynaptic calcium accumulation and vesicle depletion<sup>155</sup>. This form of plasticity is thought to play a role in information transfer across synaptic connections, activity-dependent synaptic efficacy modulation, promoting synchronization and working memory<sup>155-157</sup>. Careful coordination of the firing of populations of neurons in time supports appropriate short and long-term forms of plasticity that are critical for information processing, learning and memory.

In addition to this coordination, two key mechanisms, spike timing-dependent plasticity and homeostatic plasticity, play essential roles in fine-tuning synaptic connections and maintaining network stability.

Spike timing-dependent plasticity (STDP) is a critical mechanism by which synaptic connections are adjusted based on the precise timing between pre- and post-synaptic neuronal firing<sup>158,159</sup>. When a presynaptic spike precedes a postsynaptic spike by a few milliseconds, the synapse is typically strengthened, whereas the reverse timing generally leads to synaptic weakening. This bidirectional modulation enables neurons to fine-tune their connectivity in an activity-dependent manner. STDP is thought to underlie the encoding of temporal sequences and the formation of cell assemblies that support learning and memory, providing a neural substrate for experience-driven synaptic modifications<sup>160</sup>. In contrast, homeostatic plasticity acts as a stabilizing force within neural circuits. Unlike the rapid, synapse-specific changes mediated by STDP, homeostatic mechanisms such as synaptic scaling adjust the strength of all synapses on a neuron in response to prolonged changes in network activity<sup>161,162</sup>. This process ensures that overall neuronal excitability remains within an

optimal range, preventing conditions of excessive excitation or depression that could impair information processing. Homeostatic plasticity maintains network stability while still permitting the flexible reorganization of synaptic connections required for long-term memory consolidation.

The interplay between STDP and homeostatic plasticity is essential for the proper functioning of neural networks. While STDP sharpens synaptic connections based on the timing of activity to encode specific patterns and experiences, homeostatic plasticity ensures that the overall level of activity remains balanced over time. This dynamic equilibrium allows the brain to remain both adaptable, stable, and capable of forming new memories and integrating them into existing networks without destabilizing the system. Together, these processes support robust information processing, learning, and memory by enabling precise, experience-dependent modifications while maintaining overall neural circuit integrity.

### **2.3 Network Disruption as a Central Mechanism in Cognitive Impairment**

Research has increasingly shifted from viewing cognitive deficits as arising solely from focal lesions or direct consequences of an injury, to recognizing that widespread disruptions in neural network dynamics are the critical underlying factors. This network-centric perspective holds that alterations in the coordinated activity of neurons across neural circuits are central to the cognitive and behavioral impairments observed in a variety of neurological and neurodevelopmental disorders. In this chapter we will discuss how network disruption underlies the cognitive impairments in different neurological diseases.

### **2.3.1 Evidence from Epilepsy and Early Life Insults**

Traditionally, the cognitive impairments associated with epilepsy were attributed to the direct effects of recurrent seizures. However, a growing body of evidence indicates that the underlying disruption of neural networks plays a more central role. For instance, studies have demonstrated that children with early-onset epilepsy exhibit cognitive deficits even before seizure onset, suggesting that preexisting network dysfunction contributes to these impairments<sup>163,164</sup>. Similarly, animal models of early life seizures (ELS) show that seizures occurring during critical developmental windows result in lasting alterations in hippocampal and prefrontal circuitry that correlate more strongly with cognitive deficits than do with seizure frequency or severity alone<sup>32,37,41,163,165–168</sup>.

Memory impairments are common in individuals with temporal lobe epilepsy, with both short-term and long-term memory being affected. Specifically, episodic autobiographical and semantic memory deficits are prominent<sup>169–171</sup>. However, the severity and type of impairment can vary based on epilepsy subtype and affected circuits. Research indicates that these memory deficits are closely linked to dysfunction in hippocampal circuits critical for memory consolidation. Network dysfunction is evident not only during seizures, but also between seizures and even in seizure-free states. Even during seizure-free periods, spatial memory deficits are observed in animal models, suggesting that network dysfunctions precede seizures<sup>119,172,173</sup>.

Mechanistically, information processing through the mechanisms discussed earlier is shown to be altered in epilepsy and associated disorders. CA1 place cells are unstable in epileptic mice and undergo remapping a few weeks after pilocarpine-induced temporal lobe epilepsy (TLE). CA1 place cell representations become

unstable, degrade over time, and place cell spatial tuning becomes less consistent across days<sup>174,175</sup>. Prolonged recording over days from populations of neurons in CA1 and dentate gyrus has shown desynchronized interneuron firing between these two areas<sup>57</sup>, which suggests that disruption of spatial coding is due to the loss of information processing control by interneurons. The desynchronized interneuron firing can affect the timing of the inputs being sent to the CA1. This idea was supported by the observation of theta rhythm temporal coordination loss in the dentate gyrus, where these neurons were firing at inconsistent phases of the CA1 theta rhythm<sup>57</sup>. Spatial memory alteration was previously shown to be present even during the latent, seizure-free, period after either the pilocarpine-induced status epilepticus (SE) or early life seizures during the 1st weeks of life<sup>119,172,173</sup>. These deficits were associated with a decrease in hippocampal theta power<sup>172</sup> and were not influenced by the occurrence of spontaneous seizures.. Interestingly, Shuman et al.<sup>57</sup>, found that the loss of spatial coding precision in CA1 emerged weeks after pilocarpine induction, even before frequent seizures developed. This suggests that impaired place representation is not a direct consequence of seizure activity but rather reflects underlying circuit instability.. Notably, place coding alteration, place cell deterioration, more dispersed place fields, and fewer place field responses were also seen after silencing either CA3, MEC or both<sup>57,176,177</sup>. This is important because it shows that degrading inputs from upstream regions, like CA3 and MEC, can mimic the same impairments in CA1 spatial coding as seen after seizures. It suggests that seizures, and specific upstream input loss, may converge on shared mechanisms that destabilize hippocampal information processing.

In addition, we and others have shown dysregulated population coding in induced early life seizures models. In-vivo single-unit recording showed that CA1 pyramidal cells are functionally connected to other pyramidal cells and fire in a coordinated fashion during spatial memory tasks; this connectivity is altered in TLE where neuronal reactivation and synchrony predicts the behavioral outcome in a TLE model<sup>178</sup>. Population functional connectivity is also crucial within the hippocampus and between the hippocampus and PFC to underlie spatial working memory (SWM)<sup>37,179</sup>. During a SWM task, the hippocampal-PFC network shows a distributed dynamic code, seen through temporally regulated firing within and between brain regions, which is needed to combine separate processes together to execute a SWM task<sup>37</sup>. The coordinated firing of cells in time is important for several components like attention, decision making and long-term memory, which can predict task performance. The temporal modulation of populations of neurons predicted SWM accuracy in a delayed non-match-to-sample task in control rats and rats with a cortical malformation that, in humans, is an important etiology in epilepsy. Animals with cortical malformations showed deficits in hippocampal firing modulation in addition to decreased functional connectivity between neurons<sup>37</sup>.

Furthermore, population coding and neural dynamics are important for pattern separation and this process has been shown to be altered in hippocampal injury and epilepsy. The pattern separation depends on a network spanning different brain regions other than hippocampus, like the dorsal medial prefrontal cortex (dmPFC), however the hippocampus and the parahippocampal cortex serve as a hub for this network<sup>180</sup>, thus it is expected that a hippocampal injury will alter the network communication causing pattern separation deficits<sup>95,181,182</sup>. TLE patients and amnesic

mild cognitive impairment (aMCI) patients have pattern separation deficits, and this could be due to hippocampal dysfunction involving DG and CA3<sup>93,183</sup>. Another reason could be due to the failure of separating similar information during encoding by the hippocampus, hence memories will not be accurately encoded or retrieved. Studies investigating aMCI and TLE patients have shown that aMCI patients have an excess activation of the DG/CA3 area in fMRI compared to control groups and this excess activation is correlated with poor performance on pattern separation tasks. The same poor performance was seen in TLE patients performing the Mnemonic Similarity Task (MST). TLE patients demonstrated poor pattern separation performance compared to controls, however, it is important to note seizure and hippocampal sclerosis did not affect the performance of patients in this task<sup>93,181</sup>. Following studies showing that TLE patients have spatial mnemonic discrimination impairment and that TLE mice have DG-dependent object location memory deficits<sup>98,184</sup>, Madar et al.<sup>100</sup> tested pattern separation in TLE patients and mice with TLE, and then used mouse brain slices to record the spiking patterns of single granule cells (GC) in the dentate gyrus. TLE patients performing object recognition-based MST had a significant deficit in identifying similar but not identical objects suggesting that TLE might be impairing the DG-dependent mnemonic discrimination. Similar deficits were seen in mice with TLE as the mice had a decrease in object-location mnemonic discrimination compared to control mice<sup>100</sup>. Slice electrophysiology in the same mice utilized inputs mimicking the same recorded inputs during behavior and indicated that the output spike-trains of GCs had a higher average correlation compared to input correlation, which signifies a deficit in pattern separation in mice with TLE. Different input ranges demonstrated decreased pattern separation and convergence in DG at multiple timescale levels<sup>100</sup>.

This result shows the importance of population dynamics underlying spatial deficits and signals the importance of assessing functional connectivity.

Imaging and histological experiments showed that structural and functional connectivity were altered in TLE patients as well<sup>168,185</sup>. Histological changes have been observed in the amygdala, entorhinal and parahippocampal cortices in TLE patients<sup>168,186–190</sup>. MRI images investigating hippocampal sclerosis associated with TLE, found that in addition to hippocampus, atrophy is present in the adjacent mesiotemporal, temporopolar structures, and thalamus<sup>168,191–194</sup>, and this atrophy increases over time<sup>194–197</sup>. Experiments investigating tissue microstructure and structural covariance indicate that structural connectivity was impacted in TLE. Diffusion tensor MRI showed a disorganization in fiber arrangement in temporo limbic and adjacent regions<sup>168,198–201</sup>. Structural covariance such as cortical thickness or gray matter volume was altered between the mesiotemporal and neocortical regions and within the corticocortical networks<sup>202–204</sup>. Resting state functional connectivity revealed a deficit in network connectivity in TLE patients compared to healthy controls. TLE patients had a decrease in ipsilateral mesiotemporal networks connectivity and ipsilateral and contralateral hippocampi connectivity<sup>168,201,205–207</sup>. This decrease in connectivity extends beyond the temporal lobes into the posterior cingulate, inferior parietal, and medial prefrontal cortices disrupting the default mode network (DMN)<sup>208–212</sup>. These changes and deficits suggest that structural connectivity is impacted in TLE patients and that TLE is also associated with functional connectivity deficits and reorganization.

Early stage TLE patients experience functional connectivity deficits mainly in the ipsilateral hemisphere<sup>211,213</sup> in addition to disturbed interhemispheric

connections<sup>168,206,214</sup>. However, in patients with generalized epilepsy, there is an increase in the interhemispheric connectivity in addition to reduced functional connectivity<sup>215–219</sup>. fMRI studies investigating the network connections in epileptic brains showed an increase in baseline functional connectivity within the temporal lobe, alongside a decrease between temporal and other regions compared to healthy controls. Also, there is a decrease in the connection probability between neighboring brain regions, known as the clustering coefficient, within the DMN<sup>210,220</sup>. This decrease in clustering coefficient as well as increased path length, i.e., distance between one node and another, was revealed to be associated with cognitive decline in patients with cryptogenic epilepsy and only seen in patients with cognitive decline<sup>220–222</sup>. The decreased cluster coefficient within the DMN could underlie the language impairment in patients with generalized epilepsy without focal brain damage. Gauffin et al.<sup>223</sup> conducted an experiment in which patients with generalized epilepsy without focal damage performed a sentence-reading task during an fMRI experiment. Patients with generalized epilepsy took a longer time to read both congruent (simple) and incongruent (complex) sentences compared to healthy controls with no reading time difference between congruent and incongruent sentences in the patients group which suggests that patients perceived both types as complex<sup>223</sup>. BOLD fMRI indicated the activation of a left-lateralized frontotemporal network, anterior cingulate cortex and occipital cortex in both patients and controls upon reading both types of sentences, however, patients with generalized epilepsy had reduced DMN suppression compared to healthy controls<sup>223</sup>. Further lack of suppression was seen in the left anterior temporal lobe and the posterior cingulate cortex, in addition to irregular activation of the right hippocampus proper and right parahippocampal gyrus<sup>223</sup>. This reduced

suppression of DMN activity may reflect the inability of the brain to appropriately disengage task-negative networks such as the DMN when attention and language networks are engaged<sup>218</sup>. This imbalance between task-positive and task-negative networks can impair cognitive efficiency and flexibility<sup>224,225</sup>. Further evidence of network alteration in TLE patients was seen by Bernhardt et al.<sup>226</sup> upon analyzing hub nodes between controls and TLE patients. Hubs are also known as nodes that have multiple connections within a network with one central position and the connections formed by the hub nodes are essential for communication and network synchronization<sup>49</sup>. Using diffusion tensor imaging (DTI), they found that hub nodes in TLE patients were mainly located in the limbic and temporal association cortices instead of being evenly distributed between different lobes and this was thought to be due to connectivity disturbances between the temporo limbic and extratemporal neocortical structures<sup>226</sup> providing evidence that epileptic brains express decreased integration and enhanced segregation<sup>220</sup>. It is also important to note that memory impairments are present in patients who don't show a lesion with MRI<sup>227</sup> which further supports the notion that cognitive impairments depend on the affected network rather than a structural lesion<sup>171</sup>. These studies emphasize the necessity to move beyond the classical lesion model into a network approach which can provide several advantages by helping track or predict cognitive decline in epilepsy patients, improving diagnosis, and developing more accurate resection surgeries by targeting the areas where the hub nodes are mostly concentrated.

It is critical to note that experimental designs that induce an underlying disorder associated with epilepsy, but in which there are no overt seizures or subclinical epileptiform activity, show changes in information processing and

behavioral deficits compared to controls. Loss of function of sodium channels Nav1.1 associated with human epilepsy in CA1 can cause disruptions to place cells and spatial cognition without producing seizures<sup>56</sup>. Nav1.1 knockdown in the medial septum causes alterations in temporal and rate coding in those neurons, and deficits in working memory that are correlated with the degree of LFP alteration in the hippocampus rather than seizure frequency<sup>119,228</sup>. Similar effects are seen in animals with a malformation of cortical development where no overt or subclinical seizures were noted. These animals have reduced fidelity of place cells, reduction in the magnitude of theta modulation, and disrupted population coding in addition to spatial and working memory deficits. The addition of induced seizures in this model did not make the behavioral deficits worse, indicating that the main contributor to the cognitive impairment was the underlying brain substrate and not seizures<sup>36</sup>.

Notably, subclinical epileptiform activity or inter-ictal spikes (IIS) are associated with disrupted cognitive function; however the number of spikes is not a reliable indicator of the associated cognitive impairment. Kleen et al.<sup>229</sup> investigated the effect of focal IIS on hippocampus in TLE. They showed that rats with unilateral intrahippocampal pilocarpine infusion developed hippocampal spikes that caused a response latency deficit in hippocampal-dependent operant behavior task, delayed-match-to-sample<sup>229</sup>. However, the hippocampal spikes only altered the cognitive performance when they occur at the same time during memory retrieval; spikes occurring during memory encoding or maintenance did not affect the cognitive performance and overall IIS frequency during a trial was not predictive of accuracy during that trial<sup>229</sup>. Similar results were seen in patients with refractory seizures performing Sternberg task, a delayed information task that depends on short-term

memory processes, along with EEG recordings<sup>230</sup>. Contralateral or bilateral to seizure focus hippocampal interictal epileptiform discharges (IED) during memory retrieval disrupted memory retrieval, and bilateral IED during memory maintenance disrupted that process, however no effect was seen on memory encoding<sup>230</sup>. These studies show that focal IIS and hippocampal IED are associated with disruptions in memory maintenance and retrieval only when they occur during the same time window as the memory processes. Taken together, this suggests that IIS/IED are indicators of disrupted network processing underlying cognition.

In addition to deficits in rate, temporal and population coding, plasticity deficits are also present in epilepsy, in accordance with the view that these neural coding mechanisms support plasticity. Kainic-acid induced status epilepticus (SE) model in rats shows a significant decrease in hippocampal LTP in addition to cell loss, and signs of hippocampal sclerosis<sup>231</sup>. These rats also have deficits in the hippocampal-dependent novel object recognition spatial memory task that positively correlated with LTP magnitudes<sup>231</sup>. These findings were also seen in the pilocarpine-induced seizures model where the mice showed a significant decrease in the hippocampal synaptopodin acting-binding protein in CA1 region which alters the ability of the neurons to express synaptic plasticity leading to a decrease in LTP induction in Schaffer collateral-CA1 synapses<sup>232</sup>. STP and working memory are also altered in kainic acid-induced SE. Following kainic acid-induced SE, there was a decrease in STP, reduced LTP capacity, impaired spatial learning, and increased inhibition in the dentate gyrus<sup>233</sup>. STP was altered in a model with recurrent hyperexcitability leading to seizures during development<sup>41</sup>, as well as a model with aberrant GABA signaling during development leading to frequent interictal

discharges. Animals with frequent IIS/IED in the developing PFC showed a decrease in attention, and sociability alongside these changes in STP<sup>234</sup>.

The growing evidence on neural networks and epilepsy shows that these disrupted neural networks are likely responsible for the cognitive impairments seen with the disease and that the underlying etiology is the cause of both the disease and coding impairments seen in epilepsy animals and patients as well. The corollary is that recovering neural networks toward normal has potential for recovering cognitive impairments.

### **2.3.2 Network Disruptions in Diverse Neurological Disorders**

The concept of network disruption is not unique to epilepsy and early life seizures. A range of neurological conditions, each with distinct etiologies, exhibit similar alterations in network dynamics that underlie cognitive impairment:

#### **2.3.2.1 Alzheimer's Disease (AD)**

Alzheimer's disease (AD) has been conceptualized as a neurodegenerative condition primarily defined by amyloid plaques, tau pathology, and regional neuronal loss. However, a growing body of evidence indicates that the cognitive deficits observed in AD are not the result of isolated regional atrophy or the accumulation of pathological proteins. Instead, they arise from widespread disruptions in the coordinated activity of neural networks. These disruptions span structural, functional, and electrophysiological levels, each of which plays a distinct role in impairing cognitive functions such as episodic memory, executive function, and spatial navigation. Research has shown that disrupted connectivity within the default mode network (DMN) and between hippocampal and cortical regions has been linked to

deficits in episodic memory and executive function<sup>235,236</sup>. Altered rate and temporal coding have been observed in patients with AD<sup>237–239</sup> and animal models of AD<sup>240–242</sup>, suggesting that the deterioration of coordinated neuronal activity is a hallmark of the disease.

High-resolution structural MRI combined with diffusion tensor imaging (DTI) and graph theoretical analyses has revealed that AD brains exhibit a profound reorganization of their network architecture and altered network topology. Several studies have reported that AD patients show increased network path lengths and decreased global efficiency, indicating that the overall network is less optimally connected<sup>243–245</sup>. For example, increased network path lengths and decreased global efficiency suggest that the brain's capacity to rapidly transfer information between distant regions is compromised<sup>243–245</sup>. Also, degradation in white matter tracts linking the hippocampus with the neocortex was shown to correlate with deficits in episodic memory and spatial orientation<sup>246,247</sup>.

Further, at the local network level, the hippocampus and medial temporal lobe regions, which are critical nodes for memory consolidation and emotional processing, display altered functional connectivity with significant reductions in clustering coefficients and node centrality<sup>248–250</sup> which are essential for episodic memory and spatial processing. The compromised integrity of local circuits is associated with cognitive deficits as it leads to disrupted information processing<sup>248</sup>. In addition, it is also associated with abnormal amyloid levels and phosphorylated tau in cognitively unimpaired individuals with AD<sup>251,252</sup>, further supporting the notion that a disorganized brain underlies both the disease progression and the information

processing inefficiency, directly contributing to the disease development and cognitive decline.

Also, functional neuroimaging has been pivotal in identifying widespread connectivity deficits in AD. Resting-state fMRI studies consistently show that the default mode network (DMN), specially the posterior cingulate cortex (PCC) and medial prefrontal cortex, is significantly less connected in AD patients<sup>253-256</sup>. This reduced connectivity within the DMN which is critical for memory retrieval is correlated with episodic memory and executive function deficits<sup>253-256</sup>. These alterations often appear before clinical symptoms manifest<sup>236</sup>, suggesting that the progressive decoupling of the DMN underlies the early cognitive deficits seen in AD.

Beyond the DMN, other large-scale networks such as the dorsal attention network (DAN) and the salience network (SAN) also show altered connectivity. For example, studies have demonstrated that reduced inter-regional synchrony in these networks is linked to impairments in executive function and attentional control<sup>257</sup>. In early stages of AD, including in individuals with amnesic mild cognitive impairment (aMCI), a compensatory reorganization of network hubs has been observed. MEG studies reveal a shift in network centrality from posterior to anterior regions, suggesting that the brain may attempt to rewire or bolster alternative circuits in response to emerging pathology<sup>244</sup>.

The dynamic nature of these functional changes is also evident in task-based fMRI studies. The task-based studies used different stimuli and reported decreased hippocampal activity in AD patients compared to healthy controls during the encoding phase of the stimuli<sup>258-262</sup>. Also, a decrease in temporal and prefrontal regions was observed during the tasks<sup>263</sup>. This indicates that AD patients exhibit diminished

activation in memory-related regions and a loss of coordinated temporal activity across distributed networks. This disruption in temporal synchronization is thought to impair the integration of sensory, mnemonic, and executive processes necessary for successful cognitive performance.

Furthermore, studies that utilized electrophysiological recordings provide insights into the disruptions that underlie network dysfunction in AD. These studies reveal that the disease is associated with marked impairments in multiple coding dynamics. In the APP/PS1 transgenic mouse model for example, hippocampal neurons exhibit significant increase in firing rates, hyperexcitability, and LTP deficits<sup>264–266</sup>. Elevated firing rates in CA1 pyramidal cells were shown to compromise the fidelity of rate coding necessary for accurate memory encoding seen by the deteriorating stability of hippocampal place cells over time<sup>267</sup>.

Temporal coding is essential for organizing the timing of neuronal discharges, particularly in the hippocampus, where theta (4–8 Hz) and gamma (30–80 Hz) oscillations give information about the underlying memory function. In mouse models of AD, alterations in hippocampal network oscillations and theta-gamma coupling arise before A $\beta$  overproduction<sup>268–270</sup>. Loss of theta-gamma coupling has been observed in human patients as well<sup>271</sup>. These oscillatory deficits are further linked to aberrant phase precession and diminished temporal precision in neuronal firing, directly impacting the brain's capacity to form coherent memory traces.

Coordinated population coding is crucial for integrating information across distributed circuits. In AD, temporal coherence of neuronal populations in both the hippocampus and neocortex is markedly reduced<sup>272,273</sup>. This disintegration of ensemble activity disrupts the coordinated network communication necessary for

working memory and cognitive flexibility. As a result, AD patients often exhibit fragmented memory retrieval and difficulties in maintaining coherent representations of spatial environments<sup>274,275</sup>.

Notably, longitudinal studies have shown that early network alterations, detected via fMRI and EEG, can predict subsequent cognitive decline, emphasizing that network dysfunction is not only a correlate but a likely driver of the disease's clinical progression<sup>262,276,277</sup>. These studies underscore that Alzheimer's disease is not a focal disorder of amyloid deposition or tau pathology, but it is fundamentally a disorder of network dysfunction where structural disintegration, functional desynchronization, and electrophysiological alterations converge to impair the coding and integration of neural information across critical circuits.

### **2.3.2.2 Network Disruptions in Fragile X Syndrome**

Fragile X syndrome (FXS) is increasingly being recognized as a disorder of the neural network disruptions rather than solely due to a single gene mutation. Mutations in the FMR1 gene reduces or eliminates the production of Fragile X mental retardation protein (FMRP), and leads to significant alterations in brain's circuitry that affect structural integrity, functional connectivity, and the dynamics of neuronal coding, contributing to the cognitive and behavioral deficits observed in FXS.

Neuroimaging studies have identified structural abnormalities in several brain regions in individuals with FXS<sup>278,279</sup>. Notably, there is an enlargement of the caudate nucleus, thalamus, and specific cortical areas such as the frontal, cingulate, and fusiform gyri<sup>280</sup>. Studies have also shown that these structural changes are associated with hyperactivity, sensory processing deficits, cognitive deficits and aberrant behaviors in FXS<sup>278-280</sup>. For example, an enlarged caudate nucleus has been associated

with repetitive behaviors and attention deficits<sup>281-284</sup>, while alterations in the fusiform gyrus may relate to difficulties in facial recognition and social interactions<sup>285</sup>. These structural abnormalities were further seen with FMR1 KO animal models. FMR1 KO mice have deficits in dendritic spines, characterized by an increased density of immature, long, and thin spines<sup>286-288</sup>. This aberrant spine morphology is indicative of disrupted synaptic development and plasticity, which are essential for learning and memory processes.

Altered functional connectivity was also seen in FXS. Resting-state and task-based fMRI studies have shown that individuals with FXS exhibit decreased functional connectivity within the default mode network (DMN) and between critical brain regions, like fronto-parietal circuits, in addition to decreased nodal strength during the tasks showing decreased connectivity strength<sup>289-291</sup>. The decreased DMN connectivity has been linked to impairments in social interactions and communication. In *Fmr1* KO models, abnormal synchrony between the hippocampus and PFC was manifested as impaired performance in tasks requiring cognitive flexibility and decision-making<sup>292-294</sup>. For example, *Fmr1* KO rats exhibit impaired hippocampal-prefrontal networks, leading to deficits in working memory and decision-making<sup>294</sup>. These disruptions in functional connectivity result in inefficient information processing, further exacerbating cognitive deficits.

Neural coding abnormalities in FXS encompass deficits in rate, temporal, and population coding. *Fmr1* KO mice and zebrafish models show impairments in learning, memory, and attention. These behavioral deficits have been directly linked to disruptions in the dynamics of neural coding, including abnormalities in rate, temporal, and population coding. *Fmr1* KO mice exhibit significant hyperexcitability

in cortical and hippocampal circuits. Neurons in the neocortex of Fmr1-KO mice show elevated spontaneous firing activity accompanied with reduced spike timing precision<sup>295</sup>. These deficits are associated with impaired long-term potentiation (LTP) which is essential for learning and memory formation, shown by impaired performance in spatial memory tasks<sup>296</sup>. Moreover, Fmr1 KO mice demonstrate disrupted theta-gamma coupling in the hippocampus. Theta-gamma coupling, an indication of information organization and representation in memory, is disrupted in Fmr1 KO mice specifically in tasks that involve working memory<sup>292,296</sup>. Further, the spatial and temporal coordination among groups of neurons is also compromised, resulting in more variable and less robust population responses<sup>295</sup>.

Finally, a recent study using an Fmr1 KO rat model has highlighted significant disruptions in hippocampal-prefrontal cortex (HC-PFC) networks, critically underlying cognitive deficits associated with the disorder. Single-unit recordings in the hippocampus and prefrontal cortex of Fmr1-KO rats revealed significant abnormalities in neuronal firing patterns<sup>294</sup>. Hippocampal neurons exhibited atypical action potential dynamics characterized by reduced theta-modulated burst firing, essential for spatial learning and memory consolidation. However, neurons within the prefrontal cortex demonstrated abnormal, disorganized firing patterns and diminished temporal precision, hence significantly impairing executive functioning and behavioral flexibility<sup>294</sup>. Advanced network analyses in this study further demonstrated significant disruptions in neural network connectivity within and between the hippocampus and prefrontal cortex. Specifically, networks in Fmr1 KO rats exhibited reduced connection density, lower clustering coefficients, and decreased neuronal co-modulation which are key indicators of impaired information integration across neural

circuits<sup>294</sup>. These network-level disruptions were associated with significant behavioral deficits, including impaired spatial navigation, decreased sociability, and increased anxiety-like behaviors. This highlights how the disruptions in hippocampal-prefrontal network dynamics underlies the cognitive and behavioral impairments in Fragile X syndrome.

Understanding FXS as a network disorder shifts the focus of therapeutic interventions towards restoring neural connectivity and regulating neuronal excitability. Targeting network-level dysfunction in FXS can offer promising avenues for improving cognitive and behavioral outcomes in affected individuals.

### **2.3.2.3 Traumatic Brain Injury and Post-Traumatic Epilepsy**

Traumatic brain injury (TBI) is a major public health concern, affecting approximately 69 million people globally each year<sup>297-302</sup>. While TBI severity varies from mild to severe, even mild injuries contribute to long-term cognitive and psychiatric impairments, including deficits in attention, executive function, spatial learning, and memory, as well as increased risk for anxiety and psychiatric illnesses<sup>297-302</sup>. Beyond these cognitive consequences, 10–20% of TBI patients develop post-traumatic epilepsy (PTE), characterized by recurrent unprovoked seizures emerging at least one week after injury<sup>303-305</sup>. Current treatment strategies focus primarily on reducing intracranial pressure via decompressive craniectomy<sup>306,307</sup>, which, while preventing immediate brain tissue loss, paradoxically increases PTE incidence by up to 76%<sup>306</sup>. Anti-epileptic drugs (AEDs) fail to prevent epileptogenesis and do not address the progressive network dysfunctions underlying both seizure activity and cognitive decline<sup>308</sup>. Given that cognitive dysfunction and epilepsy both emerge from widespread disruptions in brain network function, further investigation

into how TBI leads to maladaptive network remodeling is critical to developing effective therapeutic strategies.

Seizures are the result of abnormal hypersynchronous network activity in the brain and are considered to be a symptom of epilepsy. Cognitive and behavioral impairments start appearing after TBI and before PTE develops. This period between the initial injury and the onset of chronic seizures is marked by progressive alterations in neural circuit function, including changes in neuronal excitability, connectivity, and synchronization. These chronic network disruptions not only increase seizure susceptibility but also contribute to the cognitive and behavioral impairments observed in TBI survivors. Given that both epilepsy and cognitive impairment are the result of the network dysfunction, this suggests that TBI induces persistent network dysfunctions that may serve as common pathological substrates for both conditions.

Neural network reorganization following TBI is a dynamic process that involves changes at multiple levels, including synaptic, circuit, and global connectivity. At the network level, increased hyperexcitability and hypersynchrony have been implicated in epileptogenesis. Studies investigating seizure susceptibility after TBI using pentylenetetrazole (PTZ) have demonstrated a reduction in seizure threshold, indicating a hyperexcitable network state<sup>301,309–313</sup>. Beyond hyperexcitability, abnormal increases in functional connectivity between brain regions are a hallmark of epileptogenesis. Functional connectivity, defined as the correlated activity between distinct neural populations, has been shown to increase between the hippocampus and cortex in hippocampal slices from early post-traumatic epileptogenesis models<sup>314,315</sup>. Similar findings have been observed in kainic acid and status epilepticus models, where enhanced connectivity within cortical and thalamic-

hippocampal circuits correlates with increased seizure susceptibility<sup>314,316</sup>. These findings suggest that epileptogenesis results from large-scale maladaptive network reorganization rather than localized neuronal dysfunction alone.

Network dysfunction in PTE is not limited to epilepsy but is also linked to the cognitive and psychiatric impairments observed after TBI<sup>300-302,317</sup>. TBI models demonstrate significant deficits in learning, memory, and anxiety regulation. Increased depression- and anxiety-like behaviors have been observed in post-injury models using burrowing and elevated plus maze (EPM) tasks<sup>301</sup>, while novel object recognition (NOR) tests indicate recognition-memory deficits following TBI<sup>301,318,319</sup>. Spatial learning impairments, assessed using the Morris water maze (MWM) and Barnes maze, are prominent in post-injury animals<sup>320-323</sup>. These cognitive impairments arise from disruptions in key neural coding mechanisms that underlie information processing, like rate and temporal coding, which are significantly altered in TBI. Cortical recordings reveal increased firing rates following controlled cortical impact (CCI) in mice<sup>324</sup>, while hippocampal neurons in fluid percussion injury (FPI) models exhibit reduced spike-time reliability, directly correlating with memory recall deficits in the Morris water maze<sup>325</sup>.

Neural coding deficits in TBI extend beyond individual neuron firing to broader network dynamics. At the population level, synchrony between brain regions is crucial for task performance and cognitive flexibility<sup>38</sup>. Hippocampal-prefrontal cortex (HC-PFC) synchrony, essential for working memory and spatial navigation<sup>37,326,327</sup>, is significantly altered after TBI, with excessive synchrony emerging as a feature of epileptogenesis. These findings suggest that while the specific neural dynamics underlying cognitive dysfunction and epileptogenesis may differ,

they share common features such as hyperexcitable firing patterns and maladaptive network synchrony. This highlights the importance of developing interventions that restore normal network connectivity and function as a key strategy for preventing both epileptogenesis and TBI-related cognitive deficits.

Understanding that cognitive impairments stem primarily from network disruption rather than isolated neuronal loss opens new avenues for treatment. Rather than focusing solely on protecting individual neurons, therapeutic strategies should aim to restore the coordinated network dynamics essential for cognitive function. Interventions that enhance synaptic plasticity, normalize oscillatory activity, and improve connectivity may ultimately yield better cognitive outcomes. This network-centric approach provides the rationale for exploring treatments such as ACTH, which as discussed in subsequent sections, appears to have neuroprotective effects that restore network function across a variety of neurological conditions.

#### **2.4 The Neuroprotective Effects of ACTH Across Neurological Disorders**

Adrenocorticotrophic hormone (ACTH) is a pivotal neuropeptide involved in regulating the hypothalamic-pituitary-adrenal (HPA) axis. Synthesized from proopiomelanocortin (POMC) in the anterior pituitary gland, ACTH is released in response to corticotropin-releasing hormone (CRH) from the hypothalamus, leading to cortisol secretion from the adrenal cortex through activation of the melanocortin-2 receptor (MC2R)<sup>328-330</sup>. This hormonal cascade plays a critical role in metabolic regulation, immune function, and the cognitive response to stressors<sup>328-330</sup>. ACTH also interacts with other melanocortin receptors, influencing pigmentation, appetite, and inflammation, working in harmony with circadian and ultradian rhythms to facilitate both immediate and long-term adaptation to stressors<sup>331</sup>.

Although it has been recognized for its role in regulating adrenal function and stimulating glucocorticoid release, research has demonstrated that ACTH exerts direct neuroprotective effects independent of its endocrine functions. These effects have been observed in a variety of neurological conditions, ranging from neurodegenerative diseases and epilepsy to ischemic stroke, multiple sclerosis, and neonatal brain injury. ACTH and its synthetic analogs have been shown to modulate neuronal survival, synaptic plasticity, neuroinflammation, and neurotrophic signaling, making ACTH a promising therapeutic candidate for neuroprotection.

While ACTH was tested in controlling seizures, research has highlighted its direct cognitive benefits. In a study using *Kcna1*-KO mice, a model of chronic epilepsy with severe cognitive impairments, administration of ACTH was found to maintain hippocampal synaptic plasticity by preventing deficits in long-term potentiation (LTP) in the CA1 region<sup>332</sup>. Moreover, mice treated with ACTH performed significantly better in Barnes Maze indicating preserved spatial learning and memory function<sup>332</sup>. It is important to note that the positive effects of ACTH occurred without altering seizure frequency, which suggests that ACTH exerts its neuroprotective effects beyond its anticonvulsant properties. Further supporting this, ACTH analog ACTH4-10 that binds melanocortin receptors without stimulating steroid secretion, has been shown to modulate limbic circuits by downregulating corticotropin-releasing hormone (CRH) expression in the amygdala independent of glucocorticoid signaling<sup>333</sup>. This finding further highlights that ACTH can activate central melanocortin receptors, in a steroid-independent manner.

Beyond epilepsy, ACTH has shown profound neuroprotective effects in ischemic stroke models. Stroke leads to a cascade of gene expression changes that

exacerbate neuronal death and neuroinflammation. In a transient middle cerebral artery occlusion (tMCAO) model in rats, it was revealed that ACTH administration significantly counteracted stroke-induced transcriptional dysregulation<sup>334</sup>.

Transcriptomic analyses demonstrated that ACTH mediated a protecting effect against ischemia-induced alterations in over 1,100 genes associated with immune response, neurosignaling, and neurogenesis<sup>335</sup>. Additionally, it was shown that the rats that did receive ACTH exhibited angiogenesis and enhanced glial proliferation in peri-infarct regions<sup>335</sup>, showing that ACTH mediated its neuroprotective effects through anti-inflammatory properties and direct modulation of neurotrophic signaling pathways.

The neuroprotective potential of ACTH extends beyond acute brain injuries to neurodegenerative disorders, particularly Parkinson's disease. In a model of MPTP-induced dopaminergic neurotoxicity, administration of ACTH prevented the loss of dopaminergic neurons in the substantia nigra, decreased anxiety and improved motor function in rodents<sup>336</sup>. For example, ACTH enhanced the expression of neurotrophic factors, including brain-derived neurotrophic factor (BDNF), to counteract the selective damage of dopaminergic pathways through MPTP-induced mitochondrial dysfunction and oxidative stress. Additionally, rats that received ACTH were shown to express control-like dopamine levels in the striatum compared to vehicle treated rats, which is crucial for motor function<sup>336</sup>. This shows ACTH's ability to preserve dopaminergic integrity highlighting its possible potential role in mitigating neurodegeneration in Parkinson's disease.

In addition to its neuroprotective effects in adult neurological disorders, ACTH has been investigated for its ability to mitigate peri-intraventricular hemorrhage (PIVH), a neonatal brain injury, that leads to long-term neurodevelopmental

impairments. In a neonatal rat model of PIVH, administration of ACTH significantly reduced the extent of striatal lesions, preserved neuronal and glial populations, and decreased the expression of astrocytic and microglial activation markers<sup>337</sup>. These findings suggest that ACTH plays a critical role in protecting the developing brain from hemorrhagic insults by modulating inflammatory responses and promoting neuronal and glial resilience.

Further supporting ACTH's role in cognitive protection, it was previously shown that ACTH treatment ameliorates attention deficits associated with early-life interictal spikes (IIS) in the prefrontal cortex<sup>338</sup>. Rats with bicuculline-induced IIS treated with ACTH exhibit significantly reduced attention deficits in a delayed non-match to sample (DNMS) task, showing that ACTH improved cognitive function even when it did not alter the underlying IIS activity<sup>338</sup>. Similarly, ACTH was able to prevent deficits in fear extinction which is a prefrontal cortex-dependent cognitive task, after ELS<sup>339</sup>. Rats with a history of flurothyl-induced seizures treated with ACTH, were able to acquire and extinguish the fear conditioning task compared to the vehicle and corticosteroid treated groups. Notably, ACTH's effects were independent of seizure suppression and possibly mediated through melanocortin receptors MC3R and MC4R signaling in the prefrontal cortex<sup>339</sup>. Rats with a history of induced ELS exhibited significant downregulation of these receptors, which may hint to a protective effect of ACTH on these receptors and explain the persistent cognitive impairments observed in the vehicle and corticosteroid treated groups. The fact that ACTH, but not dexamethasone, restored normal cognitive function further underscores ACTH's neuroprotective properties beyond its corticosteroid secreting role.

Another neurological condition where ACTH has shown promise is multiple sclerosis (MS), a demyelinating disorder characterized by immune-mediated damage to the central nervous system. Traditionally, corticosteroids have been the primary treatment for acute MS relapses, however, ACTH was shown to be a treatment option due to its ability to modulate immune responses through melanocortin receptor activation. Clinical studies have demonstrated that ACTH therapy can significantly reduce inflammation in MS patients, leading to improved neurological outcomes, even in those who fail to respond to corticosteroids<sup>340</sup>. The anti-inflammatory effects of ACTH are attributed to its ability to downregulate pro-inflammatory cytokines while simultaneously promoting remyelination and neuroprotection<sup>340</sup>.

In addition to these disease models, ACTH has also been shown to promote peripheral nerve regeneration and protection against neurotoxic insults. ACTH treatment in chemotherapy-induced neuropathy has revealed that it prevents axonal degeneration and enhances nerve repair by stimulating neurotrophic factor signaling in both humans and animals<sup>341</sup>. Similarly, in models of diabetic and autoimmune neuropathy, ACTH peptides facilitated neurite outgrowth and preserved myelinated axons<sup>342</sup>, further supporting their role in nerve repair mechanisms.

Together, these findings show the effect of ACTH on mitigating neuronal damage and enhancing recovery in the context of epilepsy, stroke, neurodegenerative disease, neonatal brain injury, or autoimmune conditions, underscoring its potential as a neuroprotectant.

## 2.5 The Melanocortin System and MC4R in Cognitive Function

### 2.5.1 Overview of the Melanocortin Receptors (MCRs)

The melanocortin system consists of five known melanocortin receptors (MC1R–MC5R), which are G protein-coupled receptors (GPCRs) involved in diverse physiological functions. These receptors, encoded by distinct genes, respond to peptides derived from proopiomelanocortin (POMC), including adrenocorticotrophic hormone (ACTH) and melanocyte-stimulating hormones ( $\alpha$ -MSH,  $\beta$ -MSH, and  $\gamma$ -MSH)<sup>343,344</sup>. Each melanocortin receptor subtype has specific roles across different tissues: MC1R is primarily expressed on melanocytes and various immune cells, where it influences pigmentation and anti-inflammatory processes<sup>343,345</sup>. MC2R, known for its role in the adrenal cortex, regulates steroidogenesis, particularly cortisol production<sup>345,346</sup>. MC3R and MC4R, however, are highly expressed in the central nervous system (CNS) and play a significant role in neurocognitive and metabolic functions. MC3R is mainly found in the brain and gastrointestinal tract, where it regulates energy homeostasis and immunomodulation<sup>343,347</sup>. MC4R regulates food intake, energy expenditure, and sexual function, with significant expression in the hypothalamus and other brain regions<sup>343,348</sup>. Lastly, MC5R is associated with exocrine gland function and the regulation of sebaceous gland activity in tissues such as the skin and adrenal glands<sup>343,349</sup>.

ACTH binds to these melanocortin receptors with varying affinities, with the highest affinity for MC2R, making it the primary receptor for ACTH's steroidogenic effects in the adrenal cortex. MC1R, MC3R, and MC4R can also bind ACTH, though they respond more sensitively to other melanocortins like  $\alpha$ -MSH and  $\gamma$ -MSH<sup>343,348,350,351</sup>. Given the selective expression of MC3R and MC4R in the brain and

glial cells, these receptors are suggested to play significant roles in various physiological processes, cognition and neuroprotective processes<sup>352,353</sup>. Our research focuses on MC4R due to its broader implications in neurodegenerative diseases and other neurological conditions. Traditionally, MC4R has been studied in the context of feeding behaviors and obesity, with approximately 6% of obesity cases attributed to loss-of-function mutations in this receptor<sup>349</sup>. Interestingly, new-onset patients with pediatric epilepsy are more likely to be obese than neurotypical children, potentially suggesting dysregulation of the MC4R system in these patients<sup>354</sup>. Beyond its role in energy homeostasis, recent evidence has shown that activation of MC4R can decrease cell death in various disease models, improve cognitive outcomes in models of Alzheimer's disease and cerebral ischemia, and regulate synaptic plasticity in the hippocampus.

### **2.5.2 MC4R and Diseases**

In the brain, the melanocortin receptor MC4R plays a pivotal role in the pathophysiology of various neurological disorders, such as Alzheimer's disease and cerebral ischemia. Activation of MC4R has been shown to promote neuroprotection and enhance cognitive function through multiple mechanisms. Recent studies indicate that MC4R activation can decrease cell death, enhance cognitive performance in disease models, and regulate synaptic plasticity in the hippocampus<sup>349,351,354–358</sup>. For instance, it was demonstrated that melanocortins protect against the progression of Alzheimer's disease in triple-transgenic mice (3xTg). The study found that treatment with  $\alpha$ -melanocyte-stimulating hormone (NDP- $\alpha$ -MSH) reduced cerebral cortex and hippocampus phosphorylation levels of amyloid/tau cascade proteins, inflammation, and apoptosis. Treated mice exhibited decreased neuronal loss and improved learning

and memory<sup>357</sup>. Another study utilizing the TgCRND8 Alzheimer's disease mouse model found that  $\alpha$ -MSH treatment prevents GABAergic neuronal loss and improves cognitive function. Treated mice demonstrated improved spatial memory and reduced anxiety during the Y-maze task<sup>359</sup>.

MC4R agonists also counteract late inflammatory and apoptotic responses, improving neuronal functionality after cerebral ischemia<sup>356</sup>. MC4R agonists counteract late inflammatory and apoptotic responses post-ischemia in a transient global brain ischemia model. Treatment with MC4R agonists reduced levels of pro-inflammatory cytokines and markers of apoptosis in the brain, enhancing neuronal survival and functionality, which further improved cognitive performance in the Morris Water Maze task<sup>356</sup>. Furthermore, other studies demonstrated that activating MC4R impacts neuronal viability and synaptic plasticity. For example,  $\alpha$ -MSH treatment rescued neurons from excitotoxic cell death following kainic acid-induced damage, resulting in a significantly higher number of viable neurons in the hippocampal CA1 pyramidal cell layer<sup>360,361</sup>. Moreover, activation of MC4R enhanced synaptic plasticity by increasing the number of mature dendritic spines and enhancing the surface expression of the AMPA receptor subunit GluA1, which mediates neurotransmission enhancement and hippocampal long-term potentiation<sup>362</sup>.

Interestingly, recent research has shown that MC4R is also involved in diseases like intracerebral hemorrhage (ICH), autism and schizophrenia. ICH studies demonstrated that selective injection of MC4R agonist was able to increase the expression of MC4R in microglia, neurons and astrocytes and the activation of the MC4R was able to decrease brain edema, suppress microglia activation and neutrophil infiltration after the ICH<sup>363,364</sup>. In addition, the levels of the inflammation markers like

TNF- $\alpha$ , and IL-1 $\beta$  were decreased after the MC4R agonist injection. MC4R activation did not only decrease inflammation and edema but also improved neurobehavioral functions. CD1 mice injected with an MC4R agonist had better spatial learning and memory in Morris Water Maze as well as improved long-term movement coordination ability in rotarod task<sup>363,364</sup>.

MC4R agonist was further tested in several neurodevelopmental disorders such as schizophrenia and autism which are characterized by social behavioral deficits. Drugs for neurodevelopmental disorders are mainly symptomatic and mostly they don't target the behavioral deficits. Administration of a selective MC4R agonist in p50 KO mice, a model used to study autism and schizophrenia due to its similar cortical and behavioral alteration, was able to acutely increase the social interaction in p50 KO mice to levels analogous that of basal WT mice<sup>365</sup>. Interestingly, intranasal treatment with an oxytocin antagonist blocked the positive effects of the MC4R agonist, demonstrating that these positive social effects were mediated by the oxytocin pathway<sup>365</sup>. Another study investigated the effects of MC4R agonist on oxytocin and behavioral deficits in a maternal immune activation (MIA) mouse model of autism. Injecting the MC4R agonist took place 4-6 months in male MIA mice exhibiting autism-like features like impaired social behavioral metrics, diminished vocal communication, and increased repetitive behaviors. After the activation of the MC4R, MIA adult male mice showed an improvement in sociability deficits along with increase in the oxytocin receptor density in the anterior cingulate cortex, a region involved in complex cognitive functions, including empathy, emotion, and decision making<sup>366</sup>. Another study using CNTNAP2 KO mice, an autism mouse model, found that administration of a selective MC4R agonist caused endogenous oxytocin release

and acutely rescued the social deficits, an effect blocked by an oxytocin antagonist<sup>367</sup>. This shows that MC4R has acute positive implications in different neurodegenerative and neuropsychiatric disease mouse models.

## **2.6 Astrocytes Function and Alteration in Neurological Disorders**

### **2.6.1 Astrocytic Function in the Brain**

Astrocytes, the most abundant glial cells in the central nervous system, play a crucial role in maintaining neural homeostasis, supporting neuronal function, modulating synaptic transmission and contributing to cognition<sup>368-370</sup>. These cells regulate the extracellular environment by modulating ion concentrations, managing neurotransmitter levels, and maintaining water balance<sup>368-370</sup>. One of their key roles is in regulating glutamate levels through uptake transporters, primarily glutamate aspartate transporter (GLAST) and glutamate transporter-1 (GLT-1), which are crucial for preventing excitotoxicity by maintaining extracellular glutamate levels<sup>371,372</sup>. Astrocytes also support overall brain health by providing metabolic substrates like lactate to neurons and by regulating water balance via Aquaporin-4 (AQP4), the main water channel in the CNS, predominantly located on astrocytic end-feet at the blood-brain barrier (BBB) interface, and it is essential for maintaining water homeostasis and preventing edema<sup>373,374</sup>. In addition, astrocytes contribute to structural integrity and cellular communication through Glial Fibrillary Acidic Protein (GFAP), a cytoskeletal key marker of reactive gliosis, a process where astrocytes proliferate and undergo hypertrophy in response to injury, inflammation, or stress. Connexin-43 (Cx43), a gap junction protein facilitating intercellular signaling and ion buffering<sup>375-378</sup>. Together,

these astrocytic components help maintain an environment that supports proper neuronal function and cognitive processes.

Astrocytes influence synaptic activity and plasticity through processes like the tripartite synapse, where astrocytic processes envelop synapses and modulate the availability of neurotransmitters, ions, and other signaling molecules<sup>379</sup>. This dynamic interaction contributes to long-term potentiation (LTP) and long-term depression (LTD), both essential for learning and memory<sup>380</sup>. Additionally, astrocytes contribute to neurovascular coupling, linking neural activity with local blood flow by releasing vasoactive substances in response to increased neuronal activity, thereby ensuring adequate oxygen and nutrient delivery to active brain regions<sup>381</sup>.

## **2.6.2 Astrocytes in Diseases**

The central role astrocytes play in maintaining neural networks has led to increasing recognition of their potential contribution to the pathophysiology of different neurological disorders.

### **2.6.2.1 Alzheimer's Disease (AD)**

Astrocytes dysfunction is increasingly recognized as a key contributor to AD's pathophysiology. Astrocyte alterations in AD significantly affects neuronal function, synaptic plasticity, and network communication, contributing to disease progression and cognitive deficits. Several astrocytic markers, including GFAP, AQP4, GLAST, and connexin-43, are altered in AD, reflecting significantly impaired astrocytic function. These alterations disrupt astrocyte-neuron interactions, leading to neural network dysregulation.

One of the earliest astrocytic changes in AD is reactive astrogliosis, marked by increased GFAP expression and hypertrophic astrocytes clustering around amyloid-beta (A $\beta$ ) plaques<sup>382,383</sup>. This change is seen in both human AD brains and AD mouse models, such as the 5xFAD and APP/PS1 transgenic mice<sup>384-386</sup>. Studies have shown a significant increase in astrocytic GFAP expression in both the hippocampus and cortex, correlating with disease severity and cognitive impairments<sup>387,388</sup>. Initially, this increase in GFAP expression can serve a protective role, however, continuously elevated GFAP levels become indicative of astrogliosis that exacerbates neuroinflammation and contributes to neurodegeneration. In addition, astrocytic atrophy, characterized by decreased astrocyte volume and reduced support for neuronal synapses, is also seen in the hippocampus, entorhinal cortex and medial prefrontal cortex of AD brains. For instance, APP/PS1 and Tau-P301S mouse models exhibit astrocytic atrophy in hippocampus and entorhinal cortex<sup>389,390</sup>, and 3xTg exhibit astrocytic atrophy in the medial prefrontal cortex<sup>391</sup> that significantly correlates with synaptic loss and impaired spatial memory performance, highlighting the critical role of astrocytes in maintaining cognitive function.

Astrocyte dysfunction in AD is also characterized by altered calcium signaling, impaired neurotransmitter regulation and metabolic support<sup>98,392</sup>. It is thought that early astrocytic calcium dysfunction plays a key role in network hyperactivity and impaired neuronal synchronization. In vivo calcium imaging in APPNL-F mouse model demonstrated significantly reduced calcium signaling in the cingulate cortex even before amyloid plaque deposition and was associated with significant spatial learning and memory impairments in the Morris water maze and novel object recognition tasks<sup>393</sup>. Another study using the 5xFAD mice demonstrated increased

spontaneous astrocytic calcium activity disrupting neuronal firing and contributing to cognitive decline<sup>394,395</sup>. The cognitive deficits were highly correlated with the network dysfunction, which suggests that astrocytic calcium dysregulation directly contributes to cognitive decline in AD. Notably, restoring astrocytic calcium homeostasis, via DREADDs-mediated modulation of astrocytes, effectively normalized neuronal activity, rescued functional connectivity, and improved cognitive performance<sup>393</sup>. These findings further highlight the critical role of astrocytic calcium regulation in maintaining cognitive function.

Furthermore, reactive astrocytes can contribute to neurotoxicity and synaptic dysfunction in AD. For example, exposing astrocytes to A $\beta$ 42 in a neuron-astrocyte co-culture led to a reactive phenotype characterized by morphological changes, increased cytokine release, and increased synaptotoxicity<sup>396</sup>. Also, the neurons in the co-culture exhibited significant dendritic atrophy and synapse loss, emphasizing the detrimental role of astrocytes in AD-related synaptic degeneration<sup>396</sup>.

Aberrant gliotransmission also plays a role in AD, shown by the excessive release of GABA neurotransmitter by reactive astrocytes, which suppresses neuronal activity and impairs synaptic plasticity. Hippocampal slices from APP/PS1 mice show excessive astrocytic GABA release leading to impaired synaptic plasticity and memory deficits. Inhibiting astrocytic GABA synthesis pharmacologically rescued memory impairments in these models<sup>397</sup>. Moreover, glutamate homeostasis is altered in AD underscoring another astrocytic dysfunction. Studies in post-mortem AD brains and AD mouse models have shown a significant downregulation of GLAST and GLT-1 transporters, resulting in elevated extracellular glutamate levels and neuronal excitotoxicity<sup>398-400</sup>. For example, reduced expression of GLAST and GLT-1 in

APP/PS1 mice leads to excessive glutamate accumulation in the hippocampus, exacerbating synaptic loss and cognitive deficits seen in spatial learning and memory in the water maze<sup>401-403</sup>. This highlights the critical role of astrocytic glutamate transporters in maintaining cognitive function.

In addition to neurotransmitter dysregulation, astrocytic network communication is also impaired in AD. AQP4 and connexin-43 expression is altered in AD<sup>404,405</sup>, which disrupts astrocyte-neuron and astrocyte-astrocyte communication. AQP4 expression and localization are disrupted which impair glymphatic clearance and exacerbate A $\beta$  accumulation. Studies using AQP4 knockout mice have shown increased A $\beta$  deposition and cerebral amyloid angiopathy, loss of synaptic protein and brain-derived neurotrophic factor in the hippocampus and cortex, and worsened cognitive deficits in APP/PS1 mice<sup>406</sup>. Similarly, connexin-43 expression and function are dysregulated, leading to impaired astrocytic gap junction coupling and cortical desynchronization<sup>397,407</sup>.

#### **2.6.2.2 Parkinson's Disease (PD)**

Parkinson's disease (PD) is characterized by loss of dopaminergic neurons in the substantia nigra, but astrocytes in the basal ganglia and other brain regions also undergo significant changes in PD. Even though astrocytes are not extensively studied, it was shown that brain homeostasis is significantly altered in PD through astrocytic alterations contributing to disease progression. Astrocytic alterations in PD are associated with both loss-of-function and toxic gain-of-function mechanisms, leading to disrupted neuroprotection and exacerbation of neuroinflammation<sup>408</sup>. GFAP and AQP4 expression is altered which indicates disrupted astrocytic homeostasis. Increased GFAP expression and hypertrophic morphology indicative of astrogliosis is

seen in both post-mortem human PD brains and animal models, including those overexpressing  $\alpha$ -synuclein<sup>409</sup>. Reactive astrocytes in PD release pro-inflammatory cytokines such as tumor necrosis factor-alpha (TNF- $\alpha$ ) and interleukin-1 beta (IL-1 $\beta$ ), which contribute to neurotoxicity and neuronal degeneration<sup>408</sup>. Furthermore, PD brains were shown to express reactive astrocytes that contribute to dopaminergic neuron loss<sup>410,411</sup>. Preventing neurotoxic astrocytic activation through Glucagon-like peptide-1 receptor (GLP1R) agonists, a potential neuroprotectant in AD and PD, reduced neuronal degeneration and motor deficits in  $\alpha$ -synuclein preformed fibril ( $\alpha$ -syn PFF) mouse model of sporadic Parkinson's disease<sup>411</sup>.

Astrocytic involvement in PD extends beyond inflammation to include disruptions in glymphatic clearance and metabolic support. It has been shown that mice overexpressing  $\alpha$ -synuclein exhibit a significant decrease in AQP4 expression in the substantia nigra, along with reduced glymphatic activity, impairing the clearance of extracellular  $\alpha$ -synuclein aggregates<sup>409,412</sup>. Interestingly, AQP4 KO mice overexpressing human A53T  $\alpha$ -synuclein in the SN, exhibited increased accumulation of  $\alpha$ -synuclein monomers in the brain parenchyma two weeks after the start of the experiment<sup>409</sup>, indicating a close interaction between AQP4 function and  $\alpha$ -synuclein located in the brain parenchyma. Additionally, astrocytes contribute to blood-brain barrier (BBB) integrity which was shown to be disrupted in PD, partially due to astrocyte dysfunction<sup>412,413</sup>. The reduced expression of AQP4 and connexins in astrocytes affect the BBB stability and impairs astrocyte-neuron metabolic coupling<sup>408</sup>. This loss of astrocyte-regulated homeostasis increases the passage of peripheral immune cells and toxic proteins to the brain, exacerbating neurodegeneration<sup>412</sup>.

Further, proteomic and RNA profiling studies have revealed that striatal astrocytes exhibit lower gap junction coupling, potassium buffering, and neuroprotective interactions compared to hippocampal astrocytes, which may underlie the selective vulnerability of the nigrostriatal pathway in PD<sup>414,415</sup>. Loss of astrocyte-secreted neurotrophic factors, such as glial cell line-derived neurotrophic factor (GDNF), impairs the survival of dopaminergic neurons. Astrocytes in PD models showed reduced GDNF expression that contributed to disease progression<sup>416</sup>.

### **2.6.2.3 Schizophrenia**

Schizophrenia has been considered a disorder of neurons and neurotransmitters, however, astrocytes have emerged as important players in its pathophysiology. Studies in post-mortem brains of schizophrenia patients have shown reduced GFAP expression in certain brain regions, suggesting astrocyte atrophy or loss<sup>417,418</sup>. For example, GFAP protein was reduced in the white matter of the anterior cingulate cortex in schizophrenia patients, while S100B, an astrocyte-derived calcium-binding protein, was elevated in both the brain and peripheral blood of individuals with schizophrenia<sup>419</sup>. Additionally, transcriptomic analyses of patient brains showed an increase in astrocyte-related genes, indicating that astrocytes undergo molecular changes in schizophrenia<sup>420</sup>. Further, some studies suggested that astrocytes through AQP4 expression might contribute to the BBB impairment seen in schizophrenia, impacting the vascular integrity and contributing to neuroinflammation in the brain<sup>421,422</sup>. Moreover, abnormalities in GLT-1 expression have been shown in the prefrontal cortex of schizophrenia patients and further confirmed in animal studies<sup>423,424</sup>. For instance, upregulating astrocytic GLT-1 expression in rodents was correlated with impairments in sensorimotor gating, learning, and memory<sup>425</sup>. This

highlights that normal cognitive function requires optimal astrocytic support of neurotransmission. This was further seen in mice models with selective deletion of adenosine A2A receptors on astrocytes. This disrupts astrocyte regulation of glutamate release and uptake and induces schizophrenia-like neural changes including abnormal glutamate receptor expression and altered synaptic plasticity along with psychomotor and working memory deficits<sup>426</sup>. This highlights that astrocytic dysfunction can cause cognitive symptoms same as the ones seen in the disorder.

#### **2.6.2.4 Epilepsy**

Preclinical studies highlight the critical role of astrocyte dysfunction in the pathogenesis of epilepsy-associated cognitive deficits. Impairments in astrocyte functions including glutamate homeostasis, ion buffering, water regulation, and gap junction communication are seen in epilepsy models. These impairments correlate with synaptic instability, hyperexcitability, and memory deficits seen with the disease.

Elevated GFAP levels are observed in epilepsy models, reflecting the heightened state of astrocytic activation and gliosis<sup>427</sup>. Astrocytic gliosis is initially a protective reaction to neuronal injury, characterized by increased GFAP expression, hypertrophy, and proliferation of astrocytes around the epileptic focus. However, chronic activation transitions into maladaptive gliosis, perpetuating inflammation, neuronal excitability, and exacerbating epileptogenesis through excessive cytokine production and altered neurotransmitter homeostasis<sup>370,375,427</sup>.

In addition to that, GLAST and GLT-1 transporters expression is often reduced in epilepsy, leading to impaired glutamate clearance and heightened excitability in neuronal circuits<sup>371,372,428,429</sup>. Specifically, decreased expression and function of GLT-1 results in elevated extracellular glutamate levels, prolonging postsynaptic receptor

activation. This disruption exacerbates neuronal excitotoxicity, contributing directly to neuronal death and further epileptogenesis<sup>428,429</sup>. Additionally, loss of GLAST functionality also aggravates seizure susceptibility by allowing excess glutamate accumulation and subsequent hyperactivation of neuronal networks<sup>371,372</sup>.

Chronic high extracellular glutamate can damage neurons, further worsening cognitive impairment and epileptogenesis<sup>427,428,430,431</sup>. Repeated seizures and glutamate-mediated excitotoxicity induce long-term structural and functional neuronal changes, characterized by dendritic atrophy, loss of synaptic spines, and alterations in synaptic plasticity<sup>430,431</sup>. These morphological and functional impairments directly link chronic glutamate dysregulation to persistent cognitive deficits observed in epilepsy models, specifically deficits in spatial learning and memory task such as impaired performance in the Morris water maze<sup>430,431</sup>.

Moreover, AQP4 dysregulation can lead to impaired water clearance, resulting in cellular swelling and BBB breakdown, which exacerbates seizure susceptibility and promotes neuroinflammation<sup>370–372,432–434</sup>. Astrocytic AQP4 channels, localized primarily at perivascular endfeet, play an essential role in water homeostasis, glymphatic clearance, and maintaining the integrity of the blood-brain barrier (BBB). Dysfunctional AQP4 expression contributes significantly to cytotoxic edema, impaired glymphatic clearance of extracellular metabolites, and exacerbation of neuroinflammatory responses<sup>370–373,432–434</sup>. Studies in epilepsy models have shown altered localization of AQP4 from perivascular astrocytic endfeet to the astrocytic soma and processes, correlating with worsened edema formation, increased seizure frequency, and significant cognitive impairments including deficits in LTP and location-specific object memory task<sup>434,435</sup>.

Lastly, changes in Connexin-43 (Cx43) expression can disrupt astroglial networks, impacting neuronal synchronization and contributing to hyperexcitability. Cx43, a major gap junction protein, facilitates astrocytic intercellular communication essential for potassium buffering and neurotransmitter clearance<sup>436,437</sup>. Reduced Cx43 expression impairs astrocytic coupling, thus disrupting the astrocytic syncytium required for efficient buffering of extracellular potassium and neurotransmitter uptake<sup>436</sup>. This dysregulation significantly enhances neuronal excitability and predisposes the network to seizure activity<sup>427,436-438</sup>. Experimental reduction of Cx43 in animal models increases seizure frequency and duration, highlighting its critical role in maintaining neural circuit stability<sup>438</sup>.

### **2.6.3 MC4R Expression in Astrocytes**

Recent studies suggest that MC4R is expressed in astrocytes, indicating that ACTH and melanocortin peptides might exert effects not only through neurons but also through glial cells. While MC4R was traditionally associated with neuronal modulation of appetite, metabolism, and inflammation, its presence in astrocytes opens new potential mechanisms of action. MC4R in astrocytes may influence calcium signaling, glutamate uptake, and inflammatory responses, which are crucial in conditions like epilepsy and cognitive impairment. This astrocytic MC4R expression may help explain the neuroprotective and anti-inflammatory effects observed with MC4R activation<sup>439</sup>. For example, MC4R activation in astrocytes could modulate the release of cytokines and other inflammatory mediators, dampening neuroinflammation.

Multiple studies investigated the effects of astrocyte MC4R activation. One study found out that activating MC4R through  $\alpha$ -MSH in astrocytes culture reduced

the nitric oxide production and the expression of inducible nitric oxide synthase (iNOS) induced by bacterial lipopolysaccharide and interferon- $\gamma$ <sup>440</sup>. This anti-inflammatory effect was lost with the use of an MC4R antagonist, suggesting a MC4R-mediated mechanism in the action of this melanocortin. The activation of the MC4R also increased astrocyte viability by modulating apoptotic protein expression<sup>440</sup>. Interestingly, the MC4R activation in astrocytes induced BDNF expression through the cAMP-PKA-CREB pathway as well potentially linking MC4R activation to increased BDNF expression<sup>441</sup>. In addition to that, MC4R anti-inflammatory effects were also seen in primary cultured rat hypothalamic neurons. MC4R activation decreased TNF- $\alpha$  expression induced by the administration of a combination of LPS and interferon- $\gamma$ <sup>442</sup>. Another study investigated astrocyte MC4R activation in a Multiple Sclerosis (MS) disease in humans. The study showed the presence of MC4R mRNA and protein in human astrocytes and an increased astrocytic MC4R immunoreactivity in human active MS lesions<sup>443</sup>. Activating the astrocytic MC4R via Setmelanotide, a selective MC4R agonist, in lesion tissue culture reduced inflammation-driven chemokine expression and induced the production of the cryoprotective interleukins IL-6 and IL-11 by increasing CREB phosphorylation<sup>443</sup>. Interestingly, the setmelanotide treated astrocytes skewed macrophages toward an anti-inflammatory phenotype, which could limit a local inflammatory response in MS<sup>443</sup>. MC4R's anti-inflammatory effect in MS was also previously investigated in cell culture where ACTH treated astrocytes and microglia were able to prevent damage to oligodendrocytes, a damage usually observed with MS<sup>444</sup>. This shows that targeting astrocytic MC4R limits neuroinflammation by activation of the cytoprotective IL-6 cytokine family and by modulation of macrophage phenotype.

These findings underscore the important role of astrocytes in neurological diseases and how dysfunctions that include disrupted water balance, impaired neurotransmitter clearance, compromised intercellular communication, and maladaptive inflammatory responses are present in different diseases. Targeting astrocytic pathways may offer therapeutic or protective benefits. In particular, activating MC4R in astrocytes via ACTH or  $\alpha$ -MSH seems to modulate astrocytic activity, promoting anti-inflammatory and neuroprotective effects. Such intervention has shown reduction in neuroinflammation, enhancement of cellular viability, and potential mitigation of the negative outcomes associated with various diseases. Restoring astrocytic homeostasis or preventing astrocytic alterations, may offer a viable pathway for neuroprotection and disease modification, for potentially improving cognitive and functional outcomes across neurological disorders.

## Chapter 3

### COMMON METHODOLOGIES

#### 3.1 Animals

Male and female C57BL/6J (strain#:000664) and MC4r KO (B6.129S4-Mc4rtm1Lowl/J, Strain #:032518) mice from the Jackson Laboratory were used in the experiments. MC4R knockout mice were maintained as homozygous, and littermates with both copies of the receptor were obtained from Jackson Labs and used as controls. This strain has a floxed stop codon in front of the MC4R gene, allowing us to knock the receptor back using cre-recombinase. We used littermates and equivalently bred mice (WTs and KOs from the same corresponding litters, and wildtype, knock-in and knockout animals bred in parallel whenever possible) to reduce confounding genetic variability. All mice were housed in the same animal room and provided with food and water *ad libitum* and maintained on a 12-h light-dark cycle with consistent temperature and humidity, identical bedding, and enrichment. Each cage contained 3-5 mice of the same sex and treatment group to avoid social stress. The same experimenter provided regular husbandry and was the sole handler for all behavioral assays. This approach minimized discrepancies in handling or environment that could inadvertently influence anxiety measures. All procedures were conducted in compliance with the ARRIVE 2.0 guidelines to ensure methodological transparency and reproducibility. The experimental protocol was approved by the Institutional Animal Care and Use Committee (IACUC) at Nemours Children's Health and was

performed in accordance with the National Institutes of Health *Guide for the Care and Use of Laboratory Animals*.

### **3.2 Animal Handling and Habituation**

All animals were handled daily by a single experienced experimenter for routine husbandry and any procedural injections. The same experimenter conducted all behavior tests, minimizing variability due to multiple handlers. Mice were transferred to the testing room at least 60 minutes prior to the start of any behavioral task for habituation. During testing, the experimenter remained outside the room to reduce potential stress or distraction. This consistent handling and habituation protocol was designed to minimize anxiety and thigmotaxis, enhancing the validity of locomotion, exploration and anxiety measures.

### **3.3 Early Life Seizure Mouse Model**

Seizures begin on postnatal day 10 (p10). 20 total seizures were administered for 5 days from p10-p14. Wild type and knockout mice were divided into three groups each: WT control vehicle-treated, vehicle-treated ELS, and ACTH-treated ELS; and KO control vehicle-treated, vehicle-treated ELS, and ACTH-treated ELS. An hour before every seizure, mice received subcutaneous injections of their respective drug or vehicle. Animals took a one-hour break between each of their four daily seizure sessions. 4-animal groups were housed in individual sections of a custom-designed and built plexiglass chamber, which were linked to a central chamber that contained flurothyl. All sections of the chamber have equal access to the central chamber containing the flurothyl when the section doors are closed, but a sliding plastic panel

cuts off flurothyl access once the section is opened for quick evacuation of the flurothyl.

### **3.4 Flurothyl Induction**

0.02mL of Flurothyl (Sigma-Aldrich) was dispensed into the central chamber on a filter paper and allowed to diffuse into the connected chambers containing individually placed animals. At incremental doses of 0.01mL or 0.02mL, flurothyl was given to elicit seizures with a minimum interval of one minute between each administration. The animal's chamber was immediately evacuated upon the onset of a tonic-clonic seizure. Seizure sessions were recorded through webcams for close monitoring and further offline analysis. Animal-specific metrics, such as latency to seizure and duration of seizure, were documented by an observer and confirmed through video analysis.

### **3.5 Drug Administration**

Mice in the ACTH group received subcutaneous injections with an ACTH in 5% gelatin solution at a dose of 150 IU/m<sup>2</sup>, diluted with 5% gelatin to a total volume of 0.1mL. Vehicle Control and Vehicle ELS littermates received 0.1mL subcutaneous injections of the same solution vehicle as their littermates. All mice received drug administration once daily, one hour prior to each day's seizure inductions.

### **3.6 Open Field Task**

At p50, mice were placed in a 46 cm x 46 cm squared arena in an isolated room and allowed to explore freely for 10 minutes. Sessions were video recorded and analyzed via ANY-maze for total locomotion, center entries as well as relative time

spent in the center in order to obtain measures for spontaneous activity and exploration.

### **3.7 Seizure Latency and Duration**

To evaluate the differences in seizure latency and duration between various experimental groups, we conducted a time-to-event analysis using the Cox Proportional-Hazards model. We employed a shared frailty Cox Proportional-Hazards model due to its robustness in handling time-to-event data, allowing us to assess the effect of multiple covariates on the hazard of seizure occurrence adjusting for multiple measurements per animal. To account for day-specific effects, we stratified the Cox model by Seizure Day. This stratification ensures that our results are adjusted for any variations in seizure risk that may occur from day to day. This method enabled us to compare the seizure characteristics across different treatment and genotype groups, providing insights into the effects of various interventions on seizure dynamics.

### **3.8 Software Validation**

The behavioral tasks were recorded and analyzed using ANY-maze (Stoelting Co.), an automated video tracking software widely used for rodent behavior assessments<sup>445</sup>. ANY-maze offers accurate real-time tracking of each animal's position, speed, and zone entries, with a reported high concordance to manual scoring in multiple paradigms<sup>446</sup>. To further ensure accuracy, we manually check approximately 20% of the sessions to verify that the automated scoring matched the animal's actual position and movements. No discrepancies were detected, supporting the reliability of the software's measures in our setup.

### 3.9 Statistical Analysis

Data were analyzed using a generalized estimating equation (GEE) model, a multivariable, repeated-measures, regression model. This approach allows for modeling data with multiple measures per animal and adjusts for potential confounding variables like sex and litter. Sex, genotype and group were used as factors. Sex and litter were not significant and were therefore removed from the final analyses. Non-significance is defined as  $p > 0.05$ ; p values for all significant results are reported in the results section ( $p < 0.05$  \*,  $p < 0.01$  \*\*,  $p < 0.001$  \*\*\*,  $p < 0.0001$  \*\*\*\*).

To ensure that our study was sufficiently powered to detect group differences, we conducted a post hoc power analysis for each GEE model using G\*Power<sup>447</sup>. Effect sizes (Cohen's  $f^2$ ) were derived from the Wald Chi-Square ( $\chi^2$ ) values reported in the GEE output using the formula  $f^2 = X^2/N$ , where N represents the total number of animals analyzed in each model.

## Chapter 4

### MELANOCORTIN 4 RECEPTOR-DEPENDENT MECHANISM OF ACTH IN PREVENTING ANXIETY-LIKE BEHAVIORS AND NORMALIZING ASTROCYTE PROTEINS AFTER EARLY LIFE SEIZURES <sup>448</sup>

#### 4.1 Introduction

Epilepsy, affecting 50-65 million people worldwide, is a neurological condition characterized by an enduring predisposition to generate seizures with significant neurobiological, cognitive, and social implications<sup>449,450</sup>. Approximately 30–40% of children with epilepsy experience cognitive, psychiatric, or behavioral comorbidities, particularly anxiety disorders<sup>33,451,452</sup>, significantly impacting quality of life<sup>34,453–455</sup>. Current anti-seizure therapies fail to adequately address these comorbidities<sup>38,453,456</sup>.

ACTH, a melanocortin family peptide within the hypothalamus-pituitary-adrenal (HPA) axis, has been utilized as a treatment for decades in childhood epilepsies, particularly infantile spasms<sup>457–460</sup>. The canonical mechanism of ACTH involves activating the melanocortin 2 receptor (MC2R) in the adrenal glands, playing a role in steroidogenesis<sup>346,461</sup>. However, because ACTH agonizes all melanocortin receptors, not just the canonical MC2R, we demonstrated that rodents with a history of early life seizures (ELS) treated with ACTH, but not a corticosteroid, showed significant improvements in fear extinction learning and attention<sup>338,339</sup>, as well as normalized gene expression in the brain related to synaptic plasticity and cell communication, without altering seizure parameters<sup>462</sup>. Taken together, these data

support a role for ACTH acting at an additional pathway, with actions above and beyond canonical corticosteroid release.

The melanocortin receptors, MCRs1-5, exhibit distinct tissue distributions and functions<sup>463,464</sup>. Activation of MC4R, primarily expressed in the CNS, has been shown to be neuroprotective in neurodegenerative diseases<sup>349,351,354</sup>. Recent studies indicate that MC4R activation can decrease cell death, enhance cognitive performance, and regulate synaptic plasticity in the hippocampus<sup>349,351,354,356–358,362</sup>. For instance, activating the hippocampal MC4R circuit alleviated synaptic plasticity impairments in Alzheimer's disease<sup>358</sup> indicating that MC4R has therapeutic potential in conditions where synaptic function is compromised.

Research has mainly focused on neuronal function after ELS and it was shown that ELS can disrupt the hippocampal-prefrontal cortex network and alter synaptic plasticity leading to cognitive and psychiatric deficits. However, there is a significant gap in the understanding of the role of astrocytes, which play a vital role in the brain's response to injury, after ELS. Activation of MC4R in astrocytes promotes anti-inflammatory effects and modulates cell survival proteins<sup>440</sup>. Astrocytes are crucial in epilepsy, resetting ion balance and recycling neurotransmitters after seizure<sup>370</sup>. Astrocyte alterations contribute significantly to seizure predisposition<sup>465</sup>. For instance, increased levels of Glial Fibrillary Acidic Protein (GFAP) and altered Aquaporin-4 (AQP4) expression are both linked to increased seizure susceptibility and worsened seizure activity<sup>370–372,432–434</sup>. However, the role of MC4R activation in mitigating astrocyte dysfunction in epilepsy has not been explored.

We have previously shown in two rat models that ACTH can improve cognitive outcome after ELS and that ACTH treatment in control rats did not alter

cognitive function<sup>338,339</sup>. Here we show for the first time that ELS is associated with significant anxiety in a mouse model, which is ameliorated by ACTH. We hypothesized that ACTH exerts its beneficial effects through activation of MC4R signaling in both neuronal and astrocyte populations. Our findings underscore a crucial role for MC4R in ACTH's positive effects and its potential to alleviate anxiety-like behavior.

## **4.2 Methods**

### **4.2.1 Animals**

In addition to WT and MC4R KO animals, Syn1-cre (B6.Cg-Tg(Syn1-cre)671Jxm/J, Strain #:003966) and Gfap-cre (B6.Cg-Tg(Gfap-cre)77.6Mvs/2J, Strain #:024098) mice from the Jackson Laboratory were used in the experiments.

For the knock-in experiments, we used a breeding strategy with homozygous MC4R KO mice and hemizygous GFAP Cre or Syn1 Cre mice to re-express MC4R in astrocytes or neurons, respectively. Multiple lines of evidence have confirmed the astrocyte-specific expression of GFAP-Cre (B6.Cg-Tg(Gfap-cre)77.6Mvs/2J) through strong colocalization of Cre with GFAP immunoreactivity in various brain regions<sup>466-468</sup>, while Syn1-Cre (B6.Cg-Tg(Syn1-cre)671Jxm/J) has been validated as neuron-specific<sup>469,470</sup>, both with no off-target effects. We verified the presence of the Cre transgene by polymerase chain reaction (PCR) genotyping. Male hemizygous GFAP Cre, male hemizygous Syn1 Cre and homozygous KO female mice were used. We bred homozygous MC4R KO females with hemizygous GFAP Cre males in the first cross. We genotyped the F1 generation and selected heterozygous KO mice that were also Cre positive. The one floxed allele of the MC4R gene was reintroduced by the

Cre recombinase, resulting in heterozygous MC4R knockout mice. F1 generation heterozygous KO/Cre+ mice were bred with homozygous MC4R KO mice. 75% of the offspring from breeding a heterozygous KO/Cre+ mouse with a homozygous KO mouse will be Cre positive. The Syn1 Cre mice were bred in a similar manner.

#### **4.2.2 Early Life Seizure Animals**

Wild type and knockout mice were divided into three groups each: WT control vehicle-treated, vehicle-treated ELS, and ACTH-treated ELS; and KO control vehicle-treated, vehicle-treated ELS, and ACTH-treated ELS. (WT: N = 7 control vehicle-treated, N = 8 vehicle-treated ELS, N = 9 ACTH-treated ELS; KO: N = 7 control vehicle-treated, N = 7 vehicle-treated ELS, N = 6 ACTH-treated ELS). Knock-in mice were split into 2 groups each: (N = 6 MC4R Syn1 KI vehicle-treated ELS, N = 8 MC4R Syn1 KI ACTH-treated ELS, N = 5 MC4R GFAP KI vehicle-treated ELS, N = 5 MC4R GFAP KI ACTH-treated ELS).

#### **4.2.3 Light/Dark Box Task**

At p50, mice were placed in a 46cm x 27cm x 30cm acrylic box. 1/3 of the box was a dark area, while 2/3 of the box was exposed to light. A plexiglass door allowed the animals to enter either compartment of the box. The mouse was placed in the light compartment of the box and allowed to freely explore for 10 minutes. Animals were video recorded and analyzed via ANY-maze for time spent in each compartment in order to test anxiety-like behavior.

#### **4.2.4 Immunohistochemistry**

48 hours after the last seizure, animals were perfused followed by brain collection. Brains were fixed with 4% paraformaldehyde (PFA) for 4 hours and then

transferred into 20% sucrose solution for cryopreservation. Brains were sliced at 40 microns for the prefrontal cortex (PFC) and hippocampus (HC) and fixed on charged slides for staining. A two-day immunohistochemistry protocol was used. Day 1 consisted of two 15-minute washes in 1X PBS, one hour of blocking and tissue permeabilization, followed by an overnight primary antibody incubation at 4C. Day 2 consisted of three 15-minute washes in 1X PBS, one two-hour secondary antibody incubation in the dark at room temperature, three additional 15-minute washes in 1X PBS, coverslip mounting using Fluoroshield with DAPI, and coverslip sealing. Blocking buffer was composed of 10% Normal Goat Serum and 0.5% Triton X-100 in 1X PBS. Tissues were co-stained with primary antibody, Glial Fibrillary Acidic Protein (GFAP) [1:1000] (ab4674, ABCAM LTD), and the conjugated secondary antibody, Alexa Fluor 555 (ab150170, ABCAM LTD), alongside another astrocytic biomarker Aquaporin-4 (AQP4) [1:500] (NBP1-87679, Novus Biologicals INC) and the secondary antibody, Alexa Fluor 488 [1:1000] (ab150077, ABCAM LTD). Stained sections were imaged at 40x using confocal microscopy, processing Z-stacks into maximum-intensity projections to visualize all tissue depths of fluorescent regions of interest (ROIs), and image analysis using ImageJ and the Colocalization Finder plugin.

#### **4.2.5 Power Analysis**

For the WT/KO dataset (N = 44), the Wald Chi-Square was  $\chi^2 = 17.6$  (df = 5,  $p < 0.001$ ), yielding an effect size of  $f^2 = 0.40$ , which resulted in 87.2% power at  $\alpha = 0.05$ . For the KI dataset (N = 24), the Wald Chi-Square was  $\chi^2 = 13.7$  (df = 3,  $p < 0.001$ ), yielding an effect size of  $f^2 = 0.57$ , achieving 81.3% power at  $\alpha = 0.05$ .

## 4.3 Results

### 4.3.1 Seizure Latency and Duration Is Unaffected by Treatment or MC4R knockout

We first asked whether our treatment differentially affected seizure induction in any of our groups. To do this, we analyzed seizure latency and duration. The mean latency and duration of seizures, along with their standard errors of the mean (SEM), were calculated for each group: WT ELS Vehicle (Latency:  $344.73 \pm 7.62$  s, Duration:  $68.06 \pm 1.57$  s), WT ELS ACTH (Latency:  $298.52 \pm 7.06$  s, Duration:  $72.97 \pm 1.66$  s), KO ELS Vehicle (Latency:  $326.77 \pm 9.59$  s, Duration:  $80.88 \pm 3.47$  s), KO ELS ACTH (Latency:  $314.71 \pm 9.69$  s, Duration:  $75.55 \pm 2.31$  s). Cox Proportional-Hazards analysis was employed to assess the impact of treatment and genotype on seizure latency and duration, adjusting for multiple measurements per animal and day-specific effects. For seizure latency, the analysis revealed no significant effect of treatment ( $p = 0.73$ , Cox Proportional-Hazards) or genotype ( $p = 0.81$ , Cox Proportional-Hazards) across days (Figure 4.1A). For seizure duration, the analysis showed no significant effect of treatment ( $p = 0.16$ , Cox Proportional-Hazards) or genotype ( $p = 0.22$ , Cox Proportional-Hazards) across days (Figure 4.1B). Overall, our findings suggest that neither treatment nor genotype significantly influenced seizure latency or duration when adjusted for day-specific effects and multiple measurements per animal.

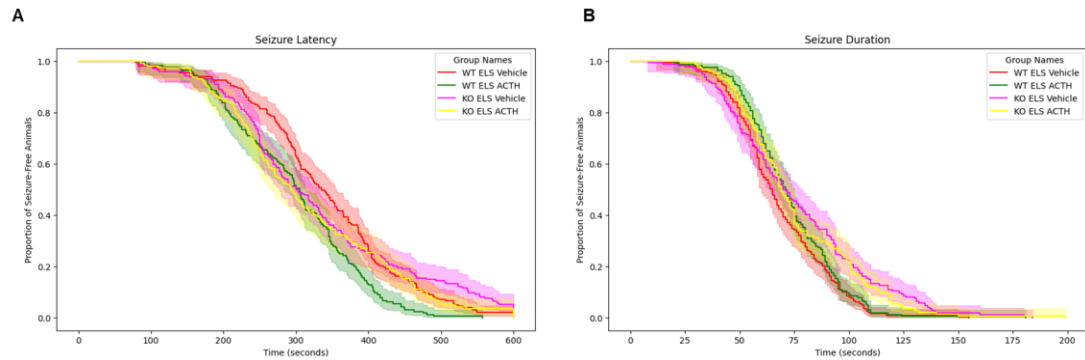


Figure 4.1: Seizure parameters are not altered by ACTH treatments  
 Treatment with ACTH does not alter latency to flurothyl seizure compared to vehicle-treatment groups across the different genotypes (A). Similarly, treatment with ACTH did not significantly alter seizure duration across different genotypes (B).

#### 4.3.2 ELS Did Not Affect Exploration and Spontaneous Activity in Open Field Task

The open field behavior test was conducted to assess spontaneous activity and exploration behavior in the experimental groups. This task measures the time spent in the center of the open field, the number of entries into the center, and the total distance traveled. These parameters provide insights into the animals' willingness to explore a new environment and their activity. There were no significant differences in the time spent in the center of the open field between the control ( $140.7 \pm 17$  ms), vehicle-treated ELS ( $145.9 \pm 22$  ms), and ACTH-treated ELS ( $166.5 \pm 25$  ms) ( $p > 0.05$ , GEE) (Figure 4.2A). Similarly, the number of entries into the center did not differ significantly between the groups ( $p > 0.05$ , GEE) (Figure 4.2B). Lastly, there was no significant variation in the total distance traveled by the animals across the different groups ( $p > 0.05$ , GEE) (Figure 4.2C). These results indicate that neither treatment nor genotype had a significant effect on spontaneous activity or exploration in the open field task (genotype\*treatment effect,  $p > 0.05$ , GEE).

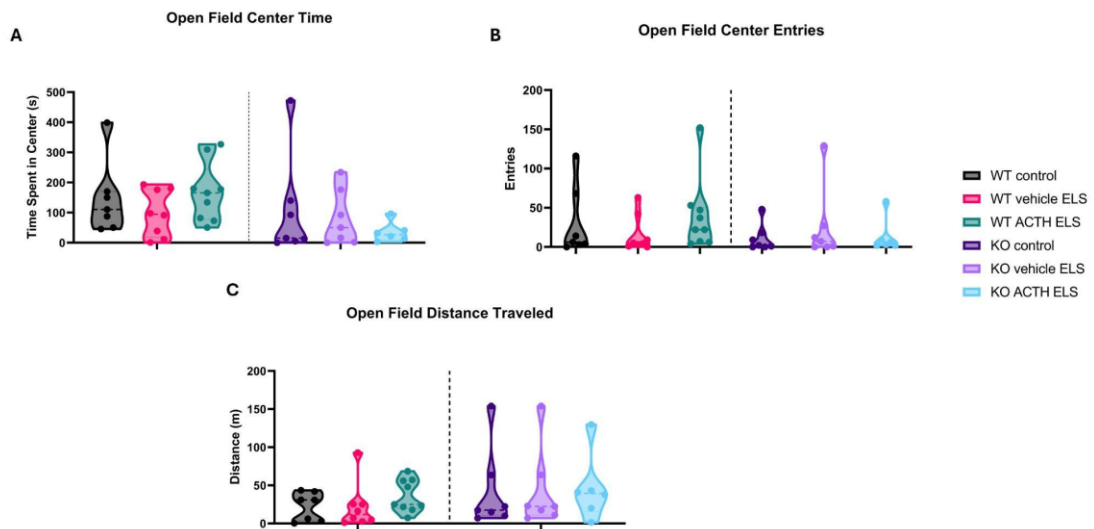


Figure 4.2. No behavioral differences in open field task parameters

There were no significant differences in the time spent in the center of the open field between the WT and KO groups (A). Similarly, the number of entries into the center did not differ significantly between the WT and KO groups (B). The total distance traveled by the subjects also showed no significant variation across the WT and KO groups (C).

### 4.3.3 ACTH Ameliorates Anxiety in Light/Dark Box Task

The light/dark box task was conducted to specifically assess anxiety-related behavior in the experimental groups. This task measures the time spent in the light zone of a box with both lighted and dark chambers, based on the natural aversion of rodents to brightly lit areas. Increased time in the light zone indicates reduced anxiety. Unlike the open field task, which primarily measures general locomotor activity and exploration, the light/dark box task is more sensitive to detecting anxiety-related behaviors.

WT vehicle-treated ELS mice spent significantly less time in the light zone compared to the WT controls (Figure 4.3;  $p = 0.005$ , GEE). Interestingly, ACTH was able to ameliorate the anxiety in mice with a history of ELS. ACTH-treated ELS mice

spent significantly more time in the light zone compared to the vehicle-treated group ( $p = 0.00049$ , GEE). Similarly to the WT group, the MC4R KO vehicle-treated ELS spent significantly less time in the light zone compared to MC4R KO controls ( $p = 0.003$ , GEE), however, ACTH treatment was not able to ameliorate the anxiety ( $p = 0.005$  to KO control group) indicating a MC4R-dependent mechanism for this amelioration, with a significant genotype\*treatment effect ( $p = 0.000061$ , GEE).

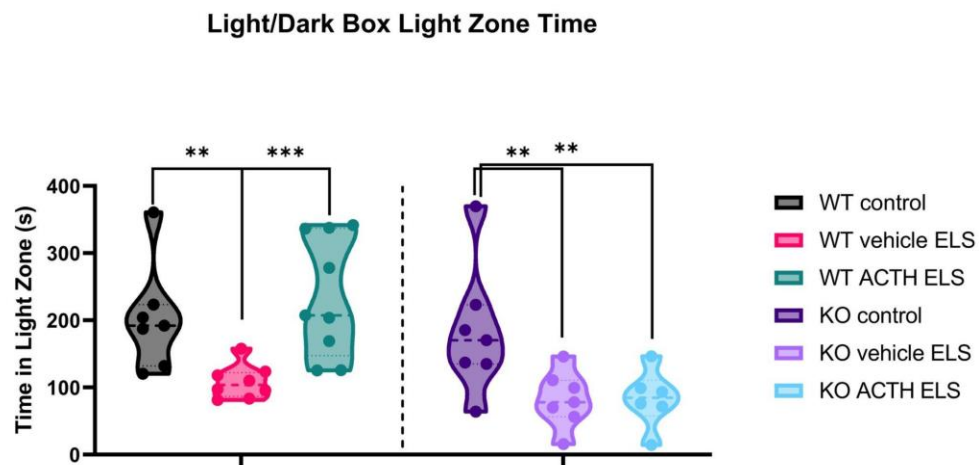


Figure 4.3. ACTH ameliorates the anxiety phenotype in mice with ELS

The light/dark box task was used to assess anxiety-related behavior by measuring the time spent in the light zone and the number of entries into the light zone. WT ELS mice treated with ACTH spent significantly more time in the light zone compared to WT ELS vehicle-treated mice. ACTH did not rescue the anxiety phenotype in MC4R KO ELS ACTH-treated mice compared to MC4R KO ELS vehicle-treated mice.

#### 4.3.4 Acute astrocyte dysfunction in the prefrontal cortex and hippocampus after recurrent early life seizures

Extensive research has focused on neuronal function, neuronal alterations and their long-term consequences following early life seizures. For instance, it was shown

that early life seizures can disrupt the hippocampal-prefrontal cortex network and lead to cognitive deficits and psychiatric-like manifestations<sup>471</sup>. It was further shown that these deficits and manifestations occur due to changes in synaptic plasticity, such as an aberrant increase in long-term potentiation (LTP), rather than neuronal loss<sup>471</sup>. Other studies have also demonstrated that ELS does not result in cell death however it causes alterations in short- and long-term plasticity<sup>41,472</sup> and reduced neurogenesis<sup>473–477</sup>. In addition to that, after ELS there is a decrease in inhibitory currents in hippocampus and neocortex, and hyperexcitation in neocortex<sup>39,478</sup>. While much is known about the neuronal alterations following ELS, there remains a significant gap in our understanding of astrocytic responses, their contributions to early life epilepsy and seizures, and their modulation of the MC4R effect. To address this gap, we used immunohistochemistry to examine acute astrocyte protein expression in the prefrontal cortex and hippocampus after ELS with and without ACTH treatment as astrocytes are involved in various neuroprotective and neuroinflammatory processes that could influence seizure outcomes (Figure 4.4A). 48 hours after seizures, we saw a significant increase in GFAP expression in both brain regions ( $p=0.048$ , GEE) (Figure 4.4B, C), indicating enhanced astrocytic activation and gliosis. We also saw a significant decrease in AQP4 expression in both brain regions after ELS ( $p=0.003$ , GEE) (Figure 4.4B, C). Dysregulation of AQP4 has been linked to increased seizure susceptibility through astrocyte proliferation, hypertrophy, impaired water balance, and edema<sup>370–372,432–434</sup>. The results suggest that ELS is associated with astrocytic dysfunction. ACTH treatment was able to recover GFAP and AQP4 levels. These findings highlight the acute impact of ELS on astrocytic populations and the potential of ACTH treatment to mitigate these effects.

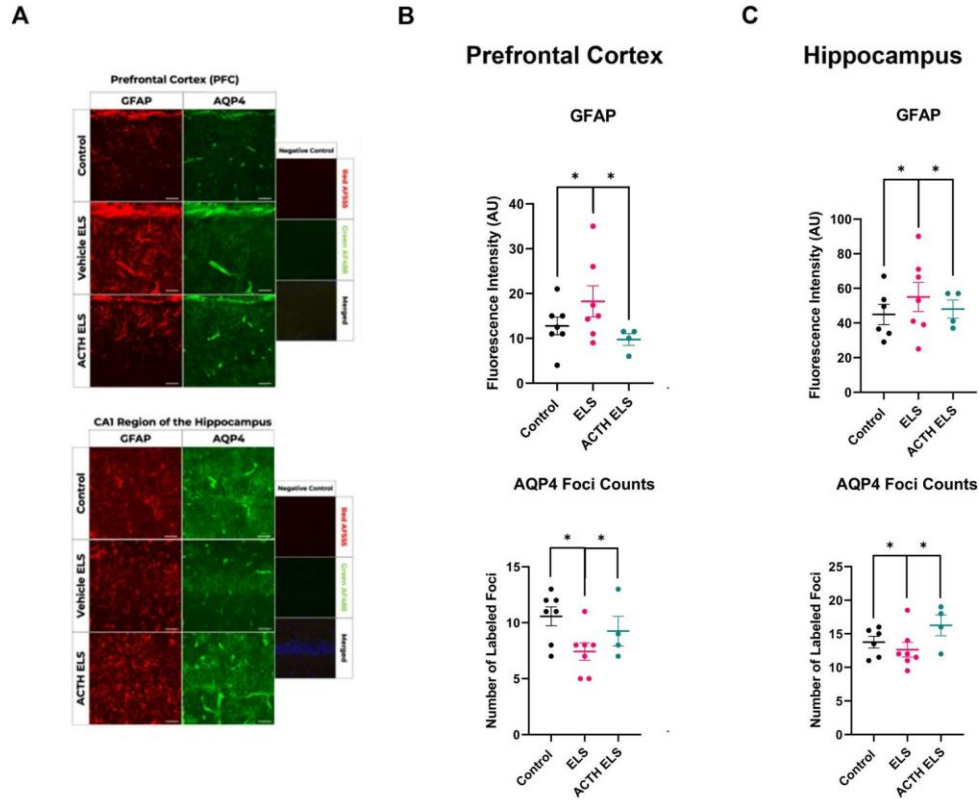


Figure 4.4. ACTH mitigates the astrocytic dysfunction in mice with ELS  
 Immunohistochemistry assessed astrocytic dysfunction after early life seizures (A). Mice treated with ACTH showed a recovery in astrocytic function. ACTH normalized GFAP and AQP4 levels in the PFC after early life seizures (B, C). ACTH normalized GFAP and AQP4 levels in the HC after early life seizures (B, C).

#### 4.3.5 Cell-type specific re-expression of MC4R in neurons and astrocytes

Given that astrocyte protein expression was altered after ELS and that MC4Rs are expressed in both neurons and astrocytes, we asked whether MC4Rs in these cell types differentially contribute to anxiety prevention following ELS. We therefore generated knock-in (KI) mice by re-expressing MC4R in either neurons or astrocytes, followed by ELS and ACTH treatment. We emphasize that the GFAP-Cre line used

here has been shown to colocalize specifically with GFAP+ astrocytes in multiple brain regions<sup>466-468</sup>, and the Syn1-Cre line exhibits robust Cre expression in neurons<sup>469,470</sup>. Although no Cre driver is 100% cell-type restricted, these lines are widely regarded as reliable tools to target neurons or astrocytes, respectively, with extensive published evidence, particularly lineage-tracing and immunohistochemical analyses, demonstrating minimal off-target expression<sup>479</sup>. By using these well-characterized lines, we minimized potential confounds arising from ectopic recombination and effectively isolated the roles of neuronal vs. astrocytic MC4R in our ELS model.

KI of the receptor did not change seizure parameters, and there were no significant effects of treatment ( $p = 0.68$  for latency and  $p = 0.40$  for duration, GEE) on either the astrocyte- or neuron- re-expression group (Figure 4.5A, B GFAP KI ELS Vehicle latency:  $309.29 \pm 9.28$  s, duration:  $79.02 \pm 2.33$  s; GFAP KI ELS ACTH Latency:  $317.83 \pm 10.86$  s, Duration:  $78.50 \pm 2.64$  s; Syn1 KI ELS Vehicle latency:  $332.98 \pm 8.89$  s, duration:  $82.04 \pm 2.21$  s; and Syn1 KI ELS ACTH latency:  $347.32 \pm 8.04$  s, duration:  $85.19 \pm 2.14$  s).

We saw no significant differences in time spent in the center (Figure 4.5C), number of entries to the center (Figure 4.5D) or the total distance traveled (Figure 4.5E) between the vehicle-treated and ACTH-treated ELS knock-in (KI) groups in the open field. It is important to note that the vehicle-treated groups represent two distinct Cre+ genotypes: Syn1-Cre+ for neuronal MC4R re-expression and GFAP-Cre+ for astrocytic MC4R re-expression. Although both are vehicle-treated, they differ in the promoter driving Cre (Syn1 vs. GFAP), which can possibly introduce baseline behavioral differences. However, our analysis uses genotype and treatment as factors

to account for these baseline differences with no significant difference between the vehicle-treated ELS KI groups for center entries (GEE,  $p=0.758634$ ), distance (GEE,  $p=0.063050$ ) or time in light zone (GEE,  $p=0.727150$ ). A significant genotype\*treatment effect ( $p=0.000006$ , GEE) for open field center entries, indicating that the treatment differentially affected the two reexpression groups. Post-hoc comparisons show that treatment with ACTH in animals where MC4Rs were re-expressed in astrocytes was significantly associated with an increase in the number of center entries compared to MC4R neuron KI groups ( $p=0.00000374$  to syn1-cre ELS vehicle and  $p=0.000154$  to syn1-cre ELS ACTH groups).

In the light/dark box task, ACTH treatment decreased anxiety in both the animals with MC4R re-expressed in neurons and animals with the receptor re-expressed in astrocytes (Figure 4.5F). Neuronal KI ELS mice treated with ACTH showed a significant increase in light zone time compared to neuronal KI mice treated with vehicle ( $p=0.034$ , GEE). Similarly, the astrocyte KI ACTH-treated mice spent more time in the light zone compared to the vehicle-treated astrocyte KI ELS mice ( $p=0.006$ , GEE). Notably, there is a genotype\*treatment effect ( $p=0.00089$ , GEE) for the light zone time. This was again driven by the ACTH-treated animals in the astrocyte-reexpression group, whose time spent in the light zone was significantly higher than all other groups ( $p<0.001$ , GEE). This suggests that re-expression in astrocytes was more effective at recovering the treatment effect than reexpression in neurons.

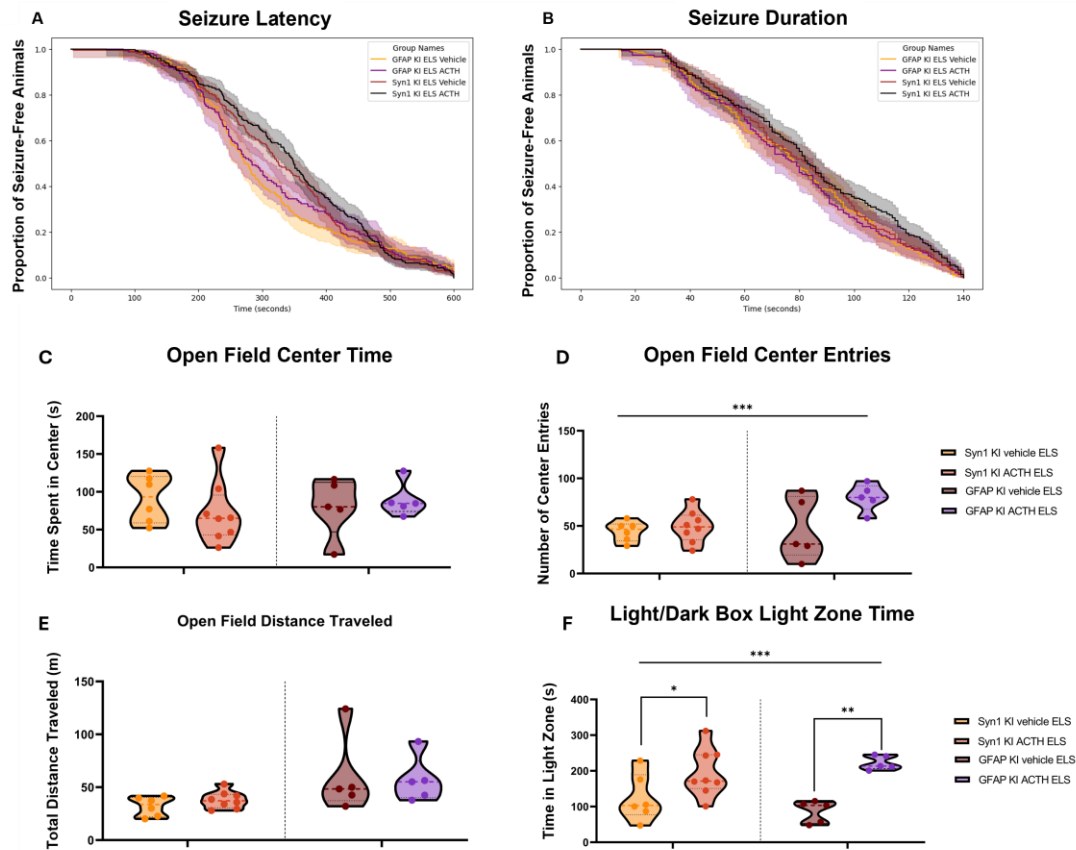


Figure 4.5. ACTH-treated KI mice with ELS show less anxiety compared to vehicle-treated mice with no differences in seizure parameters or spontaneous activity.

Survival analysis plot indicates no differences in latency to tonic-clonic seizure between animals with MC4R re-expression in astrocytes and without treatment with ACTH (yellow vs purple line and envelope) or animals with MC4R re-expression in neurons with and without treatment with ACTH (red vs blue line) (A). Similarly, treatment with ACTH did not significantly alter seizure duration in different groups of KI mice (B). There were no significant differences in the time spent in the center of the open field between the vehicle treated and ACTH treated KI ELS groups (C). Similarly, the number of entries into the center did not differ significantly between the vehicle treated and ACTH treated KI ELS groups, however, there is a genotype\*treatment effect with post-hoc comparisons showing that treatment with ACTH in MC4R astrocyte KI animals was significantly associated with an increase in the number of center entries compared to other groups (D). The total distance traveled by the subjects also showed no significant variation across the vehicle

treated and ACTH treated KI ELS groups (E). Both KI ELS mice treated with ACTH spent significantly more time in the light zone compared to KI ELS vehicle-treated mice, however there is a genotype\*treatment effect with post-hoc comparisons showing that treatment with ACTH in MC4R astrocyte KI animals was significantly associated with an increase in the time spent in the light zone compared to other groups (F).

#### 4.4 Discussion

The present study aimed to elucidate the mechanism by which ACTH can improve psychiatric comorbidities after ELS. Deficits are a well-documented consequence of ELS, with up to 65% of patients experiencing impairments in anxiety, learning, memory, and executive function<sup>34,453–455,480,481</sup>. These deficits are particularly concerning as they can persist into adulthood, significantly impacting quality of life<sup>34,453–455,481</sup>. Traditional anti-seizure medications primarily focus on controlling seizure activity but do not address these cognitive comorbidities associated with epilepsy<sup>38,453,456</sup>. This gap in treatment highlights the need for therapeutic strategies that can mitigate these cognitive comorbidities. Our study investigated ACTH's effect on anxiety, showing MC4R-dependent improvements, which challenge the notion that ACTH's primary effects are mediated through MC2Rs in the adrenal cortex for systemic glucocorticoid release<sup>346,461</sup>. In support of actions above and beyond corticosteroids, we previously showed that dexamethasone treatment failed to recapitulate the positive effects on behavior seen with ACTH treatment<sup>339</sup> and that ACTH, but not dexamethasone, normalizes gene expression after ELS with no effects of ACTH on seizure parameters<sup>339,462</sup>.

ACTH belongs to the melanocortin family of neuropeptide hormones, all derived from proopiomelanocortin (POMC), and binds with varying affinity to melanocortin receptors (MCRs). MC2R is exclusively activated by ACTH, while the

other 4 receptors respond to both ACTH and other POMC peptides, with different binding affinities. These G protein-coupled receptors also exhibit distinct tissue distributions and functions<sup>339,345,463,464,482</sup>. In the brain, melanocortin receptor MC4R was shown to have important roles in the pathophysiology of various neurological disorders like Alzheimer's disease and cerebral ischemia. Activation of MC4R has been shown to promote neuroprotection and enhance cognitive function through multiple mechanisms. It was previously demonstrated that melanocortins protect against the progression of Alzheimer's disease in triple-transgenic mice (3xTg); the study found that treatment with  $\alpha$ -melanocyte-stimulating hormone (NDP- $\alpha$ -MSH) reduced cerebral cortex and hippocampus phosphorylation levels of amyloid/tau cascade proteins, inflammation, and apoptosis. Treated mice demonstrated decreased neuronal loss and improved learning and memory<sup>357</sup>. Another study, utilizing the TgCRND8 Alzheimer's disease mouse model, found that  $\alpha$ -MSH treatment prevents GABAergic neuronal loss and improves cognitive function. Treated mice exhibited improved spatial memory and reduced anxiety during the Y-maze task<sup>359</sup>. In the context of cerebral ischemia, MC4R agonists counteract late inflammatory and apoptotic responses post-ischemia in a transient global brain ischemia model. Treatment with MC4R agonists reduced the levels of pro-inflammatory cytokines and apoptosis markers, leading to enhanced neuronal survival and functionality further improving cognitive performance in Morris Water Maze task<sup>356</sup>.

Furthermore, other studies demonstrated that activating MC4R has an impact on neuronal viability and synaptic plasticity.  $\alpha$ -MSH treatment was shown to rescue neurons from excitotoxic cell death following kainic acid-induced damage resulting in a significantly higher number of viable neurons in the hippocampal CA1 pyramidal

cell layer<sup>360</sup>. Moreover, activation of MC4R enhanced synaptic plasticity by increasing the number of mature dendritic spines and enhancing the surface expression of AMPA receptor subunit GluA1 mediating neurotransmission enhancement and hippocampal long-term potentiation<sup>362</sup>.

In our study, ACTH treatment administered 1 hour before each seizure day did not alter seizure latency or duration, which shows that ACTH's therapeutic effects extend beyond seizure modification and are likely mediated by MC4R pathways unrelated to seizure modulation<sup>338,339</sup>. This finding challenges the prevailing assumption that deficits after ELS are a result of the seizures themselves.

The open field task results indicated that ELS did not significantly affect general locomotor activity or exploration behavior, as there were no differences in time spent in the center, number of entries into the center, or total distance traveled across the groups. This suggests that ELS and subsequent ACTH treatment do not impact the animals' general activity levels or willingness to explore a new environment. In contrast, the light/dark box task revealed significant anxiety-related behaviors in ELS mice, which were ameliorated by ACTH treatment. WT ELS mice exhibited increased anxiety, spending less time in the light zone compared to controls. ACTH treatment significantly reduced this anxiety-like behavior, indicating its potential therapeutic effect. However, in MC4R KO mice, ACTH treatment did not ameliorate anxiety, showing that the anxiolytic effects of ACTH are mediated through MC4R signaling pathways.

Immunohistochemistry staining was performed for important astrocytic proteins like GFAP and AQP4. The selected proteins play an essential role in astrocytic function and were shown to be altered in epilepsy. Astrocytes, glial cells in

the brain, play a critical role in supporting neuronal function, modulating synaptic transmission and maintaining homeostasis within the central nervous system<sup>368–370</sup>. In epilepsy, astrocytes undergo significant alterations affecting astrocyte channels, transporters, and metabolism which are directly linked to epileptogenesis<sup>427,483,484</sup>. Specifically, disruptions in potassium, and water homeostasis, contribute to the seizure predisposition, epilepsy onset and the hyperexcitability characteristic of epilepsy<sup>465,485,486</sup>. Furthermore, astrocytes' role in synchronizing neuronal activity and regulating synaptic transmission and plasticity, by releasing transmitters and maintaining calcium signaling, makes them essential for cognitive and psychiatric functions like learning, memory and stress responses<sup>368,369,487–489</sup>. Disruptions in astrocyte function have also been linked to mood and cognitive disturbances, suggesting that interventions restoring astrocyte homeostasis could alleviate diverse neuropsychiatric symptoms<sup>487,488,490</sup>. Prolonged stimulation of hippocampal astrocytes, for instance, has been found to impair spatial memory, and working memory, indicating that astrocytic reactivity can negatively impact cognitive function<sup>413,491</sup>. However, sufficient activation of hippocampal astrocytes led to enhanced calcium activity sufficient to induce long-term potentiation (LTP) which is a cellular correlate of learning and memory. Mice performing contextual fear conditioning and T-maze tasks and undergoing hippocampal astrocyte activation during the acquisition phase demonstrated an improved memory recall in both tasks the following day<sup>490</sup>. Furthermore, another study showed that inhibition of activated astrocytes after inflammation was able to ameliorate anxiety and depressive-like behaviors induced by lipopolysaccharide in addition to decreasing GFAP and increasing BDNF levels in the

brain<sup>492</sup>. These studies highlight the importance of astrocyte homeostasis and the important role of astrocytes in neuropsychiatric deficits.

Increased levels of GFAP is observed in epilepsy and is indicative of astrogliosis<sup>370,372</sup>. AQP4 is a water channel protein involved in water homeostasis and balancing potassium concentration and its altered expression can lead to disrupted water regulation which is linked to increased worsened seizure activity<sup>433,434</sup>. This shows the importance of these proteins for proper astrocytic function.

Our immunohistochemistry staining analysis demonstrated significant astrocytic dysfunction in both the prefrontal cortex and hippocampus following ELS, as evidenced by increased GFAP levels and decreased AQP4 expression 48 hours after the last seizure. While direct evidence linking MC4R activation to changes in GFAP or AQP4 in epilepsy models is scarce, melanocortin signaling, including MC4R activation, exert anti-inflammatory and astrocytic modulation in CNS disease<sup>440,483</sup> opening an important question about the effect of MC4R activation on astrocytic protein expression normalization. GFAP upregulation and AQP4 dysregulation are hallmark features of astrocyte reactivity that can exacerbate seizure susceptibility and neural dysfunction. Thus, it is plausible that MC4R-dependent astrocyte modulation underlies the normalization of GFAP and AQP4 we observed<sup>493</sup>. First, MC4R is G-coupled, elevating intracellular cAMP upon activation, which can regulate downstream signaling cascades that modulate glial inflammation and gliosis<sup>440,483,494,495</sup>. Second, changes in cAMP-dependent pathways have been shown to affect astrocytic hypertrophy and the expression of intermediate filaments, including GFAP<sup>377,496-498</sup>. Third, water-channel proteins like AQP4 can be influenced by signaling events that also involve cAMP-regulated transcription factors<sup>499,500</sup>. Indeed,

ACTH treatment effectively normalized both markers, suggesting its potential to mitigate acute astrocytic dysfunction induced by ELS. The recovery of these astrocytic markers highlights the therapeutic potential of ACTH in restoring normal astrocytic function and, by extension, improving neural homeostasis.

The changes in astrocyte protein expression after ELS and the ability of ACTH to improve chronic anxiety in WT mice but not in KO mice, raised a question about the impact of neuronal and glial MC4R expression on ACTH positive effects. To address the question of cell-specific expression of MC4R, we re-expressed the MC4R selectively into neuronal populations or astrocytic populations. We observed that KI mice did not show significant differences in open field parameters. However, the significant genotype\*treatment effect for the number of entries, with the GFAP KI\*ACTH treatment showing a significant effect compared to the groups with MC4R neuron re-expression, highlights that the genotype influences the ACTH's effect on exploration and activity levels in the open field. In the light/dark box task, anxiety-like behaviors decreased in both Syn1 KI and GFAP KI mice treated with ACTH. Notably, the significant genotype\*treatment effect for the light zone time, with the GFAP KI\*ACTH treatment showing a significant effect compared to all other groups, suggests that the effect of treatment on reducing anxiety was more pronounced in the GFAP KI genotype group. This supports the role of MC4R in both neuronal and astrocytic populations in modulating anxiety responses following ELS, however, the expression of MC4R in astrocytes appears to have a greater impact, with less anxiety, after ELS compared to its expression in neurons.

Our findings highlight the complex interplay between ELS, astrocytic function, and behavioral outcomes. ACTH treatment, while not influencing seizure parameters

directly, shows promise in reducing ELS-associated anxiety and astrocytic dysfunction. Future research should explore precise mechanisms underlying ACTH's therapeutic effects.

## Chapter 5

### NETWORK ABNORMALITIES UNDERLYING COGNITIVE IMPAIRMENT AFTER EARLY LIFE SEIZURES ARE NORMALIZED WITH ACTH TREATMENT

#### 5.1 Introduction

The developmental period is a highly vulnerable phase for the brain, during which insults such as maternal immune activation, ischemia, traumatic brain injury or seizures are associated with disruptions in the maturing brain and can lead to enduring cognitive and behavioral deficits<sup>1-14</sup>. Understanding how early life insults alter brain function is crucial for mitigating long-term consequences. Acute recurrent early-life seizures (ELS) coinciding with critical windows of neural network formation can have enduring negative consequences on learning and memory<sup>26-28</sup>.

Experimental recurrent ELS have demonstrated definitively that there is a relationship between this early life insult, network dysfunction and abnormal cognitive performance across a range of tasks<sup>40,41,339,501</sup>, underscoring the importance of interventions that address the downstream consequences after acute ELS, which can reshape developing neural circuits<sup>38,163,168,502</sup>. Recent studies in animal models have begun to emphasize the importance of network-level exploration in understanding neuronal connectivity and firing pattern changes after early insults<sup>37,38,43,119,171</sup>. Abnormal neuronal firing rates, temporal coding patterns and population-level dynamics across multiple brain regions are all implicated in ELS<sup>37,40,41</sup>, ultimately affecting the circuits that support cognition. Consequently, interventions that either

prevent circuit disruption or promote circuit reorganization may prove effective in mitigating long-term cognitive deficits associated with ELS. However, these interventions remain understudied and poorly tested, particularly regarding their effectiveness in preventing network-level disruptions and rescuing subsequent cognitive deficits<sup>31,38,43,339</sup>.

Adrenocorticotrophic hormone (ACTH), a melanocortin peptide, is a promising neuroprotective therapy against these network disruptions that, intriguingly, has positive effects on cognitive deficits after ELS without altering seizure parameters<sup>339,503</sup>. While the canonical mechanism of action of ACTH is thought to be through glucocorticoid production via the melanocortin-2 receptor (MC2R), data suggest that ACTH also influences neural circuits directly via other melanocortin receptors<sup>339,440,503,504</sup>. We and others have previously shown that melanocortin-4 receptor (MC4R) expressed in the brain has been linked to neuroprotection, synaptic plasticity, and astrocyte function<sup>339,362,440,503</sup> and that ACTH depends on the MC4R pathway for its neuroprotective effects<sup>503</sup>. However, the network-level mechanisms of these effects remain poorly understood.

To understand these consequences, we focused on circuits within the prefrontal cortex (PFC), a brain region critical for higher-order cognitive functions including emotional regulation, learning, decision-making, and extinction of aversive memories<sup>505</sup>. Importantly, impairments in PFC-dependent cognitive functions are commonly observed following ELS and parallel deficits in humans, contributing to poor quality of life across multiple neuropsychiatric conditions including epilepsy, anxiety disorders, and post-traumatic stress disorder<sup>26,506-511</sup>. Thus, elucidating how

ACTH protection of PFC network organization against ELS-induced disruptions has significant translational relevance for improving patient outcomes.

In classical fear conditioning, the medial PFC (mPFC), especially the prelimbic region, plays an important role in fear extinction by helping the brain relearn that a previously threatening cue is now safe<sup>512,513</sup>. Fear extinction is not mediated by a single region but rather by a coordinated activity across a distributed network involving the mPFC, basolateral amygdala (BLA), and hippocampus<sup>505,514</sup>. Within this circuit, the BLA helps encode both the original fear and the extinction process, the hippocampus provides context to help the brain distinguish between safe and threatening environments, and the mPFC modulates the activity of the amygdala and adjusts its firing patterns in response to changes in emotional context, supporting flexible adapting behavior<sup>515-517</sup>. Hence, successful extinction requires dynamic, flexible modulation of population-level firing patterns and synchronized activity across these structures to modulate the acquisition and expression of fear<sup>518,519</sup>. Disrupting this coordinated network activity by ELS can interfere with the extinction learning by impairing firing flexibility and functional connectivity between PFC and downstream regions<sup>514,518,520</sup>. Such impairments in extinction are seen in multiple neuropsychiatric conditions, including post-traumatic stress disorder, anxiety disorders, and epilepsy, all of which share deficits in network-level flexibility and circuit reorganization<sup>511,520,521</sup>. Thus, examining PFC network changes and their impact on fear extinction offers a valuable window into cognitive disruptions of early life neurological insults.

In this study, we investigated long-term disruptions to PFC networks associated with ELS, and how ACTH is protective against these disruptions at both

single-neuron and neuronal population levels, focusing on how these changes affect fear extinction learning. By integrating single-unit recordings, and network analyses during baseline behavior and during fear conditioning, we show that early ACTH administration not only protects against ELS-induced network disruptions in mPFC, but also prevents fear extinction deficits. Our findings demonstrate 1) that fear extinction learning requires changes in population coding and connectivity in the mPFC, 2) recurrent ELS impairs fear extinction learning by reducing functional connectivity over the learning timescale, and 3) early administration of ACTH leads to long term neuroprotection at the network level, normalizing both neuronal firing patterns and network cohesion in the PFC, thereby improving learning and memory in animals with a history of ELS. Importantly, using a Graph Neural Network (GNN) trained on network features during the extinction task, we show that connectivity metrics are not only different between the groups but they also predict extinction learning outcomes, demonstrating the functional significance of these network-level changes and how they are required for successful learning. Our findings identify a key network mechanism of fear extinction learning and underscore the crucial value of interventions targeting broader network reorganization as a means to improve cognitive outcomes after early life insults such as ELS.

## **5.2 Methods**

### **5.2.1 Animals**

Male and female C57BL/6J (strain#:000664) mice from The Jackson Laboratory were used in all experiments. To reduce confounding variability, littermates were used whenever possible. All mice were housed in the same animal

room under a 12-hr light-dark cycle with *ad libitum* access to food and water. Environmental conditions, including temperature and humidity, were kept consistent, with identical bedding and enrichment across all cages. Each cage housed 3-5 mice of the same sex to minimize social stress. Following tetrode implantation, animals were singly housed to ensure post-surgical recovery.

### **5.2.2 Early Life Seizure Animals**

Wild type C57BL/6J mice were divided into three groups: control vehicle-treated, vehicle-treated ELS, and ACTH-treated ELS (N = 8 control vehicle-treated, N = 10 vehicle-treated ELS, N = 10 ACTH-treated ELS).

### **5.2.3 Electrode Implantation**

At p45, mice were implanted with custom 3D printed four drivable tetrodes placed into the prelimbic mPFC (+2.5 A/P and +0.5 M/L), ground wire and a reference wire placed above the cerebellar parenchyma, to record LFPs and single units. A 3 mm burr hole drilled above the mPFC, allows for electrodes to be descended into the prelimbic mPFC. The implant is glued and cemented to the skull followed by a 3 days recovery period. Electrodes were advanced 20 $\mu$ m for each recording session to ensure that different populations of neurons are being sampled during baseline. After identifying and recording PFC cells during baseline, PFC cells will be recorded during behavioral tasks.

### **5.2.4 Single Neuron Recording**

Electrodes signals were preamplified and transmitted to the Neuralynx recording system (Neuralynx, Bozeman, MT). Single neuron action potentials are identified after the signal is filtered between 500-9000 Hz and thresholded for  $3\times$  root

mean square (RMS) noise. Action potentials were then clustered and evaluated for quality control using L-ratio and isolation distance in SpikeSort3D. Number of recorded cells for each group during baseline is the following: control group (n=8, 125 cells), vehicle-treated ELS group (n=10, 138 cells) and ACTH-treated ELS group (n=10, 150 cells). The number of recorded cells for each group during fear extinction is the following: control group (n=7, 65 cells), vehicle-treated ELS group (n=7, 69 cells) and ACTH-treated ELS group (n=6, 59 cells).

### 5.2.5 Generalized Linear Modeling:

The clustered action potentials were used for further analysis through a generalized linear model (GLM). GLM is used to quantify in vivo neural dynamics in healthy and early life seizure mice. Through GLM, we are able to investigate the rate, temporal and population modulation of neurons<sup>522</sup>.

- i. **Rate modulation** investigates the rate of neuron firing with respect to an event. Peri-stimulus histograms (PSTHs) were performed for fear extinction modeling of firing rates with respect to tones.
- ii. **Temporal modulation** investigates how the neuron firing is modulated over time with respect to LFP firing. Post-spike filters (PSFs) will estimate the effect of past spikes on current spike probability or fine spike timing and it is crucial for understanding the temporal dynamics of neuronal firing.
- iii. **Population modulation** looks at how ensembles of neurons fire together.

### 5.2.6 Post-spike filters (PSFs) generation:

A PSF is a mathematical function that represents the probability density of a neuron firing an action potential or spike as a function of time after it has previously fired<sup>522</sup>. To generate PSFs, we started by analyzing the spike train of each neuron. Given that the refractory period of a neuron is approximately 2 ms, we used a 1 ms bin

size to create a binned spike train, ensuring no more than one spike per bin. This binned spike train is modeled as a Poisson process, from which we derive the probability density function that maximizes the likelihood of observing the given spike train. To account for post-spike rate modulation (auto-correlation), we modeled the spike rate  $\lambda(t)$  as:

$$\lambda(t) = \lambda_0 \exp(psf_i \times \rho^{hist}) \times t \quad (4.1)$$

- where  $(\rho^{hist})$  denotes the spiking history of the neuron, and  $(psf_i)$  is the post-spike filter encoding the firing rate modulation after a spike.

The filters were parameterized using 10 raised cosine basis functions and include an immediate post-spike impulse to capture the refractory period<sup>523</sup>. A ridge penalty was then added to the log-likelihood function to avoid overfitting<sup>524</sup>. The resulting PSFs are computed for a maximum time bin of 662 ms, resulting in a 662-component vector for each post-spike filter. This process is implemented using MATLAB.

After PSFs are implemented, principal component analysis will be performed to establish the first principal component (PC1) to investigate fine spike timing heterogeneity within the recorded brain region; thus, providing a reliable readout of the neural network.

### 5.2.7 Principal Component Analysis (PCA)

Principal Component Analysis (PCA) is a statistical technique used to reduce the dimensionality of large datasets while preserving as much variability as possible. After generating the post-spike filters (PSFs) for each neuron, PCA is applied to these filters to identify the main patterns of variability in the neuronal firing data. The PSFs,

represented as 662-component vectors, form a high-dimensional dataset that is complex to analyze directly. PCA transforms this dataset into a new coordinate system defined by the principal components (PCs), which are orthogonal directions capturing the maximum variance in the data.

The first principal component (PC1) captures the largest amount of variance. By projecting the PSFs onto these principal components, we can reduce the dataset to a lower-dimensional space, typically focusing on the first few PCs that capture the most significant patterns. This reduction simplifies the analysis and visualization of the data, allowing us to investigate fine spike timing heterogeneity within the recorded brain region. The PCA-transformed data provides a reliable readout of the neural network's activity, highlighting key differences and similarities in neuronal firing patterns across different conditions or groups. This process is implemented using MATLAB, ensuring precise and efficient computation of the principal components.

### **5.2.8 PSTH Construction and Firing Rate Percentage Change Analysis**

To analyze neuronal firing rate dynamics during fear extinction learning, we constructed peri-stimulus time histograms (PSTHs) and computed the percentage change in firing rate relative to baseline for two segments of the extinction session: the first 10 tones (early learning phase) and the last 10 tones (late learning phase).

Baseline firing rates were calculated using spike timestamps within the pre-tone preceding the onset of the first tone. The firing rate during this baseline period was determined by dividing the number of spikes by the duration. This baseline firing rate served as the reference point for calculating percentage changes in subsequent analyses.

To construct the PSTH, spike data were segmented into 3-second time bins corresponding to tone and no-tone periods. For each bin, the number of spikes was counted and normalized to compute the firing rate (spikes per second).

For each time bin, the percentage change in firing rate relative to baseline was calculated using the formula:

$$PercentageChange = \left( \frac{Firing\ Rate\ in\ Bin - Baseline\ Firing\ Rate}{Baseline\ Firing\ Rate} \right) \times 100 \quad (4.2)$$

In addition to bin-wise PSTH analysis, we calculated the overall percentage change in firing rate for each tone and no-tone segment. PSTHs were visualized as bar graphs, with firing rate values plotted for each bin. Tone periods were highlighted with yellow shading, and the baseline period was shaded in light blue. Green bars represented firing rates during tone periods, while blue bars corresponded to no-tone periods. Confidence intervals (95%) for mean percentage changes were computed and displayed for each experimental group to facilitate comparisons. The analysis was implemented in Python utilizing python NumPy, Matplotlib, and Pandas packages.

### **5.2.9 Graph Metrics Analysis for Baseline and Fear Extinction**

To analyze neural activity and brain network evolution during baseline and fear extinction tasks, we utilized a graph metrics-based approach. Graph networks were constructed independently for the baseline session and for the first and last segments of the fear extinction session. In these networks, individual neurons were represented as nodes, and functional connectivity between neurons was represented by edge weights. Edge weights were determined using the dot product of neurons' firing rates across a sliding window consisting of three consecutive data points, advancing

one data point at a time. The mean value across all sliding windows was then calculated for each neuron pair to establish the final network connectivity.

Once the networks were constructed, we performed several analyses to understand the functional connectivity and network properties.

- i. **Edge weights** represent the functional connectivity strength between pairs of neurons were computed as:

$$\omega_{ij} = \frac{1}{n} \sum_{k=1}^n (f_i^k \cdot f_j^k) \quad (4.3)$$

- where  $f_i^k$  and  $f_j^k$  are the firing rates of neurons i and j in window k, and n is the total number of sliding windows. Higher edge weights indicate stronger functional connectivity between the neuron pairs, reflecting greater synchronization of their activity.

- ii. **Weighted degree centrality** reflects the overall connectivity of a neuron within the network, considering both the number and strength of its connections. For a neuron i, it is defined as:

$$Degree_i = \sum_{j \in N(i)} \omega_{ij} \quad (4.4)$$

- where  $\omega_{ij}$  is the weight of the edge between neurons i and j, and  $N(i)$  is the set of neighbors of neuron i.

To enable comparison across networks of different sizes, the weighted degree centrality was normalized:

$$Normalized\ Degree_i = \frac{Degree_i}{|N|} \quad (4.5)$$

- where  $|N|$  is the total number of neurons in the network.

Higher values of weighted degree centrality indicate neurons that are highly connected within the network, both in terms of the number and strength of connections, emphasizing their central role in network communication.

- iii. **Weighted clustering coefficient** quantifies the tendency of neurons to form densely interconnected clusters, was computed as:

$$C_i = \frac{\sum_{j,k \in N(i)} (\omega_{ij} \cdot \omega_{ik} \cdot \omega_{ki})^{1/3}}{k_i \cdot (k_i - 1)} \quad (4.6)$$

- where  $\omega_{ij}$ ,  $\omega_{ik}$ , and  $\omega_{ki}$  are the weights of the edges forming a triangle involving neuron  $i$ ,  $k_i$  is the degree of neuron  $i$  (number of neighbors), and  $N(i)$  is the set of neighbors of neuron  $i$ .

Higher values of  $C_i$  indicate that the neuron participates in stronger and denser clusters within the network.

- iv. **Eigenvector centrality** was used to quantify the influence of individual neurons within the network, determined by their connectivity to other influential neurons. This metric assigns a score to each node ( $i$ ) based on the centrality of its connected nodes, defined as:

$$x_i = \lambda \sum_{j \in N(i)} \omega_{ij} x_j \quad (4.7)$$

- where  $x_i$  represents the eigenvector centrality of node  $i$ ,  $\omega_{ij}$  is the weight of the edge between nodes  $i$  and  $j$ ,  $N(i)$  is the set of neighbors of node  $i$ , and  $\lambda$  is the largest eigenvalue of the adjacency matrix.

The equation is solved iteratively, normalizing the centrality values such that higher scores indicate nodes that are connected to other highly central nodes. Eigenvector centrality was calculated using the NetworkX Python library, which applies spectral decomposition methods to compute the centrality scores.

v. **Network Efficiency Metrics**

1. Global Efficiency

Global efficiency ( $E_{glob}$ ), assessing the integration and efficient information transfer across the network, was computed as the average inverse shortest path length between all node pairs:

$$E_{glob} = \frac{1}{n(n-1)} \sum_{i \neq j} \frac{1}{d_{ij}} \quad (4.8)$$

- where  $d_{ij}$  is the shortest path length between nodes  $i$  and  $j$ . Nodes that are not connected (i.e.,  $d_{ij}=\infty$ ) were excluded from the calculation. Higher global efficiency values indicate a more integrated and efficient network.

## 2. Local Efficiency

Local efficiency ( $E_{loc}$ ) measures the fault tolerance and robustness of network communication within localized node neighborhoods:

$$E_{loc(v)} = \frac{1}{|N(v)|(|N(v)-1|)} \sum_{i \neq j \in N(v)} \frac{1}{d_{ij}} \quad (4.9)$$

- where  $N(v)$  is the set of neighbors of node  $v$ , and  $d_{ij}$  is the shortest path length between nodes  $i$  and  $j$  within the subgraph induced by  $N(v)$ .

The overall local efficiency of the graph is the average of  $E_{loc(v)}$  over all nodes:

$$E_{loc} = \frac{1}{n} \sum_{v \in G} E_{loc(v)} \quad (4.10)$$

## 3. Analysis Workflow

Weighted, undirected graphs were constructed for each animal and segment using normalized edge weights. To account for the importance of stronger connections, weights were inverted (1-weight) to represent path lengths. Global and local efficiency were computed using the NetworkX library in Python, and all calculations were based on the largest connected component of each graph to ensure consistency.

### **5.2.10 Graph Neural Network (GNN) Analysis for Predicting Behavioral Outcomes**

We implemented a Graph Neural Network (GNN) using a Graph Attention Network (GAT) architecture to predict behavioral outcomes (percentage freezing) from neuronal network features and functional connectivity during the fear extinction task. In this approach, each neuron was represented as a node, and functional connectivity between neuron pairs, serving as edges, was computed as the mean dot product of neurons' firing rates across sliding windows throughout each recorded segment. Neuronal features included the firing rate, mean interspike interval (mISI), maximum ISI (max ISI), coefficient of variation (CV) of ISI, and principal component (PC1 and PC2) scores of the post-spike filters. Graphs were constructed for the first and last segments of the extinction session.

The GAT model consisted of three attention layers: two hidden layers using rectified linear unit (ReLU) activations and a final output layer with a sigmoid activation output scaled from 0 to 100% to match the behavioral outcome (percentage freezing). Model regularization techniques included dropout (optimized range: 0.1–0.5), weight decay (set at  $1e-5$ ), and a cosine annealing learning rate scheduler to enhance generalization and prevent overfitting. Hyperparameter optimization with hidden channel sizes (64, 128, 256), dropout rates, learning rates (0.01, 0.001, 0.0001), and attention heads (1-4) was performed using Optuna's grid search sampler, evaluating different combinations of hyperparameters. For robust optimization, optimal hyperparameters were selected based on minimal combined validation loss and maximal  $R^2$  scores through a 5-fold cross-validation scheme.

After optimization, model performance was rigorously assessed using Leave-One-Out Cross-Validation (LOOCV), ensuring robust generalization to unseen

animals. Training efficacy and model convergence were monitored by plotting average training and validation loss curves across folds (Figure 5.1). Predictive performance was assessed using the coefficient of determination ( $R^2$ ), computed as:

$$R^2 = 1 - \frac{\sum(y_{true} - y_{pred})^2}{\sum(y_{true} - \bar{y})^2} \quad (4.11)$$

- where ( $y_{true}$ ) denotes actual freezing percentage, and ( $\bar{y}$ ) denotes their mean. An  $R^2$  greater than 0 indicates that the model explains variability better than predicting the mean outcome. An  $R^2$  of 0 indicates predictions are no better than the mean, while a negative  $R^2$  indicates the model performs worse than predicting the mean.

To interpret model predictions, feature importance scores were derived using the GNNExplainer algorithm, which assigns feature importance scores based on their influence on predictions.

As a comparative baseline, we employed linear regression with LOOCV using average neuronal features per animal, as this model cannot incorporate node-level features directly. Additionally, we performed Generalized Estimating Equations (GEE) analyses to identify significant features associated with behavioral outcomes across neurons, facilitating comparison between methods.

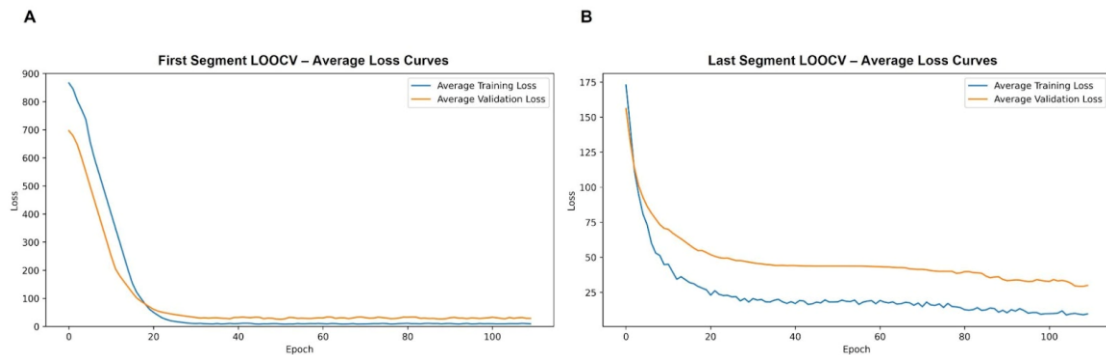


Figure 5.1: Average Training and Validation Loss Curves

Loss curves represent average training and validation losses across all Leave-One-Out Cross-Validation (LOOCV) folds for the GAT models trained to predict freezing behavior during the first segment (left panel) and last segment (right panel). The decrease and stabilization of both training and validation losses indicate successful optimization and model convergence.

### **5.2.11 Fear Conditioning**

At p55, mice (n=8 controls, n=10 vehicle-treated ELS and n=10 ACTH-treated ELS) performed a 2-day fear conditioning task.

- i. Fear acquisition takes place on day 1. During fear acquisition, mice are individually placed in an operant box. During the acquisition task, mice will experience four tone-shock pairings (28s tone followed by a 2s 0.25mA foot shock).
- ii. Fear extinction takes place on day 2. During fear extinction, mice are individually placed in the same operant box. During the extinction task, thirty 30s tones will be presented without shocks in random intervals. Mice will also be recorded for PFC cells during fear extinction. During both days, mice are video recorded and freezing time is quantified using ANY-maze. Scores were analyzed as a moving score ranging between 0 (total freezing) and 1 (total movement) or percentage freezing (0-100%).

### **5.2.12 Power Analysis**

For the dataset (N = 28), the Wald Chi-Square was  $\chi^2 = 13.546$  (df = 2,  $p < 0.001$ ), yielding an effect size of  $f^2 = 0.521$ . This resulted in an 87.88% power at  $\alpha = 0.05$ , indicating a high likelihood of detecting true group differences.

## 5.3 Results

### 5.3.1 ACTH Protects Fear Extinction Learning in Mice After ELS

The fear conditioning task is a PFC- dependent task, performed to assess fear learning acquisition and fear extinction. From postnatal day (P) 10- P14, 20 animals underwent 20 flurothyl-induced seizures with a 7% mortality rate. 10 of these animals received vehicle treatment and 10 received ACTH treatment. The 20 seizure animals, in addition to 8 control vehicle treated animals, performed the task at P55.

On day 1 during fear acquisition, all groups successfully learned the task as shown by increased freezing to the tone that is paired with a foot shock (Figure 5.2A; generalized estimating equations [GEE],  $p < 0.05$ ). There were no significant differences between the groups (GEE,  $p > 0.05$ ) and no significant effect of ELS or ACTH treatment (both GEE,  $p > 0.05$ ). On day 2, 24 hours after fear acquisition, the experimental groups performed the fear extinction component of the task. During this task, mice were exposed to a total of 30 tones without shocks and the percentage of time freezing throughout the session was assessed. Vehicle-treated ELS mice had a significant deficit in extinguishing the task as shown by the significantly higher freezing percentage by tone 30 (64.35%, IQR: 55.2%-73.5%) compared to the control group (44.4%, IQR: 34.1%-54.7%) (GEE,  $p = 0.00008$ ). However, ACTH-treated ELS mice successfully extinguished the task with a freezing percentage by tone 30 of 53.05% (IQR: 41.8%-64.3%), which was significantly lower than vehicle-treated ELS mice (GEE,  $p = 0.001$ ) and not significantly different from controls (Figure 5.2B; GEE,  $p = 0.4$ ).

Moreover, there was a group-by-time interaction effect (GEE,  $p = 0.00008$ ), so to further quantify the extinction rate, we analyzed block-level data, with each block

representing the average of 5 tones. In this analysis, we calculated the predicted mean freezing for each group at each block using the parameter estimates and determined the total decline from block 1 to block 6. The control group's freezing decreased from an estimated 86.9% at Block 1 to 44.2% at Block 6, with approximately 8.5% decrease per block. In the vehicle-treated ELS group, freezing decreased from 93.8% at Block 1 to 64.35% at Block 6, showing a 5.9% decrease per block, whereas in the ACTH-treated ELS group, the decline was from 91.9% to 53.5%, approximately 7.8% per block. Thus, while all groups exhibited significant extinction over blocks, the vehicle-treated group showed the slowest rate of decline, and ACTH-treated animals showed a rate that was intermediate but closer to the control group. These block-level findings corroborate the tone-level results and underscore that ACTH treatment partially restores the normal extinction rate following early-life seizures.

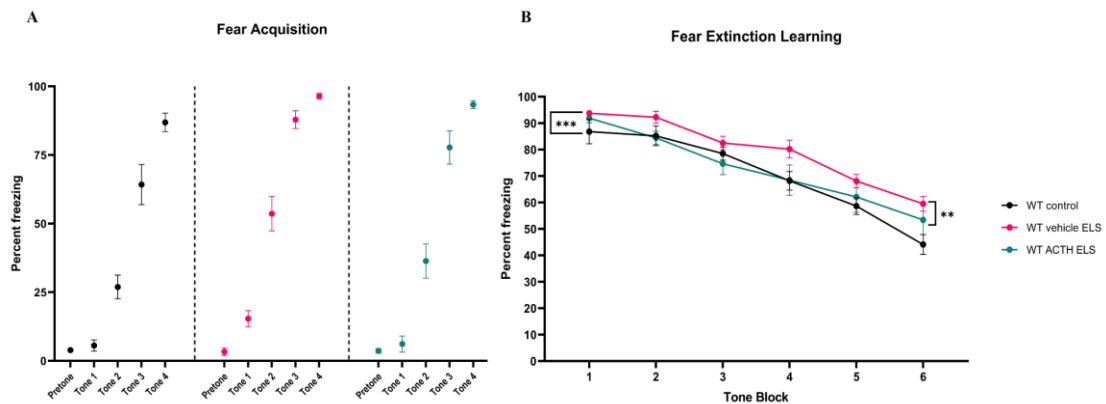


Figure 5.2: ACTH Improves Fear Extinction Deficit After ELS

All animals across all groups acquired the fear learning paradigm after two tone-shock pairings (A). However, vehicle-treated ELS animals (pink circles) had significant deficits performing the fear extinction part of the task compared to controls (black circles), even after 30 tones without shock pairing. Treatment with ACTH (teal circles) significantly prevented the fear extinction deficit in animals with a history of ELS (B).

### 5.3.2 ACTH Preserves Firing Rates During Baseline

8 control, 10 vehicle-treated ELS, and 10 ACTH-treated ELS animals were implanted with single-unit tetrodes and recorded at baseline when they were not engaged in any behavioral task. Single neuron recording shows a significant difference in the firing rate between the control (1.75 Hz, 95% CI [1.1714, 2.3210]) and vehicle-treated ELS group (0.98 Hz, 95% CI [0.86, 1.1042]) (GEE,  $p=0.01$ ). ACTH normalized the firing rate (1.73 Hz, 95% CI [1.15, 2.32]) compared to the vehicle-ELS group (Figure 5.3A; GEE,  $p=0.01$ ). There was no significant difference between the control and ACTH-treated group (GEE,  $p=1.0$ ). Further, there were no significant differences in the inter-spike intervals between the groups (Figure 5.3B; control vs ELS vehicle, GEE,  $p=0.6$  and ELS vehicle vs ELS ACTH, GEE,  $p=0.8$  and control vs ELS ACTH, GEE,  $p=0.9$ ).

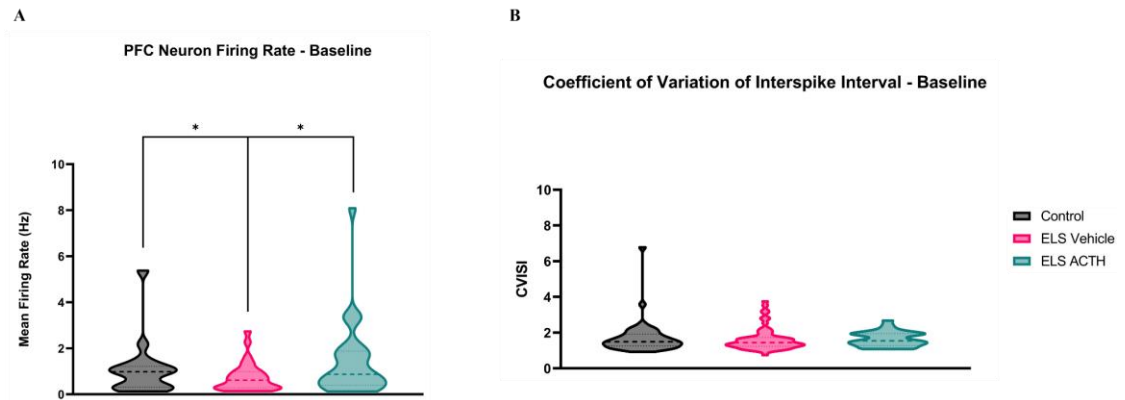


Figure 5.3: ACTH Normalizes Baseline Firing Rates of Prefrontal Cortex (PFC) Neurons at Baseline

PFC neurons from animals with a history of ELS showed a significant reduction in the mean firing rate compared to control animals. Treatment with ACTH normalized the decrease in firing rate (A). The coefficient of variation of interspike intervals did not differ significantly among control, ELS, and ACTH-treated groups (B).

### 5.3.3 ACTH Prevents Temporal Coding Deficits During Baseline

Neurons rely on the dynamic modulation of their firing probabilities to support complex cognitive processes such as learning and memory<sup>501,525,526</sup>. This plasticity in spike timing, often referred to as temporal coding, enables neurons to adapt their firing based on prior spiking activity. To model this temporal coding, we used a generalized linear model (GLM) that incorporates a neuron's past spiking history and refractory properties to estimate instantaneous firing probability<sup>37,522,523</sup>. From the GLM, we captured the properties of fine spike timing using a post-spike filter (PSF) for each neuron, which captures the temporal pattern of a neuron's likelihood of firing after an initial spike. Next, we applied principal component analysis (PCA) on all PSFs to identify the major dimensions of variation in firing patterns, focusing on the first principal component (PC1), which explained the greatest variance across neurons and was then used as a parameter in our statistical analyses. This gives us a robust, statistically principled, and data driven parameter to quantify fine spike timing.

Mean PSFs show group differences in the temporal shape of neuronal firing (Figure 5.5A). Vehicle-treated ELS neurons showed two firing peaks at approximately 42 ms and 120 ms after a spike (Figure 5.5A, middle panel). However, both Control (Figure 5.5A, top panel) and ACTH-treated ELS (Figure 5.5A, bottom panel) neurons showed an initial peak around 42 ms and a peak at around 120ms but with less amplitude and a smoother decay trajectory compared to the ELS vehicle group. To further illustrate these differences, heatmaps of post-spike filters sorted by PC1 score are provided in Figure 5.4.

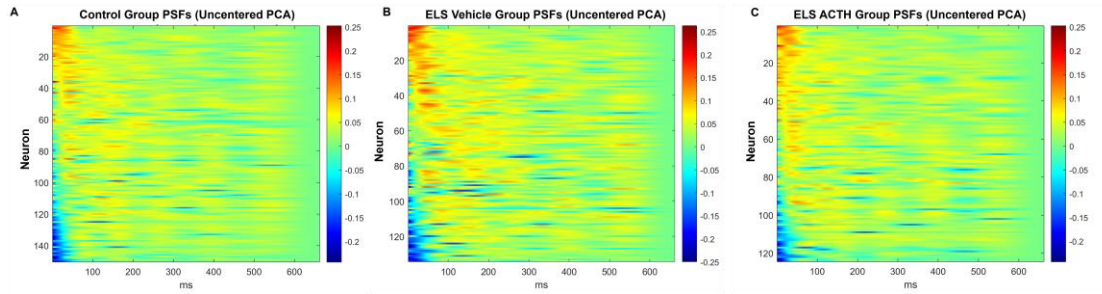
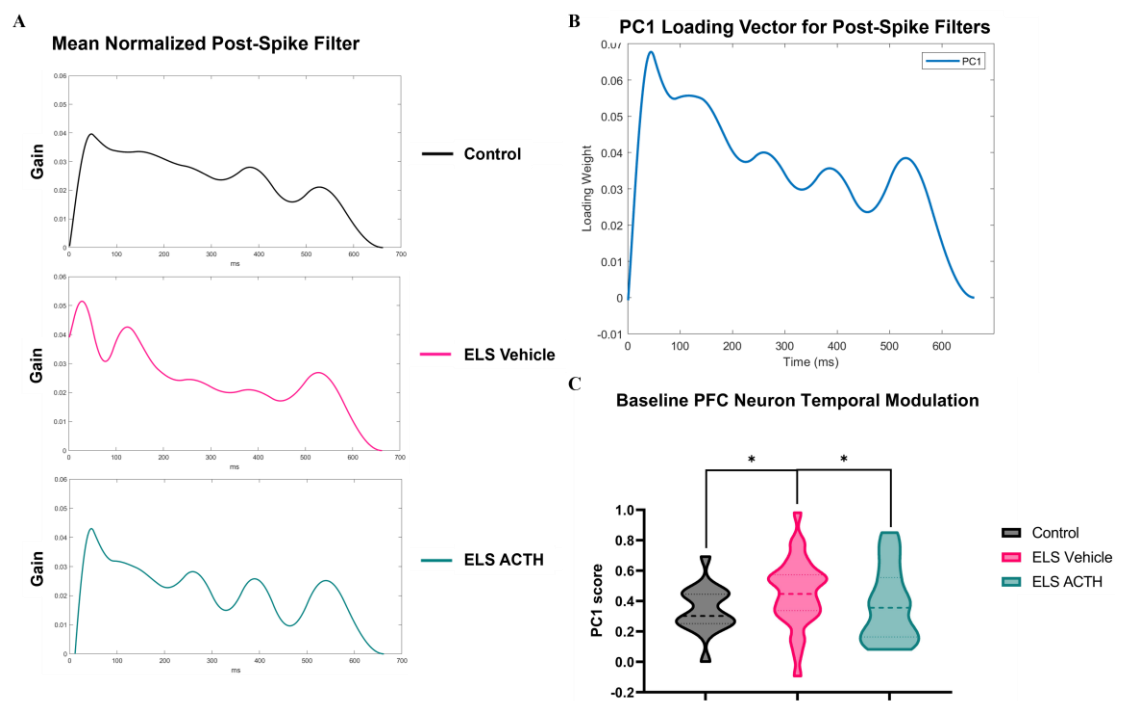


Figure 5.4: Heatmaps of post-spike filters (PSFs) sorted by PC1 score across groups. Post-spike filters (PSFs) from individual neurons are visualized as heatmaps and sorted by descending PC1 score within each group. Each row represents one neuron's normalized PSF over a 662 ms window following a spike, capturing its temporal modulation of excitability. Control neurons show heterogeneous but smooth post-spike decay patterns with moderate early beta-range and weak theta-range modulation (A). Vehicle-treated ELS neurons display prominent structure at around 42 and 120 ms, consistent with exaggerated beta and theta locking (B). ACTH-treated ELS neurons show a more variable and less structured temporal profile, close to the control group (C). These heatmaps highlight group-level differences in temporal coding and support the main findings presented in Figure 5.5.

Examination of the PC1 loading vector revealed two prominent features, an early peak at around 42 ms and a delayed rebound at around 120 ms (Figure 5.5B). The early peak corresponds to beta-range modulation (around 24 Hz), while the delayed peak aligns with theta-range activity (around 8.3 Hz). Notably, all groups exhibited this temporal structure, but the magnitude and prominence of these features differed significantly across the groups. ELS vehicle neurons exhibited stronger loading on both peaks, particularly the early beta component, indicating hypersynchrony and temporally rigid entrainment to fixed firing windows.

These dynamics were captured by the PC1 score which quantifies the neuron's alignment with the principal timing pattern seen in the loading vector. Vehicle-treated ELS neurons exhibited significantly higher PC1 scores (Figure 5.5C) compared to

Control (GEE,  $p = 0.037$ ) and ACTH-treated ELS mice (GEE,  $p = 0.025$ ), reflecting more flexible post-spike timing. Notably, ACTH treatment preserved PC1 scores at near-control levels (GEE,  $p = 0.81$ ), suggesting preserved temporal flexibility. These findings indicate that ACTH mitigates the ELS-induced shift toward a more rigid spike timing pattern, hence normalizing the temporal coding deficits in the mPFC at baseline.



**Figure 5.5: ACTH Preserves mPFC Neuron Temporal Coding After ELS**

Mean normalized PSF curves illustrate the probability of a neuron refiring over time after an initial spike. Vehicle-treated ELS neurons (pink line) displayed peaks at around 30 ms and 120 ms. However, control (black line) and ACTH-treated ELS (teal line) neurons show a peak at approximately 30 ms that gradually tapers (A). The first principal component (PC1) loading vector from the PCA on all individual PSFs reveals a pronounced positive bump near 120 ms (B). PCA analysis on the PSFs reveals that the vehicle-treated ELS group exhibits significantly higher PC1 scores compared to the control group. ACTH treatment

showed reduced scores to near-control levels, indicating a preservation of the firing repertoire disrupted by ELS (C).

#### **5.3.4 Population Dynamics Do Not Differ Between Groups at Baseline**

Population dynamics in the PFC are critical for supporting complex cognitive tasks such as decision-making, working memory, and executive control<sup>76,527–530</sup>. These tasks rely heavily on population coding where groups of neurons encode stimuli or task-related demands. Disruption of population coding could therefore compromise the neural representation of cognitive demands, potentially underlying the cognitive impairments following ELS. To evaluate if such network disruptions occur under baseline conditions with low cognitive demand, we assessed several well-established population-level network metrics. These metrics included edge weight, weighted degree centrality, weighted clustering coefficient, eigenvector centrality, global efficiency, and local efficiency, each quantifying distinct but complementary aspects of neural network function. Specifically, edge weights represent functional connectivity between neurons (Figure 5.6A). Weighted degree centrality assesses a neuron's overall connectivity strength within the network (Figure 5.6B), whereas the weighted clustering coefficient measures the tendency of neurons to form interconnected cohesive clusters (Figure 5.6C). Eigenvector centrality quantifies the influence of a neuron within a network based on the importance of its connections (Figure 5.6D). Global efficiency quantifies the overall ability of a network to transfer information (Figure 5.6E), and local efficiency measures the robustness of information transfer within local neuron neighborhoods (Figure 5.6F).

Our analysis revealed no significant differences between the groups in any of these baseline network metrics (GEE, all  $p > 0.05$ ; Figure 5.6A–F). The absence of baseline differences indicates that ELS-related network abnormalities are not

detectable under resting conditions alone. Rather, the network disruptions underlying cognitive deficits likely emerge specifically in response to cognitive demands. These findings highlight the importance of assessing network dynamics during active engagement with cognitively demanding tasks rather than solely at rest.

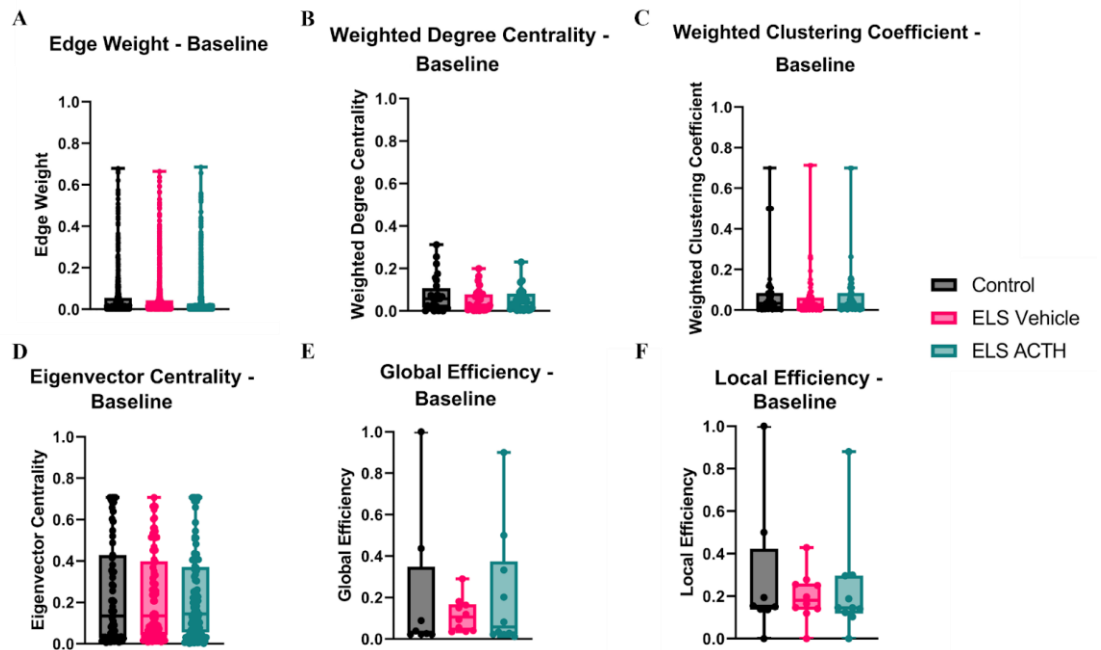


Figure 5.6: Network Metrics Show No Differences at Baseline After ELS

Analysis of PFC neural networks at baseline revealed no significant differences between control, ELS vehicle-treated, and ELS ACTH-treated animals across multiple network metrics. Edge weights (A), weighted degree centrality (B), and weighted clustering coefficient (C) showed no significant differences between the groups, suggesting no differences in functional connectivity, node importance, or network clustering propensity, respectively. Similarly, eigenvector centrality (D), global efficiency (E), and local efficiency (F) were not significantly different between the groups, indicating no difference in the network integration and communication efficiency at baseline. Collectively, these results suggest that network properties of PFC neurons are similar across all experimental groups at rest.

### 5.3.5 ACTH Conserves Rate Dynamics During Learning

We next explored how the brain network changes during fear extinction learning by quantifying the evolution of the brain network throughout the fear extinction session. To examine firing rate dynamics in response to tones, we quantified the neuron-tone response, defined as the change in neuronal firing rate during tone presentation relative to the pre-tone baseline. Peri-stimulus histograms (Figure 5.7A-C) were used to examine firing rate changes in response to tones, focusing on the first and last 10 tones of the 30-tone session (highlighted in yellow) compared to the pre-tone baseline (light blue). During the initial phase of extinction, the vehicle-treated ELS group exhibited a significant reduction in the neuron-tone response compared to the control group (87.97% vs. -6.52%, 95% CI [-2.12, 178.07] vs. [-13.00, -0.05]; GEE,  $p = 0.04$ ). However, ACTH treatment in the ELS group significantly increased the response compared to the vehicle-treated ELS group (15.53% vs. -6.52%, 95% CI [6.26, 24.82]; GEE,  $p = 0.0001$ ).

By the end of the session, firing rate dynamics had evolved across groups (Figure 5.7A-C, lower panels). However, a persistent deficit in the vehicle-treated ELS group was evident by the significantly reduced responses compared to the control group (127.44% vs. 20.61%, 95% CI [60.99, 193.91] vs. [-3.06, 44.29]; GEE,  $p = 0.003$ ). Importantly, ACTH treatment in the ELS group significantly increased responses compared to the vehicle treatment (105.32% vs. 20.61%, 95% CI [29.60, 181.04]; GEE,  $p = 0.04$ ), indicating that ACTH normalizes the deficits observed following ELS. These results indicate that while neuronal responses evolved throughout extinction, the vehicle-treated ELS group exhibited persistent deficits, whereas ACTH treatment normalized firing rate responses.

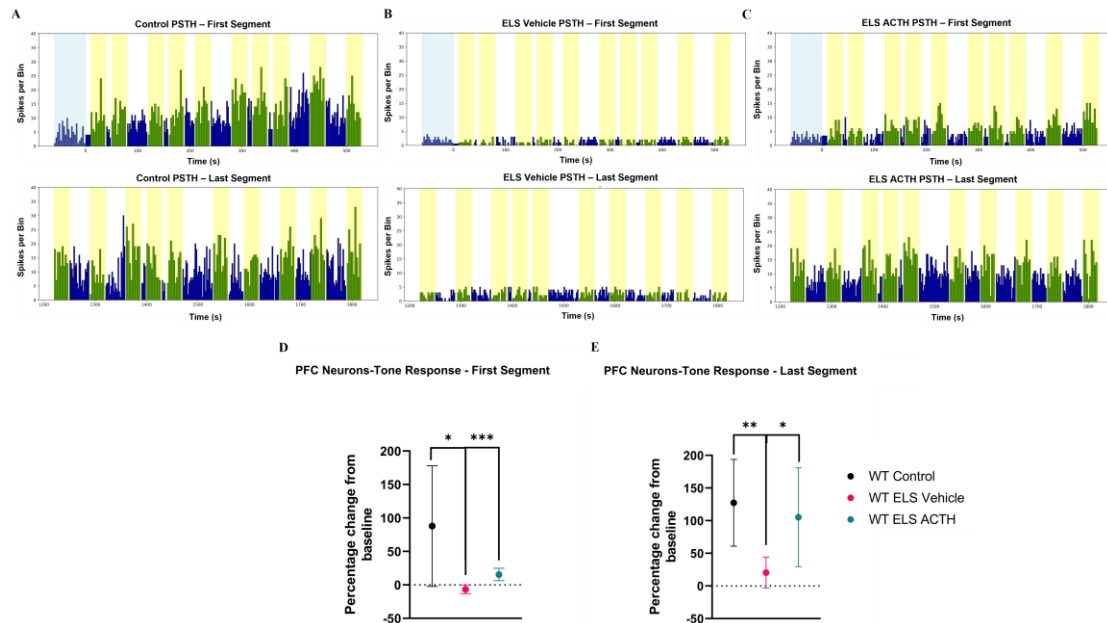


Figure 5.7: ACTH Treatment Preserves Neuronal Rate Dynamics During Extinction Learning

Peri-stimulus time histograms (PSTHs) of firing rate responses to tones during fear extinction learning in Control (A), ELS Vehicle (B), and ELS ACTH (C) groups. PSTHs are shown for the first 10 tones (upper panels) and the last 10 tones (lower panels) of the session. Yellow shading indicates tone presentation, and light blue shading indicates the pretone baseline in the first segment. Green bars represent firing during tone periods, and blue bars represent firing during non-tone periods. Quantification of percentage change in firing rate relative to baseline during the first (D) and last (E) 10 tones of the session across groups. Data are presented as mean  $\pm$  95% confidence intervals (CIs).

### 5.3.6 ACTH Preserves Population Dynamics During Learning

Investigating population dynamics is pivotal for elucidating neural mechanisms underlying cognitive tasks<sup>76,527–530</sup>. We investigated the same population metrics used at baseline at the beginning and end of fear extinction.

At the beginning of the fear extinction task, most network metrics, including edge weight, clustering coefficient, eigenvector centrality, and local and global efficiency, showed no significant differences across groups (GEE,  $p > 0.05$ ; Figure

5.8A, C-F), suggesting initially comparable network structures. However, weighted degree centrality was significantly lower in vehicle-treated ELS mice compared to control and ACTH-treated mice (Figure 5.8B), indicating early deficits in overall connectivity strength. During the last segment of the task, significant deficits across all metrics emerged in vehicle-treated ELS mice (Figure 5.8A-F), characterized by lower functional connectivity, reduced local cohesiveness, compromised influential node connectivity, and impaired global and local network efficiency. Importantly, ACTH treatment normalized these metrics at near control levels, highlighting the neuroprotective effect of ACTH against network-level disruptions following ELS. Results are summarized in Table 5.1.

To further explore relationships among these network metrics, correlation analyses were conducted separately for the initial and final segments of fear extinction (Figure 5.9). During the first segment, network metrics showed modest correlations. However, correlations among network metrics became more pronounced in the last segment, with strong positive correlations emerging between mean edge weight and eigenvector centrality ( $r=0.93$ ). Eigenvector centrality was strongly correlated with global efficiency ( $r=0.77$ ). Additionally, global and local efficiencies were highly correlated ( $r=0.84$ ). These enhanced correlations suggest that as extinction progressed, distinct network properties became increasingly coupled or coordinated, reflecting integrated changes from single-neuron interactions like edge weights to higher-order network properties like efficiency and centrality. This strengthened coupling among metrics likely represents an adaptive reconfiguration of network communication as the result of neuronal plasticity, facilitating efficient neuronal processing essential for successful extinction learning.

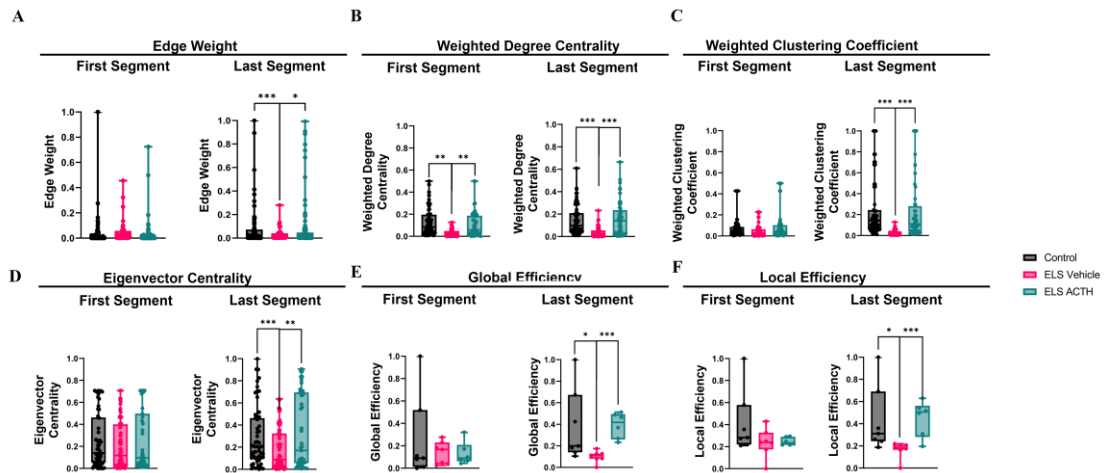


**Figure 5.8: ACTH Restores Network Properties During Fear Extinction Learning**  
 (A) Edge Weight represents the strength of functional connectivity between PFC neurons. No significant group differences (control in black, vehicle-treated ELS in pink, ACTH-treated ELS in teal) were observed in the first segment of the extinction session, but by the last segment, edge weights in the control and ACTH-treated ELS groups were significantly higher than in the vehicle-treated ELS group. (B) Weighted Degree Centrality assesses total connectivity, accounting for both the number and strength of a neuron's connections. Vehicle-treated ELS mice showed lower degree centrality relative to controls and ACTH-treated ELS mice in both the first and last segments, indicating persistent connectivity deficits in the vehicle-treated group that were rescued by ACTH. (C) Weighted Clustering Coefficient measures local network cohesiveness. Although no differences emerged in the first segment, the control and ACTH-treated ELS groups exhibited significantly higher clustering coefficients than vehicle-treated ELS mice by the end of the session, suggesting enhanced local connectivity with ACTH treatment. (D) Eigenvector Centrality quantifies each neuron's influence by weighting its connections to other highly connected neurons. All groups showed similar centrality in the first segment, but the control and ACTH-treated ELS groups exhibited a significant increase by the last segment compared to vehicle-treated ELS animals, suggesting that ACTH normalizes centrality properties critical for adaptive network function. (E) Global Efficiency reflects the ease of information flow throughout the entire network. In the first segment, no group differences were detected, however global efficiency in the vehicle-treated ELS group was significantly lower than that of control and ACTH-treated ELS mice by the end of the session, underscoring broader integration deficits in the vehicle-treated ELS group. (F) Local Efficiency is a measure of the

network's fault tolerance and communication within local neighborhoods of nodes. Similar local efficiency was observed initially across all groups, but the vehicle-treated ELS group's local efficiency was significantly lower than that of controls and ACTH-treated ELS mice in the last segment, suggesting that ACTH treatment enables effective local communication and resilience in PFC circuits.

Table 5.1: Summary of Network Metrics and Statistical Comparisons Across Groups

Network Metric	Segment	Vehicle vs. Control (p-value)	Vehicle vs. ACTH-treated ELS (p-value)	Group-by-Treatment Interaction (p-value)
Edge Weight	First	NS	NS	NS
	Last	0.0002	0.04	0.0002
Weighted Degree Centrality	First	0.006	0.001	0.001
	Last	0.0007	0.0003	0.0006
Weighted Clustering Coefficient	First	NS	NS	NS
	Last	0.0006	0.0005	0.00002
Eigenvector Centrality	First	NS	NS	NS
	Last	0.0004	0.007	0.0004
Global Efficiency	First	NS	NS	NS
	Last	0.010	0.0003	0.000001
Local Efficiency	First	NS	NS	NS
	Last	0.013	0.0003	0.0002

\*NS indicates not significant ( $p > 0.05$ ).

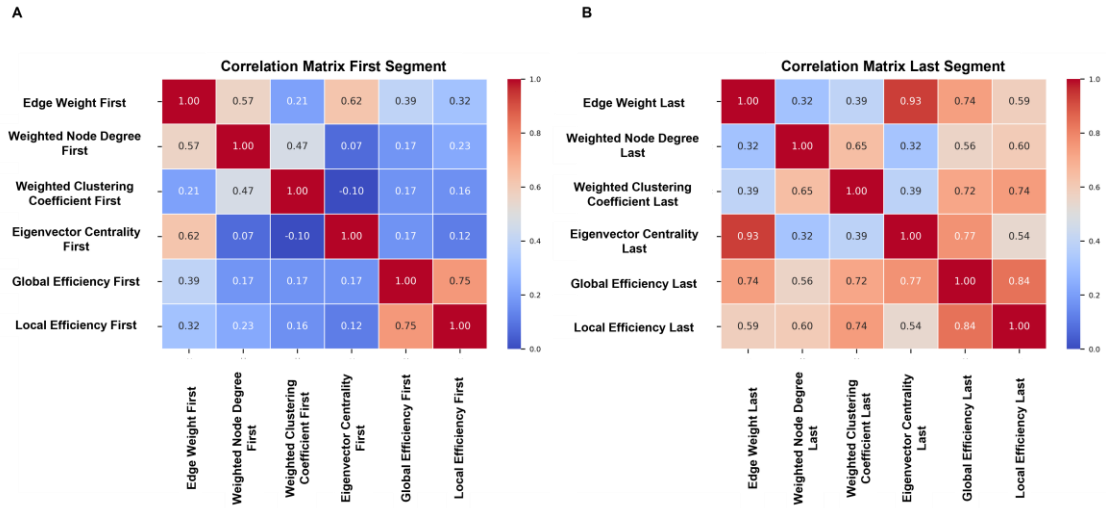


Figure 5.9: Spearman Correlation matrices of network metrics during fear extinction. Correlation matrices depicting associations between key network metrics at the first segment (left panel) and last segment (right panel) of fear extinction. Metrics include Edge Weight, Weighted Degree Centrality, Weighted Clustering Coefficient, Eigenvector Centrality, Global Efficiency, and Local Efficiency. During the initial segment, correlations were moderate, with edge weight correlating most strongly with weighted degree centrality. In the final segment, correlations among network metrics became notably stronger, highlighting the interdependent evolution of functional connectivity and network efficiency throughout extinction learning. Values indicate correlation coefficients, with color intensity proportional to correlation strength (red indicates positive correlations; blue indicates weak or negative correlations).

### 5.3.7 Neuron Features Can Predict Behavior Outcome

To move beyond traditional correlation-based analyses and assess how neural dynamics actively shape behavior, we implemented a Graph Neural Network (GNN). In this framework, each neuron recorded during the experiment is represented as a node, and edges capture functional connectivity between neuron pairs, defined by the dot product of their firing rates over a sliding window. This allows us to preserve the temporal evolution of network interactions within a graph structure. We then trained an optimized Graph Attention Network (GAT), which incorporates both node-level

neuronal features and dynamic connectivity patterns, to predict freezing behavior. This model not only captures the rich structure of population dynamics, but also offers a powerful tool to test whether and how features contribute to behavior. In doing so, it allows us to move closer to understanding network activity as a mechanistic driver of cognition, rather than a correlation.

The optimized GAT model effectively predicted freezing behavior during both first and last segments of fear extinction. The GAT achieved higher predictive performance compared to the linear regression baseline. Specifically, during the first segment, the GAT model achieved an  $R^2$  of 0.54 (Figure 5.10A), outperforming the linear regression's negative  $R^2$  of -0.24 (Figure 5.10C). In the last segment, the GAT showed further enhanced predictive capability, reaching an  $R^2$  of 0.81 (Figure 5.10B) compared to 0.28 by linear regression (Figure 5.10D). We further tested the model on permuted neuronal features or permuted behavior to make sure our model was learning from the real data instead of noise. Indeed, the predictability of the model significantly decreased with permuted features achieving an  $R^2$  of -1.40 and -0.73 (Figure 5.10E-F) and  $R^2$  of -1.58 and -1.02 (Figure 5.10G-H) with permuted behavior for first and last segments respectively.

Analysis of model feature importance using GNNExplainer identified maximum ISI, CV of ISI, and firing rate as highly influential features during the initial segment, aligning with GEE results. In the last segment, firing rate, maximum ISI, and PC scores emerged as critical predictors, also consistent with GEE findings. In contrast, linear regression identified significant effects only for maximum ISI and CV ISI in the initial segment and no significant predictors in the last segment, highlighting the limited capacity of linear regression to capture node-level network information.

These findings demonstrate that the optimized GAT model effectively bridges the analytical gap between the linear regression approach, predictive but lacking node-level integration, and the GEE method, node-level analytical power without predictive capacity, offering robust predictions alongside interpretable insights into network-level neural mechanisms underpinning fear extinction behavior. It further shows that permuting the neuronal features or behavioral data disrupts the model's converging capability leading to poor prediction which indicates that the model is predicting based on real data patterns rather than random noise.

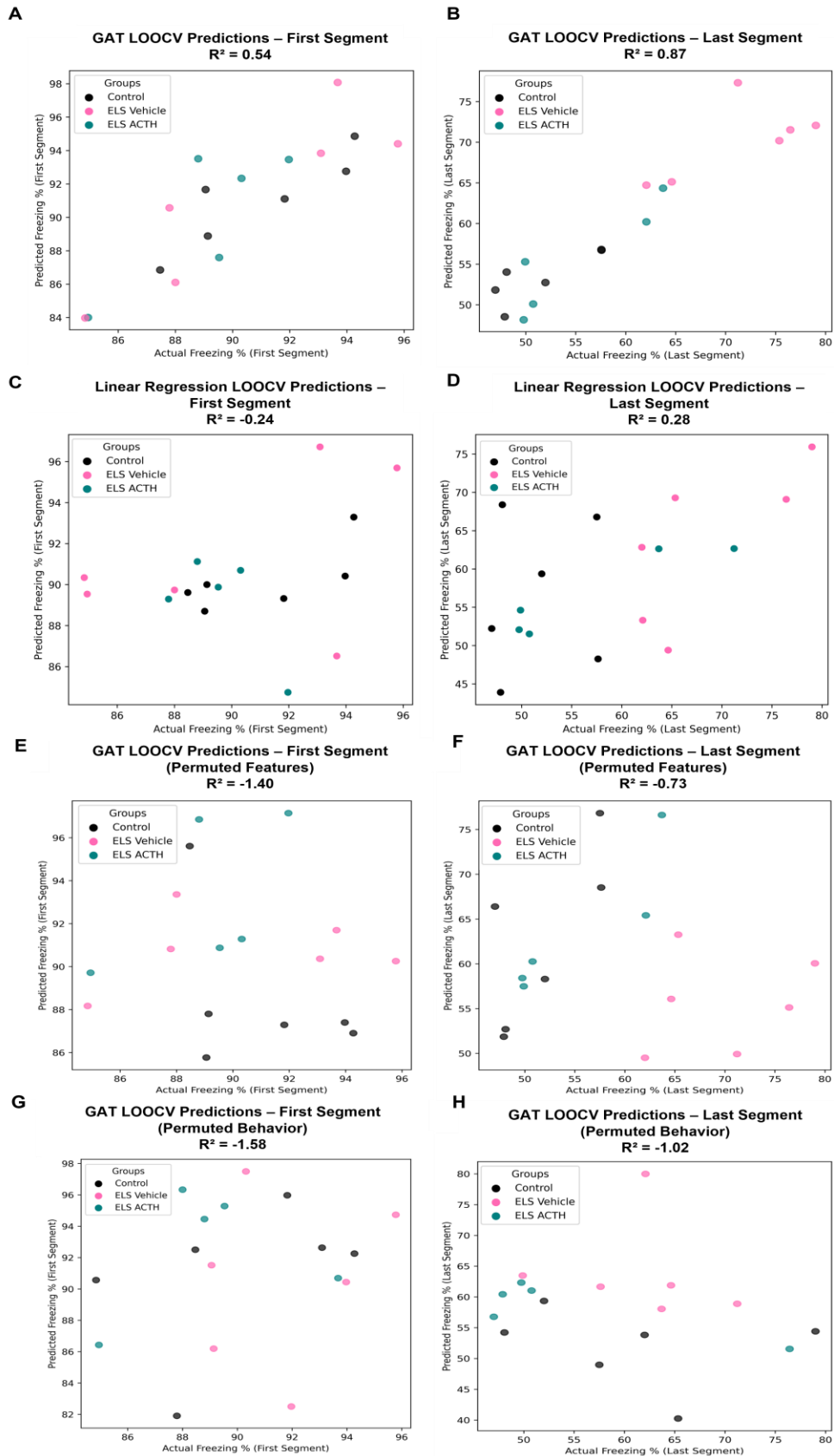


Figure 5.10: Predictive Performance of Graph Attention Network vs. Linear Regression Models.

Scatter plots show predicted versus actual freezing percentages for the first last segments of the fear extinction task. Predictions were generated using Leave-One-Out Cross-Validation (LOOCV). The optimized Graph Attention Network model outperformed linear regression by capturing node-level neuronal features and network connectivity, achieving an  $R^2$  of 0.54 during the first segment and 0.87 during the last segment(A-B). Linear regression predictions were notably less accurate, resulting in a negative  $R^2$  (-0.24) during the first segment and an  $R^2$  of 0.28 during the last segment(C-D). The Graph Attention Network model was further tested using permuted behavior or permuted features for each segment. Training the model on permuted neuronal features, achieved an  $R^2$  of -1.40 during the first segment and -0.73 during the last segment(E-F). Training the model on permuted behavior, achieved an  $R^2$  of -1.58 during the first segment and -1.02 during the last segment(G-H). Colors represent experimental groups: Control (black), Vehicle-treated ELS (pink), and ACTH-treated ELS (teal).Group-Level Network Dynamics at Baseline and During Fear Extinction

Baseline network analysis revealed no significant differences in PFC network properties between control, ELS vehicle-treated, and ELS ACTH-treated groups.

Baseline radar plot shows no significant group-level differences in terms of connectivity, clustering, integration, or efficiency, suggesting that network properties are initially similar when animals are at rest (Figure 5.11A).

During the fear extinction task, the network metrics indicate that at the beginning of the session before any learning has occurred, network properties are comparable across groups, except for significant reductions in overall connectivity in the vehicle-treated ELS group (Figure 5.11B). As the fear extinction task progressed and the animals learned, differences in network metrics emerged. Group-level radar plot analysis showed that by the late learning phase, the control and ACTH-treated ELS groups exhibited enhanced network connectivity, integration, cohesiveness, and

efficiency (Figure 5.11C). In contrast, the vehicle-treated ELS group continued to show impaired connectivity and network organization, suggestive of diminished neural flexibility and adaptation during fear extinction underlying their learning deficit.

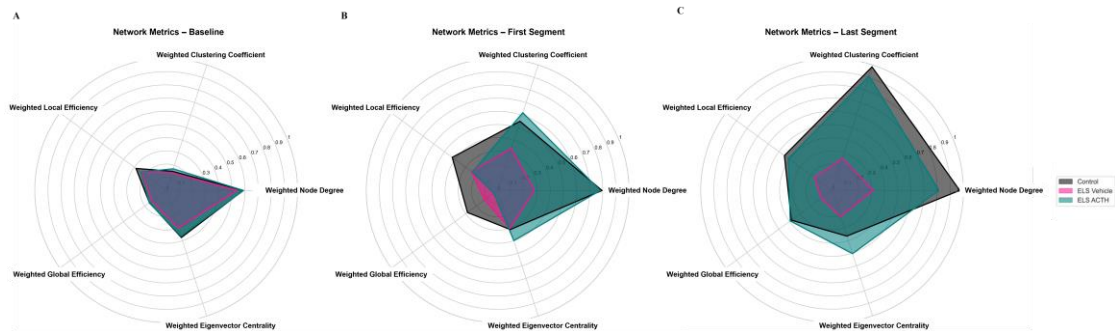


**Figure 5.11: Network Metrics Across Baseline and Fear Extinction Phases**  
Radar plots depicting normalized network metrics for control (black), ELS vehicle-treated (pink), and ELS ACTH-treated (teal) groups during baseline (A), the early learning phase of fear extinction (first segment, B), and the late learning phase (last segment, C). Metrics include edge weight, weighted degree centrality, weighted clustering coefficient, eigenvector centrality, global efficiency, and local efficiency. At baseline, no significant differences were observed between groups, indicating similar network properties during rest (A). In the first segment, significant reductions in connectivity-related metrics were observed in the vehicle-treated ELS group compared to the control and ACTH-treated groups (B). In the last segment, control and ACTH-treated ELS groups exhibited enhanced network integration and connectivity, compared to the vehicle-treated ELS group (C).

This enhancement in cohesiveness and functional organization in control and ACTH-treated ELS groups compared to vehicle-treated ELS groups was further seen with community plots between the first and last segments (Figure 5.12). These findings collectively suggest that ELS impairs mPFC plasticity underlying changes in network strength seen with learning, and that ACTH treatment not only normalizes network

properties during task-related learning but also restores organization in PFC networks, preventing the aberrant neural network development induced by ELS.

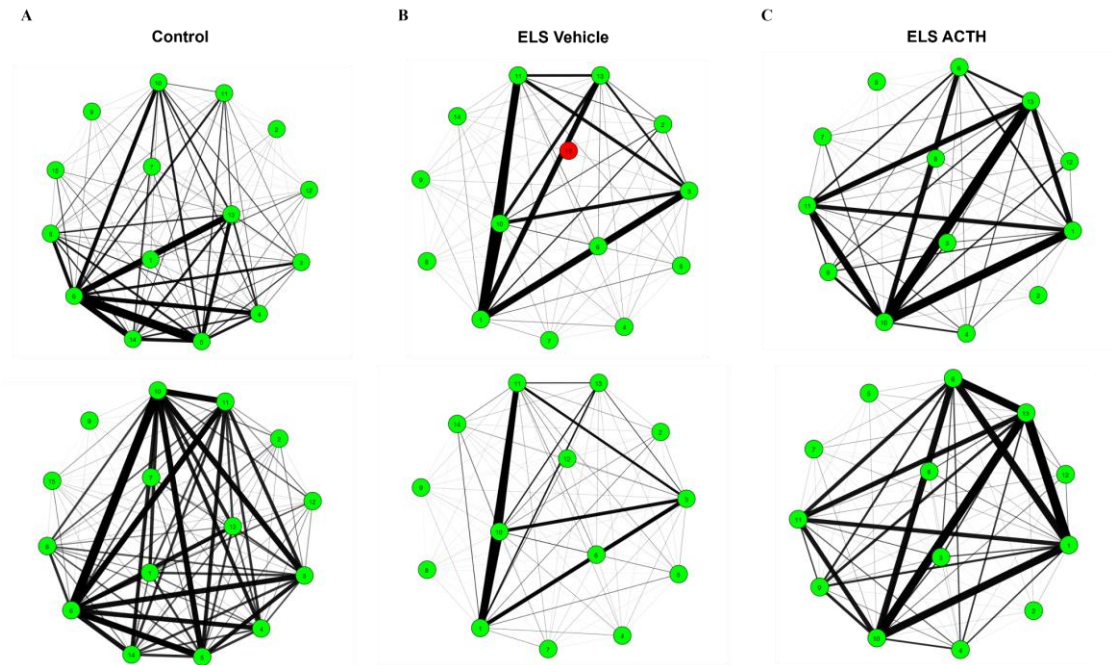


Figure 5.12: Community Structures in PFC Neural Networks During Fear Extinction  
Representative network community structures for control (A), ELS vehicle-treated (B), and ELS ACTH-treated (C) groups during fear extinction. Nodes represent neurons, with edge thickness corresponding to connection strength. Top panels depict networks during the early learning phase (first segment), while bottom panels depict networks during the late learning phase (last segment). Control and ACTH-treated ELS groups exhibit cohesive and functionally organized communities in both segments, particularly during the late learning phase (A&B). In contrast, the vehicle-treated ELS group shows less cohesive communities (C).

#### 5.4 Discussion

Early-life seizures (ELS), occurring during critical developmental windows, exert lasting effects on cortical neural networks leading to persistent cognitive deficits

characterized by impaired learning, memory, and executive functions<sup>34,453,455,531</sup>. In this study, we investigated how ELS disrupted mPFC function at both single-neuron and neuronal population levels, during baseline conditions and fear extinction learning. We found significant alterations in neuronal firing patterns, temporal fine spike-timing dynamics, and network-level connectivity that ultimately limit the cognitive flexibility required for adaptive behaviors such as fear extinction learning. Importantly, we demonstrated that ACTH administration, as a neuroprotective agent, effectively prevented these neural alterations by preserving single-neuron firing dynamics, temporal coding properties, and population-level connectivity. These findings underscore our central premise, that protecting neural network dynamics, rather than focusing solely on cellular or molecular targets, is key to preventing the long-term cognitive impairment that follows early life insults.

Fear extinction learning requires dynamic modulation of neuronal activity within mPFC-basolateral amygdala (BLA) activity to facilitate adaptive suppression of fear responses in the absence of aversive stimuli<sup>505,512,513,519,532</sup>. Dysfunction within these circuits is implicated in pathological conditions such as PTSD, anxiety disorders, and epilepsy, which are characterized by diminished neural flexibility, impaired extinction and learning<sup>506,507,511,520,521,533</sup>. Our data suggest that the reduced firing rates and restricted firing repertoire observed in ELS animals represent critical barriers to the flexible neuronal modulation (i.e. appropriate neural plasticity) necessary for extinction learning. Notably, ACTH treatment preserved intrinsic firing properties, including normalized post-spike filter and PC scores, thus expanding the firing repertoire and facilitating adaptive neuronal responses that are important for extinction learning<sup>37,534,535</sup>.

At the single-neuron level, vehicle-treated ELS mice exhibited significantly reduced baseline firing rates and abnormal temporal firing dynamics. These observations align with prior evidence highlighting disrupted intrinsic neuronal dynamics and plasticity following early life seizures<sup>37,40,41</sup>. Notably, temporal coding, viewed as the variability and precision of action potential timing, supports cognitive processes such as memory, attention, and behavioral flexibility<sup>76,131,137,529,536,537</sup>. Despite the reduced firing rate, the neurons from vehicle-treated ELS animals display a level of beta and theta modulated firing with two firing peaks at approximately 42 and a more prominent 120 ms rebound peak compared to controls and ACTH-treated ELS animals. Principal component analysis confirmed this pattern, with PC1 loadings capturing both peaks and vehicle-treated ELS neurons displaying significantly higher PC1 scores than the other groups. Thus, vehicle-treated ELS neurons retained a rigid and stereotyped temporal firing structure, firing at a lower rate but with a fixed refring window, potentially indicative of a maladaptive form of temporal coordination in neuronal firing at the single neuron level.

The early 42 ms peak falls within the beta frequency range (20–30 Hz), which has been implicated in maintaining current cognitive states, internal representation, and working memory stability<sup>538–540</sup>. While beta is a normal feature of the prefrontal coding and was present in all groups, the increased expression of this 42 ms peak in the vehicle-treated ELS group may reflect a pathological persistence indicating a failure to update or flexibly shift active states<sup>538</sup>. Such temporal rigidity is seen in Parkinson's disease, where excessive beta presence impairs behavioral flexibility and cognitive control<sup>540,541</sup>. Likewise, in healthy humans, elevated beta bursts suppress adaptive learning by reducing behavioral variability in task prediction and

overreliance on older memory representations for reward prediction<sup>542</sup>. The second peak aligns with theta rhythmicity (4-8 Hz) which is typically associated with cognitive engagement, however the emergence of a theta-modulated refring at baseline in the vehicle-treated ELS group likely reflects a constrained, inflexible temporal pattern rather than an increased rhythmic firing underlying learning over time. These findings illustrate that while beta and theta typically support cognitive stabilization and engagement, their exaggerated presence at baseline reflects pathological rigidity rather than adaptive function by locking the system into a persistent state and limiting dynamic cognitive engagement. Prominent presence of both beta and theta conveys a maladaptive form of temporal coordination which means that action potentials are locked into narrow time windows, which reduces the neuron's ability to adapt to changing inputs or participate in task-driven network dynamics. Such rigidity in spike-timing patterns can impair neuronal coding flexibility, limiting adaptive responses to changing environmental demands<sup>37,543-545</sup>. This impairment in coding flexibility will impact cognitive functions, as flexible spike timing is critical for efficient sensory coding<sup>545,546</sup>, plasticity and learning<sup>547</sup>, reliable cortical information processing<sup>536</sup>, motor output precision<sup>544</sup>, and working memory function<sup>543</sup>. Hence, the loss of spike-timing flexibility observed after ELS is one of the metrics that predicts the cognitive deficits observed in our model. Early treatment with ACTH preserved both firing rate and spike-timing variability, supporting more variable spike-timing patterns which lower PC1 scores. This supports a more dynamic and flexible neuronal firing repertoire, contributing to improved cognitive performance and facilitating extinction learning.

Interestingly, despite significant differences in firing rate and post-spike filter structure, we saw no group differences in the coefficient of variation of inter-spike interval (CV ISI) during baseline. CV ISI values across all groups were approximately 1, consistent with Poisson-like spike trains and suggesting that neurons fired randomly overall. However, CV ISI is a global measure and is insensitive to conditional spike timing patterns. It does not capture local temporal structure, such as the elevated post-spike firing probability at around 120 ms observed in the PSFs of vehicle-treated ELS neurons. This indicates that standard irregularity measures like CV ISI may fail to detect structured temporal patterns that reflect maladaptive network dynamics. These findings highlight the added value of model-based analyses, like GLM-derived PSFs, for uncovering hidden temporal constraints that may contribute to impaired cognitive flexibility. Notably, despite the differences in single-neuron firing properties, network-level graph metrics such as centrality, local clustering, and efficiency did not differ significantly between the groups. This suggests that cognitive impairments may not emerge from resting network organization alone, but instead from an inability to dynamically reorganize networks in response to task demands.

Since our goal was to characterize firing dynamics during learning, we employed a fear acquisition and extinction paradigm known to rely on mPFC. Behaviorally, all groups acquired the tone-shock association normally during the acquisition phase of the fear conditioning task, confirming intact initial fear learning. However, during extinction, vehicle-treated ELS mice displayed persistently elevated freezing, indicating impaired learning suppression of the conditioned response. In contrast, ACTH-treated ELS mice exhibited significantly reduced freezing throughout

the extinction session, suggesting that ACTH protected PFC dynamics necessary for successful fear extinction.

Single neuron analysis during extinction revealed that vehicle-treated ELS neurons exhibited impaired responsiveness to task-related stimuli during extinction learning. These neurons showed significantly reduced firing rate increases in response to tone presentations compared to both control and ACTH-treated ELS groups, as seen in the peri-stimulus time histograms. This deficit in tone-evoked response was observed both at the beginning and end of extinction, suggesting a persistent failure of stimulus engagement. In contrast, neurons from ACTH-treated animals showed restored tone-responsiveness, supporting the role of ACTH in preserving both intrinsic and task-evoked activity. These data suggest that temporal rigidity and low baseline activity in ELS neurons are accompanied by a failure to dynamically engage with task events, which further reinforces the idea that these neurons are functionally disconnected from adaptive network processes. Taken together, this suggests that the impairments in network plasticity and adaptability, rather than baseline abnormalities, underlie the observed cognitive deficits.

To understand population-level effects during the fear extinction task, we quantified multiple graph-based metrics including edge weights, weighted degree centrality, clustering coefficients, eigenvector centrality, and global/local efficiencies. These metrics collectively provide detailed insights into different aspects of functional connectivity, network integration, cohesiveness, and communication efficiency<sup>548,549</sup>. Vehicle-treated ELS mice exhibited significant impairments across these metrics during fear extinction, notably showing reduced integration, lower centrality, disrupted local clustering, and diminished global efficiency, which are features

consistent with fragmented and inefficient network communication. In contrast, networks built from neurons recorded in ACTH-treated ELS mice exhibited properties similar to control levels, indicating that maintaining these critical network features is important for adaptive fear learning. The protection of local clustering, integration, efficiency and centrality metrics in ACTH-treated animals support enhanced local and global network interactions, which are crucial for effective cognitive performance<sup>550-552</sup>. These network-level impairments likely emerge from a combination of single-neuron temporal constraints, reduced firing, impaired stimulus responsiveness leading to changes in network plasticity and ultimately poor learning in the task. Together, these results highlight that reduced firing and rigid spike-timing in ELS animals restrict the neuron's ability to engage dynamically with evolving task demands, contributing to the network-level fragmentation observed during extinction. ACTH treatment prevented these constraints, restoring responsiveness and facilitating neuronal integration, indicating that stimulus responsiveness, firing rate, and spike-timing are interconnected aspects of network adaptability that converge to support flexible cognition.

Next, we asked how the whole landscape of population dynamics relates to extinction learning. We performed correlation analyses among these metrics separately at the initial and final segments of extinction and revealed how each metric captures distinct yet interrelated aspects of network function. At the beginning of extinction, while the behavioral performance of the animals is the same, network metrics displayed moderate to weak correlations, suggesting independence in how different network properties reflect neuronal dynamics during initial task engagement. By the end of extinction, correlations among metrics became stronger, reflecting

tighter coordination among network properties. These stronger correlations during the last segment of extinction indicate increased coupling among network properties, reflecting coordinated adaptations across multiple levels, from local neuronal interactions like edge weights to broader network properties like efficiency and centrality. However, despite the global increase in correlations, the radar plots reveal that the vehicle-treated ELS group failed to evolve in the magnitude of these network features during the extinction task. While control and ACTH-treated groups showed increases in network metrics by the end of extinction, the vehicle-treated ELS group remained significantly lower across all of them, highlighting that both network integration and magnitude are required for successful fear extinction. This suggests that successful fear extinction learning relies on coordinated changes across multiple aspects of network organization within the mPFC such as local clustering, connectivity strength, and global efficiency rather than independent single parameter changes. Thus, ACTH's preservation of these integrated metrics likely facilitates the cohesive neuronal interactions and dynamics reorganization essential for learning<sup>550-</sup><sup>552</sup>. These population-level findings have significant implications, suggesting that early interventions aimed at preserving network integrity could help mitigate long-term cognitive deficits after an early-life insult.

Finally to further characterize neuronal contributions and directly link neural dynamics to behavior, we implemented a Graph Neural Network (GNN) model utilizing a Graph Attention Network (GAT) architecture. Unlike traditional statistical approaches such as linear regression, which captures population-level data, or generalized estimating equations (GEE), which provide node-level resolution without predictive capability, our optimized GAT model integrates node-level features and

their connectivity to robustly predict behavioral outcomes. Rather than identifying correlations, this model helps us ask a more important question regarding which features of neural activity are actually influencing and predicting behavior, allowing us to bridge the gap between behavior and mechanism to show whether neural dynamics *determine* cognitive outcomes. The GAT model significantly outperformed linear regression in both segments of the task suggesting that the higher  $R^2$  reflects not just improved model fit but the emergence of biologically structured dynamics over the course of learning, highlighting the value of incorporating complex neuronal interactions into behavior prediction. Feature importance analysis revealed that firing rate, ISI properties, and PSF principal components were strong predictors of freezing behavior during fear extinction, reinforcing that both firing and temporal coding are behaviorally relevant. This demonstrates the utility of the GNN approach with its capacity to integrate neuron-level analytical depth, like GEE, but with predictive power. Hence, this innovative approach not only enhances our mechanistic understanding of network dynamics but also holds promise for future applications such as predicting treatment responses and exploring network dysfunctions in other neurodevelopmental conditions.

In conclusion, our findings demonstrate that ELS produces long-lasting impairments in both spike-timing structure and network connectivity that limit cognitive flexibility during fear extinction learning. Early treatment with ACTH leads to long-lasting preservation of both firing variability and network adaptability, reinforcing the notion that interventions aimed at protecting network-level dynamics can effectively mitigate the long-term cognitive consequences of early-life insults. By normalizing firing rates, temporal coding, and key connectivity metrics, ACTH

facilitates dynamic PFC reorganization essential for adaptive learning. These results reveal a multi-scale mechanism by which rate and temporal alterations at the neuron level can propagate to network-level dysfunction, and underscore the potential of targeting neural dynamics as a mechanism to avert long-term cognitive adversity following early life insults. Future research should explore similar network-level interventions across other neurodevelopmental disorders and validate the predictive utility of network models.

## Chapter 6

### ADDITIONAL BEHAVIORAL AND ELECTROPHYSIOLOGICAL FINDINGS

The main chapters focused on core behavioral and network-level outcomes following early-life seizures (ELS) and ACTH treatment. This chapter includes additional experiments conducted alongside the experiments in chapters 4 and 5. These data include fear behavior from MC4R knockout and knock-in models, as well as baseline and fear extinction electrophysiology from MC4R KO animals. Although not all findings were significantly different or central to the main papers, they still provide insights into ACTH's MC4R-dependent modulation of neuronal and behavioral responses after ELS. Below, we present these results in full.

#### 6.1 Fear Conditioning Behavior Across WildType, MC4R Knockout, and Knock-In Lines

As previously reported in the previous chapters, wild-type (WT) animals that underwent early-life seizures (ELS) displayed a significant deficit in fear extinction learning, which was rescued by ACTH treatment. Here, we extended this analysis to include MC4R knockout (KO) and knock-in (KI) lines to examine whether ACTH's behavioral rescue depends on MC4R expression.

During fear acquisition on day 1 (Figure 6.1A), all groups including WT, MC4R KO, Synapsin1(Syn1)-Cre MC4R KI, and GFAP-Cre MC4R KI mice successfully learned the task, as indicated by increased freezing to the tone paired with foot shock (Figure 6.1A; GEE,  $p < 0.05$ ). There were no significant group differences

during acquisition (GEE,  $p > 0.05$ ), and no significant effect of ELS or ACTH treatment on learning performance across genotypes (all GEE,  $p > 0.05$ ).

On day 2, during fear extinction (Figure 6.1B), WT vehicle-treated ELS mice showed impaired extinction compared to WT controls. ACTH treatment restored extinction in WT ACTH-treated ELS mice which were not different from controls as reported in chapter 5. KO vehicle-treated ELS mice had a significant deficit in extinguishing the task as shown by the significantly higher freezing percentage by tone 30 (67%, IQR: 63.0%–69.0%) compared to KO controls (48.2%, IQR: 44.0%–70.0%; GEE,  $p = 0.018$ ). ACTH failed to improve extinction in KO ACTH-treated ELS mice (70.9%, IQR: 65.0%–77.0%; GEE,  $p = 0.273$  vs KO control). Extinction learning was not different compared to KO vehicle-treated ELS mice (GEE,  $p = 0.273$ ), indicating that ACTH did not mediate its positive effects in MC4R KO mice.

Next, we wanted to understand whether MC4Rs in neuron and astrocyte cell types differentially contribute to the improved fear extinction learning following ELS with ACTH treatment. We re-expressed MC4R in either neurons or astrocytes, followed by ELS and ACTH treatment. Syn1-Cre KI mice, in which MC4R is restored in neurons, did not benefit from ACTH. Syn-Cre ELS vehicle mice froze 66.0% (IQR: 64.0%–67.0%), and ACTH-treated Syn-Cre mice showed similar freezing levels (66.0%, IQR: 62.0%–66.0%; GEE,  $p = 0.150$ ). These findings suggest that neuronal MC4R expression alone is insufficient for behavioral rescue. In contrast, in GFAP-Cre KI mice, where MC4R is re-expressed in astrocytes, ACTH was able to rescue extinction learning. GFAP-Cre vehicle-treated ELS mice froze 67.0% (IQR: 64.0%–70.0%) compared to GFAP-Cre ACTH-treated ELS mice which showed a

significantly reduced freezing percentage of 42.0% (IQR: 38.0%–46.0%; GEE,  $p = 0.0005$ ).

Together, these data demonstrate that ACTH rescues fear extinction deficits following ELS through a mechanism that requires MC4R expression, with astrocytic MC4R significantly contributing to this effect.

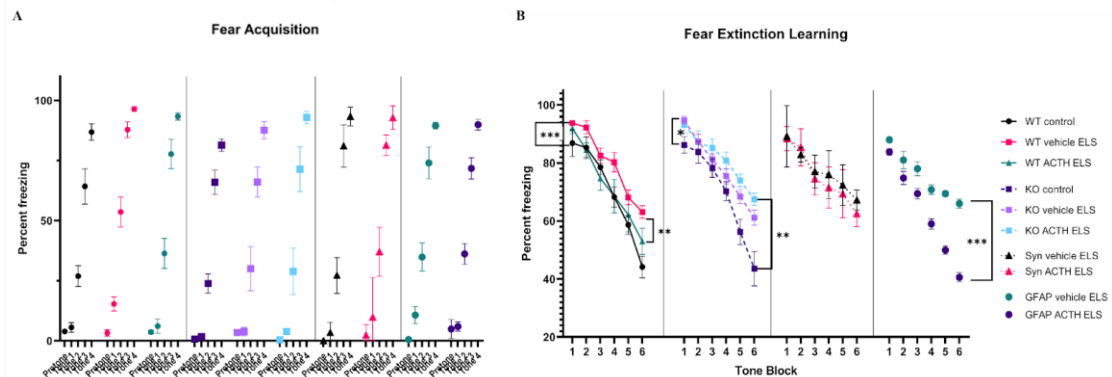


Figure 6.1: MC4R-Dependent Rescue of Fear Extinction Deficits Following Early Life Seizures

All groups acquired the fear conditioning task during tone-shock pairings on day 1, showing increasing freezing across tones (A). However, during the extinction phase (B), vehicle-treated ELS mice exhibited impaired extinction across genotypes. ACTH significantly rescued extinction learning in WT but not MC4R KO animals. ACTH restored extinction learning in GFAP-Cre MC4R KI mice but not in Syn1-Cre MC4R KI mice, indicating that neuronal MC4R expression alone is insufficient to restore learning.

## 6.2 Rate Coding Across Wildtype and MC4R KO Animals

As discussed in chapter 5, ACTH was able to preserve the firing rates in ACTH-treated ELS animals compared to vehicle-treated ELS animals which showed a significant decrease in their firing rate at baseline. Firing rates in ACTH-treated ELS

animals were comparable to control levels. In addition, there were no significant differences in the interspike interval coefficient of variation (CV ISI) between groups.

To examine whether ACTH's effects on firing rate depend on MC4R signaling, we analyzed the firing rate in MC4R KO animals. Mean firing rate in KO controls (1.58 Hz, 95% CI [1.08, 2.09]) was not significantly different from KO vehicle-treated ELS animals (1.88 Hz, 95% CI [1.16, 2.61]) or KO ACTH-treated ELS animals (1.88 Hz, 95% CI [0.13, 3.64]), all  $p > 0.05$  (Figure 6.2A). ACTH treatment in KO mice was not able to preserve firing rates at control level as we saw in the WT groups. Notably, in WT groups, the vehicle-treated ELS neurons showed a significant decrease in the firing rate, however KO vehicle-treated ELS neurons showed an increase in the firing rate compared to control even though it is not significantly different.

These findings suggest that ACTH's ability to preserve firing rate after ELS depends on intact MC4R signaling, and that MC4R KO alters the intrinsic firing rate response to ELS. The apparent increase in firing rate in KO ELS neurons, opposite to the suppression observed in WT vehicle-treated ELS neurons, may reflect a compensatory mechanism or a disinhibited firing phenotype that emerges in the absence of MC4R. Thus, this suggests that MC4R signaling may not only be necessary for ACTH's protective effects but may also to control aberrant firing rates after ELS. Also similar to WT animals, no significant group differences were seen in CV ISI across the KO groups (Figure 6.2B).

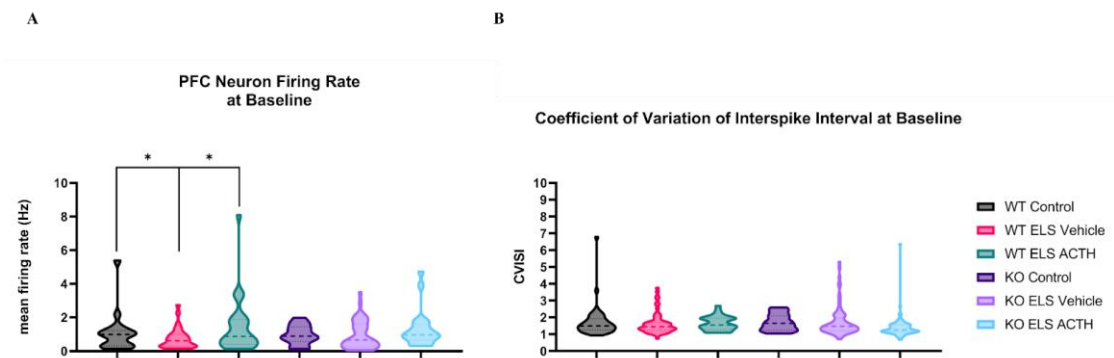


Figure 6.2: Baseline mPFC Firing Rates and Spike-Timing Variability Across Genotypes

Mean firing rates of single neurons recorded at baseline in WT and MC4R KO vehicle-treated and ACTH-treated animals. Vehicle-treated ELS mice showed significantly reduced firing compared to WT controls, an effect that was rescued by ACTH. However, ACTH failed to preserve firing rate in MC4R KO animals (A). Coefficient of variation of interspike intervals (CV ISI) showed no differences across all groups (B).

### 6.3 Temporal Coding Across MC4R KO Animals

To test whether ACTH's ability to preserve temporal coding after ELS requires MC4R signaling, we analyzed post-spike filters (PSFs) and principal component 1 (PC1) scores from medial prefrontal cortex (mPFC) neurons in MC4R KO animals. Mean normalized PSFs revealed differences in refriring timing across groups (Figure 6.3A). Unlike the canonical 42 ms and 120 ms peaks observed in WT animals, KO control neurons exhibited a delayed single peak at approximately 120 ms (Figure 6.3A, top panel). In contrast, KO vehicle-treated ELS neurons displayed prominent peaks at both around 70 ms and 150 ms post-spike (Figure 6.3A, middle panel). KO ACTH-treated ELS neurons also showed strong peaks at similar time points around 42 ms and 150 ms, indicating persistent beta and theta modulation despite ACTH

treatment (Figure 6.3A, bottom panel). PC1 scores did not significantly differ across the groups (GEE, all  $p > 0.05$ ; Figure 6.3B).

These findings suggest that in the absence of MC4R, ACTH is unable to restore temporal coding flexibility following ELS. Further, the shift in timing windows particularly the absence of a canonical beta peak in controls and the delayed theta rebound in ELS groups, indicates that MC4R signaling may be required to maintain precise rebound timing structure.

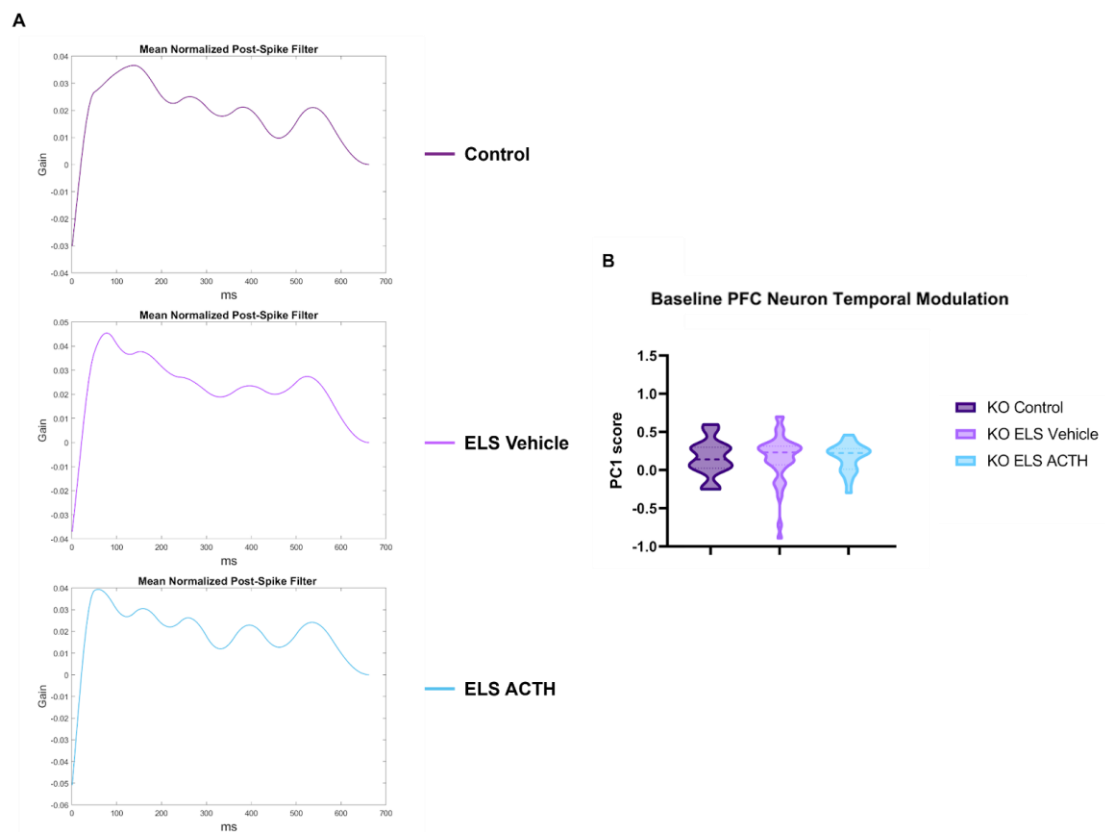


**Figure 6.3: ACTH Fails to Restore Flexible Temporal Coding in MC4R Knockout Mice at Baseline**  
Mean normalized post-spike filters (PSFs) from KO control, KO vehicle-treated ELS, and KO ACTH-treated ELS neurons. All groups showed rebound peaks, but their timing and shape varied. KO control neurons

exhibited a delayed theta-range peak around 120 ms. KO ELS vehicle neurons showed prominent peaks at around 70 ms and 150 ms. KO ACTH-treated ELS neurons displayed peaks at around 42 ms and 150 ms (A). Violin plots of PC1 scores, quantifying alignment with the principal temporal structure across neurons (B). No significant differences were observed between groups.

## Chapter 7

### OVERALL DISCUSSION AND FUTURE DIRECTIONS

Cognitive function emerges from the dynamic coordination of distributed neural circuits, yet our understanding of how these systems develop and become dysregulated especially in the prefrontal cortex (PFC) remains incomplete. To fully understand the neural dynamics underlying cognition, it is essential to test the network under both normal and pathological conditions, and importantly, under conditions of recovery or protection in order to understand how all these changes subserved cognition. To achieve this, we implemented a recurrent early-life seizures (ELS) model to investigate how PFC dynamics are altered after injury and modulated by Adrenocorticotrophic hormone (ACTH). Early-life seizures occur during critical developmental periods marked by high synaptic plasticity and circuit refinement. They disrupt not only local neuronal physiology but also the flexible, network-level interactions required for cognition. ACTH was chosen based on its neuroprotective properties across different neurological disorders. Specifically, ACTH exerts direct neuroprotective actions by modulating synaptic plasticity, reducing neuroinflammation, and promoting neuronal survival through activation of central melanocortin receptors like melanocortin receptor 4 (MC4R). For example, in epilepsy models, ACTH maintained hippocampal long-term potentiation and improved spatial learning without affecting seizure frequency and in ischemic stroke models, it counteracted widespread transcriptional dysregulation related to inflammation and synaptic signaling while enhancing angiogenesis and glial proliferation. Additionally,

in Parkinson's disease models, it preserved dopaminergic neuron integrity and normalized striatal dopamine levels by upregulating neurotrophic factors such as BDNF. This dissertation demonstrates 1) the necessary network organization in mPFC required for cognition, 2) how ELS-induced cognitive deficits arise from persistent alterations in neural coding in the mPFC rather than solely from structural damage or seizure activity, 3) how preserving the network against these coding alterations can rescue cognitive outcome after early life insult, and 4) how neuronal features and network activity predicts behavior outcome rather than being just a correlate. By targeting the mPFC, our work addresses a major gap in understanding how healthy network function supports cognition, how its dynamics are compromised by ELS, and how they can be restored.

To better conceptualize these complex neural dynamics, consider the brain as a mailing service. For the service to be efficient, mailing trucks (neuronal action potentials) must depart on a precise schedule (temporal coding) and travel at the appropriate frequency (rate coding) to deliver their packages (information) successfully. Moreover, it's not just a single truck but a coordinated fleet (population coding) that ensures messages are delivered reliably. If a route becomes damaged as what happens with ELS-induced deficits, the trucks must reorganize their schedules and routes (network reorganization) to maintain delivery efficiency. However, if some trucks become stuck, the package (information) never reaches its destination, resulting in functional deficits. This analogy underscores how disruptions in rate, temporal, and population coding can compromise cognitive performance.

Using single-unit recordings and functional network analyses during both baseline and a fear extinction task, we demonstrated that ELS causes significant

impairments across multiple scales of neural coding. Baseline recordings allowed us to assess the intrinsic properties of the mPFC network in absence of task demands, where deficits may remain hidden. However, during a fear extinction task that requires continuous reorganization of coding mechanisms to integrate contextual, emotional and cognitive signals, the network deficiencies become more evident. First, there is a reduction in mean firing rate at baseline indicating compromised rate coding which likely diminishes the network's ability to encode stimulus intensity and maintain robust signal-to-noise ratios. This deficit was exacerbated during the fear extinction where the ELS neurons failed to encode stimulus cues (tones). Second, neurons in ELS animals exhibit increased temporal rigidity during baseline, as seen in fixed post-spike firing patterns, which impairs spike-timing-dependent plasticity (STDP) and adaptive coordination of neuronal populations which in part affected the extinction performance in vehicle-treated ELS animals. Third, population-level connectivity is disrupted, with lower edge weights, reduced weighted degree centrality, and impaired graph efficiency during tasks performance. However, while baseline population measures appear to be relatively preserved, the dynamic demands of the fear extinction task reveal that ELS impairs the distributed coordination needed for adaptive cognitive functions in a task that requires the integration of hippocampal contextual input and the mPFC's regulation of amygdala's fear output.

Across baseline recordings, we observed that the mPFC neurons in the vehicle-treated ELS animals became locked into narrow timing windows. Under healthy conditions, mPFC neurons exhibited temporal coding flexibility as seen by the generalized linear model post spike filters. The PSFs show a modest beta-range peak and a low-amplitude theta-range peak in control neurons, however the majority of ELS

neurons significantly overexpressed pronounced beta and theta range peaks, not because these specific rhythms are inherently detrimental but because they reflect an aberrant restricted firing dynamic. In other words, if the underlying firing dynamics were altered in a different manner, the output might manifest in another frequency band, thus the persistent overexpression of beta and theta in ELS neurons indicates a pathological temporal lock. This rigidity reflects a deficit in the network's ability to flexibly reconfigure spike timing impairing STDP and the adaptive updating of internal representations. This observation was seen during baseline; however, this deficit may be in part responsible for the impaired response to auditory tones during fear extinction where ELS neurons were unable to respond to tone presentations. Notably, ACTH treatment restores flexible PSF profiles smoothing the rebound trajectories and reducing peak amplitudes as captured by reduced principal component 1 (PC1) scores, but only when MC4R signaling is intact. In MC4R KO mice, although the firing timescale shifts with peaks around 70 and 150 ms, the neurons remain temporally rigid. Even when the PC1 score was not significantly different between the groups, the ELS and ACTH-treated ELS neurons showed higher median on the PC1 score and higher amplitudes of these peaks compared to the KO controls highlighting a role for the MC4R in mediating proper temporal modulation. Taken together, these results demonstrate that ELS induces temporal rigidity by locking mPFC neurons into fixed oscillatory windows that impair STDP and adaptive coding, and that ACTH can restore flexible timing states thus allowing neurons to regain plasticity and support behavioral recovery only when MC4R signaling is intact.

So, in summary, I personally think that it is not about the beta and theta specifically, at the end these are an output of the underlying firing dynamics, but their

persistent expression in the ELS neurons is an output of aberrant firing dynamics. So, for example if the neurons were locked in firing to a different timescale, we would observe the output as a different frequency signature which we actually see with the MC4R KO neurons. The KO neurons shift on timescale of firing but that did not change the fact that the ELS added a more temporal lock that was not recovered by ACTH, demonstrating that the pathological effect lies in the loss of flexibility in the timing of neuronal firing and not in the specific frequency bands per se.

Beyond precise spike timing, robust synaptic plasticity in neural circuits depends on the coordinated interplay of rate coding and population coding alongside temporal coding. For instance, rate coding measuring the overall firing frequency of a neuron conveys information about the strength of an input, which modulates synaptic efficacy by influencing the magnitude of activity-dependent changes. When neurons fire at higher rates in response to a strong stimulus, they are more likely to engage mechanisms like long-term potentiation (LTP). Simultaneously, temporal coding ensures that the exact timing of these spikes is coordinated to trigger spike STDP, where the order and interval between pre- and post-synaptic spikes determine whether synapses are strengthened or weakened.

Complementing these is population coding, which refers to the coordinated activity of ensembles of neurons that collectively represent information. This distributed coding not only increases the robustness of the network by minimizing the impact of variability in individual neurons but also supports the integration of complex inputs across different brain regions. For example, in the hippocampus, place cells use their firing rate to encode spatial information while also exhibiting phase precession, a form of temporal coding that aligns their activity with theta oscillations, to create a

dynamic map of the environment. Moreover, the overlapping activation of neuronal ensembles enables the brain to form and update these spatial maps effectively, showing how population coding contributes to learning and memory.

In practice, these three coding strategies work synergistically. A reduction in overall firing rate as observed in our ELS model can decrease the potential for robust LTP, while rigid spike timing impairs STDP and disrupts the formation of flexible temporal windows necessary for synaptic adjustments. At the same time, if the coordinated activity across neuronal ensembles is compromised, the network loses its capacity to generate coherent and adaptive representations of complex stimuli. Thus, the integration of rate, temporal, and population coding is essential for dynamic synaptic modulation and cognitive plasticity, ensuring that the brain can adapt to new experiences and maintain functional flexibility.

In addition to neuronal expression, MC4R is also expressed in astrocytes, which are crucial for maintaining synaptic and network homeostasis. We performed immunohistochemical analyses for key astrocytic proteins like aquaporin-4 (AQP4) and glial fibrillary acidic protein (GFAP) and saw that ELS significantly altered their expression. Specifically, AQP4 levels were reduced, indicating impaired ion and water homeostasis, while GFAP was significantly elevated, reflecting persistent glial reactivity and inflammation. These alterations likely disrupt astrocyte–neuron communication, thereby impairing the extracellular environment essential for dynamic synaptic coding and plasticity. Given these findings, we hypothesized that ACTH's neuroprotective effects are mediated, at least in part, via astrocytic MC4R signaling. Consistent with this, ACTH treatment restored both AQP4 and GFAP expression toward control levels.

Furthermore, since vehicle-treated and ACTH-treated ELS MC4R KO animals failed to perform fear extinction and did not exhibit improvements in anxiety-like behavior in the light/dark box, we decided to dissect the contributions of neuronal versus astrocytic MC4R by conducting selective MC4R knock-in (KI) experiments. Selective re-expression of MC4R in astrocytes in global MC4R KO mice restored extinction learning with ACTH treatment. However, neuron-specific re-expression of MC4R showed no improvement in extinction learning with ACTH treatment, despite both KIs showing ACTH-mediated reductions in anxiety-like behavior. This divergence underscores the task-specific requirements for astrocytic modulation. Astrocytes modulate the local extracellular environment that determines whether neurons can engage in flexible coding. Hence, even if neurons express MC4R, a persistently ion-imbalanced or pro-inflammatory environment can prevent the restoration of normal spike-timing dynamics. ACTH requires astrocytic MC4R to unlock the neuronal capacity for plasticity by restoring the extracellular and metabolic conditions that support dynamic coding. In contrast, Syn-Cre KI animals may still receive ACTH signals in neurons, but this is insufficient if neurons remain embedded in a dysfunctional glial environment. Fear extinction specifically requires coordinated, multi-regional plasticity, and without astrocytic support, those processes can collapse. In contrast, behavioral assays such as the light/dark box test, which assess general anxiety-like responses, appear to be mediated by different circuits that do not require the same degree of coordination or spike-timing precision. Together, these findings highlight a previously underappreciated role for astrocytic MC4R signaling in shaping the neuronal coding dynamics required for cognitive flexibility.

Despite these advances, our study has several limitations that restrict the mechanistic resolution of our findings. First, we utilized fear extinction and light/dark box as our behavioral paradigms, however, they might not capture the full complexity of cognitive deficits observed in clinical populations, such as impairments in working memory, attention, or social behavior. This leaves open the possibility that other aspects of cognitive function may be differentially affected by ELS and ACTH treatment. Second, electrophysiological recordings were limited to single-unit activity in the mPFC, even though this region functions within a broader network that includes the hippocampus and basolateral amygdala. Without simultaneous recordings from these interconnected regions, we cannot determine for sure whether ACTH restores large-scale synchrony. Third, our interpretations of astrocyte–neuron interactions rely on indirect assays such as behavioral rescue data from MC4R KO and KI experiments and protein-level expression of astrocytic markers (AQP4 and GFAP). Notably, we only examined astrocytic protein expression in wild-type animals, limiting our ability to assess whether similar alterations occur in MC4R KO or KI animals. Finally, although our data suggest that ACTH's beneficial effects are mediated primarily through central melanocortin receptors particularly MC4R, we cannot completely rule out potential off-target systemic effects that might also contribute to the observed network-level changes. However, ACTH interacts with multiple melanocortin receptors distributed throughout the body. For instance, its interaction with MC2R in the adrenal cortex stimulates cortisol release, which can modulate systemic stress and inflammatory responses that might indirectly affect brain function. Additionally, ACTH may influence immune system activity or promote the peripheral release of neurotrophic factors. Although these systemic effects do not appear sufficient to

rescue network-level deficits in the absence of MC4R, as shown by the lack of behavioral recovery in MC4R KO animals, they could still contribute to the overall neuroprotective profile of ACTH. Future studies employing simultaneous multi-region recordings, real-time glial imaging, targeted manipulation across genotypes, and MC4R specific agonists will be critical for further elucidating the interplay between neuronal and astrocytic dynamics in supporting cognitive function.

Our study opens several avenues for future investigation that will help resolve remaining uncertainties about the cellular and network mechanisms underlying cognitive recovery after ELS. One critical next step is to directly test the role of astrocytes in enabling spike dynamic flexibility and behavioral rescue. Future studies can incorporate cell-type specific optogenetic and chemogenetic approaches using astrocyte-targeted tools such as GFAP- or Aldh1L1-driven Channelrhodopsin (ChR2) or Designer Receptors Exclusively Activated by Designer Drugs (DREADDs). By activating astrocytes during key phases of the fear extinction task for example during tone presentations, we can determine whether re-engaging glial signaling alone mimics ACTH's restorative effects, while suppressing astrocytic activity in ACTH-treated animals would reveal whether such glial activation is essential for behavioral rescue. Combining these manipulations with MC4R knockout backgrounds will refine our mechanistic understanding of how astrocytic MC4R regulates spike dynamics and cognition.

In parallel, real-time understanding of astrocyte-neuron coupling is very important. Astrocyte-specific calcium imaging using genetically encoded indicators like GCaMP8f, under the control of GFAP or Aldh1L1 promoters, combined with simultaneous single-unit recordings and local field potential (LFP) measurements, will

enable us to track astrocytic  $\text{Ca}^{2+}$  dynamics alongside neuronal spiking and oscillatory coherence. For instance, if ACTH treatment restores temporally coupled astrocyte  $\text{Ca}^{2+}$  bursts and neuronal spiking during extinction, this would provide robust evidence that astrocytic activity is instrumental in modulating flexible coding dynamics.

Furthermore, applying single-nucleus RNA sequencing (snRNA-seq) can offer high-resolution insights into the transcriptional states of astrocytes after ELS and ACTH treatment. This approach can identify shifts in astrocyte subtypes distinguishing between pro-inflammatory and homeostatic profiles and determine whether ACTH drives a shift toward a supportive synaptic state. While snRNA-seq does not measure neuronal dynamics directly, it provides a molecular framework that can be correlated with electrophysiological data. For example, if transcriptional restoration in astrocytes aligns with the recovery of flexible post-spike filters and improved extinction behavior, this would help trace the pathway from receptor-level activation to population-level reconfiguration.

Beyond these cellular and molecular approaches, I am personally very interested in expanding our graph metric analyses and graph attention network (GAT) framework to other neurological and neurodevelopmental disorders. The central hypothesis is that conditions from different etiologies ranging from Fragile X syndrome and Alzheimer's disease to autism spectrum disorder, schizophrenia, and traumatic brain injury may converge on shared patterns of network disintegration, such as reduced local and global efficiency, timing rigidity, and impaired population coordination. Applying uniform network metrics across multiple disease models could reveal common signatures of network dysfunction. This convergence would shift disease classification from a purely symptom-based approach to one based on

quantifiable neural dynamics and potentially uncover unified therapeutic targets. Moreover, GAT models, which in our work successfully predicted freezing behavior by integrating node-level firing properties with edge weight topology, can be extended to predict cognitive impairments across different conditions. Such predictive models may serve as dynamic markers of treatment efficacy. Together, these future directions will expand our understanding of astrocyte-neuron interactions and network dynamics in cognitive function across a range of diseases, and they will facilitate the development of novel network-centric therapeutic strategies.

To sum up, the disruptions observed after ELS in our work likely extend to other cognitive domains, including working memory, attention, and social behavior. For example, the reduction in firing rates and rigid post-spike intervals observed in ELS animals could impede the rapid updating of neuronal representations necessary for effective working memory, while impaired population coding may underlie deficits in attentional control and social cognition. These findings underscore that cognitive resilience is not about the preservation of individual neurons or the suppression of seizures but it is about the maintenance or restoration of dynamic, glia-supported network coordination.

This network-centric perspective has profound translational implications. Therapeutic strategies should shift from a lesion- or seizure-centric focus toward interventions that restore dynamic network properties such as adaptive rate coding, flexible temporal windows, and robust population synchrony. Such an approach not only reflects the emergent properties of complex neural circuits but also acknowledges the critical role of astrocyte-neuron interactions in modulating these dynamics. By

targeting these integrated network mechanisms, future treatments may achieve more meaningful cognitive recovery across diverse neurological conditions.

Ultimately, our work advocates for a paradigm shift in neurotherapeutics, one that embraces the complexity of neuronal and glial interactions and leverages advanced computational models to predict behavioral outcomes. This approach promises to bridge the gap between basic neuroscience and clinical application, paving the way for novel, network-centric interventions that can effectively restore cognitive function and improve quality of life in affected individuals.

## REFERENCES

1. Hauser, W. A. Seizure Disorders: The Changes With Age. *Epilepsia* **33**, 6–14 (1992).
2. Garfinkle, J. & Shevell, M. I. Prognostic factors and development of a scoring system for outcome of neonatal seizures in term infants. *Eur. J. Paediatr. Neurol.* **15**, 222–229 (2011).
3. Camfield, P. & Camfield, C. Incidence, prevalence and aetiology of seizures and epilepsy in children. *Epileptic. Disord.* **17**, 117–123 (2015).
4. Fiest, K. M. *et al.* Prevalence and incidence of epilepsy: A systematic review and meta-analysis of international studies. *Neurology* **88**, 296–303 (2017).
5. Volpe, J. J. Brain injury in premature infants: a complex amalgam of destructive and developmental disturbances. *Lancet Neurol.* **8**, 110–124 (2009).
6. Smith, S. E. P., Li, J., Garbett, K., Mirnics, K. & Patterson, P. H. Maternal Immune Activation Alters Fetal Brain Development through Interleukin-6. *J. Neurosci.* **27**, 10695–10702 (2007).
7. Roper, S. N. Early Life Seizures and Learning Impairment: Neither the Time nor the Place. *EBioMedicine* **7**, 19–20 (2016).
8. Rice, D. & Barone, S. Critical periods of vulnerability for the developing nervous system: evidence from humans and animal models. *Environ. Health Perspect.* **108**, 511–533 (2000).
9. Parker, K. N., Donovan, M. H., Smith, K. & Noble-Haeusslein, L. J. Traumatic Injury to the Developing Brain: Emerging Relationship to Early Life Stress. *Front. Neurol.* **12**, 708800 (2021).
10. Lockhart, S., Sawa, A. & Niwa, M. Developmental trajectories of brain maturation and behavior: Relevance to major mental illnesses. *J. Pharmacol. Sci.* **137**, 1–4 (2018).

11. Jensen, F. E. & Baram, T. Z. Developmental seizures induced by common early-life insults: Short- and long-term effects on seizure susceptibility. *Ment. Retard. Dev. Disabil. Res. Rev.* **6**, 253–257 (2000).
12. Hermann, B. Children with new-onset epilepsy: neuropsychological status and brain structure. *Brain* **129**, 2609–2619 (2006).
13. Galler, J. & Rabinowitz, D. G. The Intergenerational Effects of Early Adversity. in *Progress in Molecular Biology and Translational Science* vol. 128 177–198 (Elsevier, 2014).
14. Daval, J.-L. & Vert, P. Apoptosis and neurogenesis after transient hypoxia in the developing rat brain. *Semin. Perinatol.* **28**, 257–263 (2004).
15. Perlman, J. M. Summary Proceedings From the Neurology Group on Hypoxic-Ischemic Encephalopathy. *Pediatrics* **117**, S28–S33 (2006).
16. Schreglmann, M., Ground, A., Vollmer, B. & Johnson, M. J. Systematic review: long-term cognitive and behavioural outcomes of neonatal hypoxic–ischaemic encephalopathy in children without cerebral palsy. *Acta Paediatr.* **109**, 20–30 (2020).
17. Feng, L., Han, C.-X., Cao, S.-Y., Zhang, H.-M. & Wu, G.-Y. Deficits in motor and cognitive functions in an adult mouse model of hypoxia-ischemia induced stroke. *Sci. Rep.* **10**, 20646 (2020).
18. Lemanski, E. A. *et al.* A Novel Non-Invasive Murine Model of Neonatal Hypoxic-Ischemic Encephalopathy Demonstrates Developmental Delay and Motor Deficits with Activation of Inflammatory Pathways in Monocytes. *Cells* **13**, 1551 (2024).
19. Amodeo, D. A. *et al.* Maternal immune activation impairs cognitive flexibility and alters transcription in frontal cortex. *Neurobiol. Dis.* **125**, 211–218 (2019).
20. Woods, R. M. *et al.* Maternal Immune Activation Induces Adolescent Cognitive Deficits Preceded by Developmental Perturbations in Cortical Reelin Signalling. *Biomolecules* **13**, 489 (2023).
21. Xiong, Y., Mahmood, A. & Chopp, M. Animal models of traumatic brain injury. *Nat. Rev. Neurosci.* **14**, 128–142 (2013).
22. Mansfield, R. T., Schiding, J. K., Hamilton, R. L. & Kochanek, P. M. Effects of Hypothermia on Traumatic Brain Injury in Immature Rats. *J. Cereb. Blood Flow Metab.* **16**, 244–252 (1996).

23. Fidan, E. *et al.* Repetitive Mild Traumatic Brain Injury in the Developing Brain: Effects on Long-Term Functional Outcome and Neuropathology. *J. Neurotrauma* **33**, 641–651 (2016).
24. Kochanek, P. M., Wallisch, J. S., Bayır, H. & Clark, R. S. B. Pre-clinical models in pediatric traumatic brain injury—challenges and lessons learned. *Childs Nerv. Syst.* **33**, 1693–1701 (2017).
25. Fesharaki-Zadeh, A. & Datta, D. An overview of preclinical models of traumatic brain injury (TBI): relevance to pathophysiological mechanisms. *Front. Cell. Neurosci.* **18**, 1371213 (2024).
26. Shonkoff, J. P. & Phillips, D. A. *From Neurons to Neighborhoods: The Science of Early Childhood Development.* xviii, 588 (National Academy Press, Washington, DC, US, 2000).
27. Ben-Ari, Y. & Holmes, G. L. Effects of seizures on developmental processes in the immature brain. *Lancet Neurol.* **5**, 1055–1063 (2006).
28. Tierney, A. L. & Nelson, C. A. Brain Development and the Role of Experience in the Early Years. *Zero Three* **30**, 9–13 (2009).
29. Koh, S., Storey, T. W., Santos, T. C., Mian, A. Y. & Cole, A. J. Early-life seizures in rats increase susceptibility to seizure-induced brain injury in adulthood. *Neurology* **53**, 915–915 (1999).
30. Brunquell, P. J., Glennon, C. M., DiMario, F. J., Lerer, T. & Eisenfeld, L. Prediction of outcome based on clinical seizure type in newborn infants. *J. Pediatr.* **140**, 707–712 (2002).
31. Holmes, G. L. The Long-Term Effects of Neonatal Seizures. *Clin. Perinatol.* **36**, 901–914 (2009).
32. Lugo, J. N., Swann, J. W. & Anderson, A. E. Early-life seizures result in deficits in social behavior and learning. *Exp. Neurol.* **256**, 74–80 (2014).
33. Ekinici, O., Titus, J. B., Rodopman, A. A., Berkem, M. & Trevathan, E. Depression and anxiety in children and adolescents with epilepsy: Prevalence, risk factors, and treatment. *Epilepsy Behav.* **14**, 8–18 (2009).
34. Reilly, C. *et al.* Neurobehavioral Comorbidities in Children With Active Epilepsy: A Population-Based Study. *Pediatrics* **133**, e1586–e1593 (2014).

35. Shimizu, H. *et al.* Overlap Between Epilepsy and Neurodevelopmental Disorders: Insights from Clinical and Genetic Studies. in *Epilepsy* (eds. Department of Pathophysiology, Medical University of Lublin, Lublin, Poland & J. Czuczwar, S.) 41–54 (Exon Publications, 2022). doi:10.36255/exon-publications-epilepsy-neurodevelopmental-disorders.
36. Lucas, M. M., Lenck-Santini, P.-P., Holmes, G. L. & Scott, R. C. Impaired cognition in rats with cortical dysplasia: additional impact of early-life seizures. *Brain* **134**, 1684–1693 (2011).
37. Hernan, A. E., Mahoney, J. M., Curry, W., Mawe, S. & Scott, R. C. Fine Spike Timing in Hippocampal–Prefrontal Ensembles Predicts Poor Encoding and Underlies Behavioral Performance in Healthy and Malformed Brains. *Cereb. Cortex* **31**, 147–158 (2021).
38. Khalife, M. R., Scott, R. C. & Hernan, A. E. Mechanisms for Cognitive Impairment in Epilepsy: Moving Beyond Seizures. *Front. Neurol.* **13**, 878991 (2022).
39. Isaeva, E., Isaev, D., Khazipov, R. & Holmes, G. L. Selective impairment of GABAergic synaptic transmission in the flurothyl model of neonatal seizures. *Eur. J. Neurosci.* **23**, 1559–1566 (2006).
40. Kleen, J. K. *et al.* Early-life seizures produce lasting alterations in the structure and function of the prefrontal cortex. *Epilepsy Behav.* **22**, 214–219 (2011).
41. Hernan, A. E., Holmes, G. L., Isaev, D., Scott, R. C. & Isaeva, E. Altered short-term plasticity in the prefrontal cortex after early life seizures. *Neurobiol. Dis.* **50**, 120–126 (2013).
42. Gerstner, W., Kreiter, A. K., Markram, H. & Herz, A. V. M. Neural codes: Firing rates and beyond. *Proc. Natl. Acad. Sci.* **94**, 12740–12741 (1997).
43. Lenck-Santini, P.-P. & Scott, R. C. Mechanisms Responsible for Cognitive Impairment in Epilepsy. *Cold Spring Harb. Perspect. Med.* **5**, a022772 (2015).
44. Buzsáki, G. & Draguhn, A. Neuronal Oscillations in Cortical Networks. *Science* **304**, 1926–1929 (2004).
45. Panzeri, S., Brunel, N., Logothetis, N. K. & Kayser, C. Sensory neural codes using multiplexed temporal scales. *Trends Neurosci.* **33**, 111–120 (2010).
46. Averbeck, B. B., Latham, P. E. & Pouget, A. Neural correlations, population coding and computation. *Nat. Rev. Neurosci.* **7**, 358–366 (2006).

47. Buzsáki, G. & Mizuseki, K. The log-dynamic brain: how skewed distributions affect network operations. *Nat. Rev. Neurosci.* **15**, 264–278 (2014).
48. Lenck-Santini, P.-P. & Holmes, G. L. Altered Phase Precession and Compression of Temporal Sequences by Place Cells in Epileptic Rats. *J. Neurosci.* **28**, 5053–5062 (2008).
49. Van Diessen, E., Diederer, S. J. H., Braun, K. P. J., Jansen, F. E. & Stam, C. J. Functional and structural brain networks in epilepsy: What have we learned? *Epilepsia* **54**, 1855–1865 (2013).
50. Postnikova, T. Y. *et al.* Impairments of Long-Term Synaptic Plasticity in the Hippocampus of Young Rats during the Latent Phase of the Lithium-Pilocarpine Model of Temporal Lobe Epilepsy. *Int. J. Mol. Sci.* **22**, 13355 (2021).
51. Houweling, A. R., Bazhenov, M., Timofeev, I., Steriade, M. & Sejnowski, T. J. Homeostatic Synaptic Plasticity Can Explain Post-traumatic Epileptogenesis in Chronically Isolated Neocortex. *Cereb. Cortex* **15**, 834–845 (2005).
52. Khambhati, A. N. *et al.* Dynamic Network Drivers of Seizure Generation, Propagation and Termination in Human Neocortical Epilepsy. *PLOS Comput. Biol.* **11**, e1004608 (2015).
53. Stein, R. B., Gossen, E. R. & Jones, K. E. Neuronal variability: noise or part of the signal? *Nat. Rev. Neurosci.* **6**, 389–397 (2005).
54. Singer, W. Neuronal Synchrony: A Versatile Code for the Definition of Relations? *Neuron* **24**, 49–65 (1999).
55. Josselyn, S. A. & Tonegawa, S. Memory engrams: Recalling the past and imagining the future. *Science* **367**, eaaw4325 (2020).
56. Sakkaki, S., Barrière, S., Bender, A. C., Scott, R. C. & Lenck-Santini, P.-P. Focal Dorsal Hippocampal Nav1.1 Knock Down Alters Place Cell Temporal Coordination and Spatial Behavior. *Cereb. Cortex* **30**, 5049–5066 (2020).
57. Shuman, T. *et al.* Breakdown of spatial coding and interneuron synchronization in epileptic mice. *Nat. Neurosci.* **23**, 229–238 (2020).
58. Zuo, Y. *et al.* Complementary Contributions of Spike Timing and Spike Rate to Perceptual Decisions in Rat S1 and S2 Cortex. *Curr. Biol.* **25**, 357–363 (2015).

59. Dragoi, G., Harris, K. D. & Buzsáki, G. Place Representation within Hippocampal Networks Is Modified by Long-Term Potentiation. *Neuron* **39**, 843–853 (2003).
60. Lu, L. *et al.* Impaired hippocampal rate coding after lesions of the lateral entorhinal cortex. *Nat. Neurosci.* **16**, 1085–1093 (2013).
61. Tolman, E. C. Cognitive maps in rats and men. *Psychol. Rev.* **55**, 189–208 (1948).
62. O'Keefe, J. & Nadel, L. *The Hippocampus as a Cognitive Map*. (Clarendon Press ; Oxford University Press, Oxford : New York, 1978).
63. Davidson, T. J., Kloosterman, F. & Wilson, M. A. Hippocampal Replay of Extended Experience. *Neuron* **63**, 497–507 (2009).
64. Clark, R. E., Broadbent, N. J. & Squire, L. R. Impaired remote spatial memory after hippocampal lesions despite extensive training beginning early in life. *Hippocampus* **15**, 340–346 (2005).
65. Clark, R. E., Broadbent, N. J. & Squire, L. R. The Hippocampus and Spatial Memory: Findings with a Novel Modification of the Water Maze. *J. Neurosci.* **27**, 6647–6654 (2007).
66. Forcelli, P. A. *et al.* Memory loss in a nonnavigational spatial task after hippocampal inactivation in monkeys. *Proc. Natl. Acad. Sci.* **111**, 4315–4320 (2014).
67. Kaut, K. P. & Bunsey, M. D. The effects of lesions to the rat hippocampus or rhinal cortex on olfactory and spatial memory: Retrograde and anterograde findings. *Cogn. Affect. Behav. Neurosci.* **1**, 270–286 (2001).
68. Pastalkova, E., Itskov, V., Amarasingham, A. & Buzsáki, G. Internally Generated Cell Assembly Sequences in the Rat Hippocampus. *Science* **321**, 1322–1327 (2008).
69. Hafting, T., Fyhn, M., Molden, S., Moser, M.-B. & Moser, E. I. Microstructure of a spatial map in the entorhinal cortex. *Nature* **436**, 801–806 (2005).
70. O'Keefe, J. & Burgess, N. Dual phase and rate coding in hippocampal place cells: Theoretical significance and relationship to entorhinal grid cells. *Hippocampus* **15**, 853–866 (2005).

71. Muller, R. & Kubie, J. The effects of changes in the environment on the spatial firing of hippocampal complex-spike cells. *J. Neurosci.* **7**, 1951–1968 (1987).
72. Ruth, R. E., Collier, T. J. & Routtenberg, A. Topographical relationship between the entorhinal cortex and the septotemporal axis of the dentate gyrus in rats: II. Cells projecting from lateral entorhinal subdivision. *J. Comp. Neurol.* **270**, 506–516 (1988).
73. Wang, M. *et al.* Neuronal basis of age-related working memory decline. *Nature* **476**, 210–213 (2011).
74. Funahashi, S., Bruce, C. J. & Goldman-Rakic, P. S. Mnemonic coding of visual space in the monkey's dorsolateral prefrontal cortex. *J. Neurophysiol.* **61**, 331–349 (1989).
75. Milad, M. R. & Quirk, G. J. Neurons in medial prefrontal cortex signal memory for fear extinction. *Nature* **420**, 70–74 (2002).
76. Miller, E. K. & Cohen, J. D. An Integrative Theory of Prefrontal Cortex Function. *Annu. Rev. Neurosci.* **24**, 167–202 (2001).
77. Johnston, K., Levin, H. M., Koval, M. J. & Everling, S. Top-Down Control-Signal Dynamics in Anterior Cingulate and Prefrontal Cortex Neurons following Task Switching. *Neuron* **53**, 453–462 (2007).
78. Pouget, A., Dayan, P. & Zemel, R. Information processing with population codes. *Nat. Rev. Neurosci.* **1**, 125–132 (2000).
79. Georgopoulos, A. P., Schwartz, A. B. & Kettner, R. E. Neuronal Population Coding of Movement Direction. *Science* **233**, 1416–1419 (1986).
80. Usrey, W. M. & Reid, R. C. SYNCHRONOUS ACTIVITY IN THE VISUAL SYSTEM. *Annu. Rev. Physiol.* **61**, 435–456 (1999).
81. Tolhurst, D. J., Movshon, J. A. & Dean, A. F. The statistical reliability of signals in single neurons in cat and monkey visual cortex. *Vision Res.* **23**, 775–785 (1983).
82. Salinas, E. & Abbott, L. F. Vector reconstruction from firing rates. *J. Comput. Neurosci.* **1**, 89–107 (1994).
83. Atallah, B. V., Bruns, W., Carandini, M. & Scanziani, M. Parvalbumin-Expressing Interneurons Linearly Transform Cortical Responses to Visual Stimuli. *Neuron* **73**, 159–170 (2012).

84. Adesnik, H. Synaptic Mechanisms of Feature Coding in the Visual Cortex of Awake Mice. *Neuron* **95**, 1147–1159.e4 (2017).
85. Adesnik, H. Layer-specific excitation/inhibition balances during neuronal synchronization in the visual cortex. *J. Physiol.* **596**, 1639–1657 (2018).
86. Aertsen, A. & Braitenberg, V. *Brain Theory: Biological Basis and Computational Principles*. (Elsevier, Amsterdam; New York, 1996).
87. Carr, M. F., Jadhav, S. P. & Frank, L. M. Hippocampal replay in the awake state: a potential substrate for memory consolidation and retrieval. *Nat. Neurosci.* **14**, 147–153 (2011).
88. Anderson, J. S., Carandini, M. & Ferster, D. Orientation Tuning of Input Conductance, Excitation, and Inhibition in Cat Primary Visual Cortex. *J. Neurophysiol.* **84**, 909–926 (2000).
89. Li, Y. -t., Liu, B. -h., Chou, X. -l., Zhang, L. I. & Tao, H. W. Synaptic Basis for Differential Orientation Selectivity between Complex and Simple Cells in Mouse Visual Cortex. *J. Neurosci.* **35**, 11081–11093 (2015).
90. Li, Y., Ma, W., Pan, C., Zhang, L. I. & Tao, H. W. Broadening of Cortical Inhibition Mediates Developmental Sharpening of Orientation Selectivity. *J. Neurosci.* **32**, 3981–3991 (2012).
91. Rubin, D. B., Van Hooser, S. D. & Miller, K. D. The Stabilized Supralinear Network: A Unifying Circuit Motif Underlying Multi-Input Integration in Sensory Cortex. *Neuron* **85**, 402–417 (2015).
92. França, T. F. A. & Monserrat, J. M. Hippocampal place cells are topographically organized, but physical space has nothing to do with it. *Brain Struct. Funct.* **224**, 3019–3029 (2019).
93. Lalani, S. J. *et al.* Impaired Behavioral Pattern Separation in Refractory Temporal Lobe Epilepsy and Mild Cognitive Impairment. *J. Int. Neuropsychol. Soc.* **28**, 550–562 (2022).
94. Lohnas, L. J. *et al.* Time-resolved neural reinstatement and pattern separation during memory decisions in human hippocampus. *Proc. Natl. Acad. Sci.* **115**, (2018).
95. Leutgeb, J. K., Leutgeb, S., Moser, M.-B. & Moser, E. I. Pattern Separation in the Dentate Gyrus and CA3 of the Hippocampus. *Science* **315**, 961–966 (2007).

96. Bakker, A., Kirwan, C. B., Miller, M. & Stark, C. E. L. Pattern Separation in the Human Hippocampal CA3 and Dentate Gyrus. *Science* **319**, 1640–1642 (2008).
97. Wesnes, K. A., Annas, P., Basun, H., Edgar, C. & Blennow, K. Performance on a pattern separation task by Alzheimer’s patients shows possible links between disrupted dentate gyrus activity and apolipoprotein E  $\epsilon$ 4 status and cerebrospinal fluid amyloid- $\beta$ 42 levels. *Alzheimers Res. Ther.* **6**, 20 (2014).
98. Reyes, A. *et al.* Impaired spatial pattern separation performance in temporal lobe epilepsy is associated with visuospatial memory deficits and hippocampal volume loss. *Neuropsychologia* **111**, 209–215 (2018).
99. Madar, A. D., Ewell, L. A. & Jones, M. V. Pattern separation of spiketrains in hippocampal neurons. *Sci. Rep.* **9**, 5282 (2019).
100. Madar, A. D. *et al.* Deficits in Behavioral and Neuronal Pattern Separation in Temporal Lobe Epilepsy. Preprint at <https://doi.org/10.1101/2020.02.13.948364> (2020).
101. Baddeley, A. D. & Logie, R. H. Working Memory: The Multiple-Component Model. in *Models of Working Memory* (eds. Miyake, A. & Shah, P.) 28–61 (Cambridge University Press, 1999). doi:10.1017/CBO9781139174909.005.
102. Sreenivasan, K. K., Curtis, C. E. & D’Esposito, M. Revisiting the role of persistent neural activity during working memory. *Trends Cogn. Sci.* **18**, 82–89 (2014).
103. Sarma, A., Masse, N. Y., Wang, X.-J. & Freedman, D. J. Task-specific versus generalized mnemonic representations in parietal and prefrontal cortices. *Nat. Neurosci.* **19**, 143–149 (2016).
104. Masse, N. Y., Hodnefield, J. M. & Freedman, D. J. Mnemonic Encoding and Cortical Organization in Parietal and Prefrontal Cortices. *J. Neurosci.* **37**, 6098–6112 (2017).
105. Emrich, S. M., Riggall, A. C., LaRocque, J. J. & Postle, B. R. Distributed Patterns of Activity in Sensory Cortex Reflect the Precision of Multiple Items Maintained in Visual Short-Term Memory. *J. Neurosci.* **33**, 6516–6523 (2013).
106. Wasmuht, D. F., Spaak, E., Buschman, T. J., Miller, E. K. & Stokes, M. G. Intrinsic neuronal dynamics predict distinct functional roles during working memory. *Nat. Commun.* **9**, 3499 (2018).

107. Lundqvist, M. *et al.* Gamma and Beta Bursts Underlie Working Memory. *Neuron* **90**, 152–164 (2016).
108. Lundqvist, M., Herman, P., Warden, M. R., Brincat, S. L. & Miller, E. K. Gamma and beta bursts during working memory readout suggest roles in its volitional control. *Nat. Commun.* **9**, 394 (2018).
109. Wang, X.-J. Neurophysiological and Computational Principles of Cortical Rhythms in Cognition. *Physiol. Rev.* **90**, 1195–1268 (2010).
110. Antonovsky, A. *Unraveling the Mystery of Health: How People Manage Stress and Stay Well*. xx, 218 (Jossey-Bass, San Francisco, CA, US, 1987).
111. Buzsáki, G. Theta Oscillations in the Hippocampus. *Neuron* **33**, 325–340 (2002).
112. Buzsáki, G. Theta rhythm of navigation: Link between path integration and landmark navigation, episodic and semantic memory. *Hippocampus* **15**, 827–840 (2005).
113. Petsche, H., Stumpf, Ch. & Gogolak, G. The significance of the rabbit's septum as a relay station between the midbrain and the hippocampus I. The control of hippocampus arousal activity by the septum cells. *Electroencephalogr. Clin. Neurophysiol.* **14**, 202–211 (1962).
114. Smith, H. R. & Pang, K. C. H. Orexin-saporin lesions of the medial septum impair spatial memory. *Neuroscience* **132**, 261–271 (2005).
115. Dwyer, T. A., Servatius, R. J. & Pang, K. C. H. Noncholinergic Lesions of the Medial Septum Impair Sequential Learning of Different Spatial Locations. *J. Neurosci.* **27**, 299–303 (2007).
116. Cañas, A., Juncadella, M., Lau, R., Gabarrós, A. & Hernández, M. Working Memory Deficits After Lesions Involving the Supplementary Motor Area. *Front. Psychol.* **9**, 765 (2018).
117. Montgomery, S. M. & Buzsáki, G. Gamma oscillations dynamically couple hippocampal CA3 and CA1 regions during memory task performance. *Proc. Natl. Acad. Sci.* **104**, 14495–14500 (2007).
118. Buzsáki, G. & Wang, X.-J. Mechanisms of Gamma Oscillations. *Annu. Rev. Neurosci.* **35**, 203–225 (2012).

119. Trevelyan, A. J., Bruns, W., Mann, E. O., Crepel, V. & Scanziani, M. The information content of physiological and epileptic brain activity. *J. Physiol.* **591**, 799–805 (2013).
120. Bragin, A. *et al.* Gamma (40-100 Hz) oscillation in the hippocampus of the behaving rat. *J. Neurosci.* **15**, 47–60 (1995).
121. Colgin, L. L. *et al.* Frequency of gamma oscillations routes flow of information in the hippocampus. *Nature* **462**, 353–357 (2009).
122. Tukker, J. J. *et al.* Distinct Dendritic Arborization and *In Vivo* Firing Patterns of Parvalbumin-Expressing Basket Cells in the Hippocampal Area CA3. *J. Neurosci.* **33**, 6809–6825 (2013).
123. Harris, K. D. *et al.* Spike train dynamics predicts theta-related phase precession in hippocampal pyramidal cells. *Nature* **417**, 738–741 (2002).
124. Klausberger, T. & Somogyi, P. Neuronal Diversity and Temporal Dynamics: The Unity of Hippocampal Circuit Operations. *Science* **321**, 53–57 (2008).
125. O’Keefe, J. & Recce, M. L. Phase relationship between hippocampal place units and the EEG theta rhythm. *Hippocampus* **3**, 317–330 (1993).
126. Skaggs, W. E., McNaughton, B. L., Wilson, M. A. & Barnes, C. A. Theta phase precession in hippocampal neuronal populations and the compression of temporal sequences. *Hippocampus* **6**, 149–172 (1996).
127. Magee, J. C. & Johnston, D. A Synaptically Controlled, Associative Signal for Hebbian Plasticity in Hippocampal Neurons. *Science* **275**, 209–213 (1997).
128. MacDonald, C. J., Lepage, K. Q., Eden, U. T. & Eichenbaum, H. Hippocampal “Time Cells” Bridge the Gap in Memory for Discontiguous Events. *Neuron* **71**, 737–749 (2011).
129. Eichenbaum, H. Elements of Information Processing in Hippocampal Neuronal Activity: Space, Time, and Memory. in *The Hippocampus from Cells to Systems* (eds. Hannula, D. E. & Duff, M. C.) 69–94 (Springer International Publishing, Cham, 2017). doi:10.1007/978-3-319-50406-3\_3.
130. Umbach, G. *et al.* Time cells in the human hippocampus and entorhinal cortex support episodic memory. *Proc. Natl. Acad. Sci.* **117**, 28463–28474 (2020).
131. Fries, P. A mechanism for cognitive dynamics: neuronal communication through neuronal coherence. *Trends Cogn. Sci.* **9**, 474–480 (2005).

132. Buzsáki, G. Neural Syntax: Cell Assemblies, Synapsembles, and Readers. *Neuron* **68**, 362–385 (2010).
133. DeCoteau, W. E. *et al.* Learning-related coordination of striatal and hippocampal theta rhythms during acquisition of a procedural maze task. *Proc. Natl. Acad. Sci.* **104**, 5644–5649 (2007).
134. Stout, J. J., George, A. E., Kim, S., Hallock, H. L. & Griffin, A. L. Using synchronized brain rhythms to bias memory-guided decisions. Preprint at <https://doi.org/10.7554/eLife.92033.2> (2024).
135. Gregoriou, G. G., Gotts, S. J., Zhou, H. & Desimone, R. High-Frequency, Long-Range Coupling Between Prefrontal and Visual Cortex During Attention. *Science* **324**, 1207–1210 (2009).
136. Fell, J. *et al.* Human memory formation is accompanied by rhinal–hippocampal coupling and decoupling. *Nat. Neurosci.* **4**, 1259–1264 (2001).
137. Siegel, M., Donner, T. H. & Engel, A. K. Spectral fingerprints of large-scale neuronal interactions. *Nat. Rev. Neurosci.* **13**, 121–134 (2012).
138. Spencer, K. M. *et al.* Abnormal Neural Synchrony in Schizophrenia. *J. Neurosci.* **23**, 7407–7411 (2003).
139. Herrmann, C. & Demiralp, T. Human EEG gamma oscillations in neuropsychiatric disorders. *Clin. Neurophysiol.* **116**, 2719–2733 (2005).
140. Lega, B. C., Jacobs, J. & Kahana, M. Human hippocampal theta oscillations and the formation of episodic memories. *Hippocampus* **22**, 748–761 (2012).
141. Barry, R. J. & Clarke, A. R. Resting state brain oscillations and symptom profiles in attention deficit/hyperactivity disorder. in *Supplements to Clinical Neurophysiology* vol. 62 275–287 (Elsevier, 2013).
142. Inostroza, M., Brotons-Mas, J. R., Laurent, F., Cid, E. & De La Prida, L. M. Specific Impairment of “What-Where-When” Episodic-Like Memory in Experimental Models of Temporal Lobe Epilepsy. *J. Neurosci.* **33**, 17749–17762 (2013).
143. Wang, J. *et al.* Enhanced Gamma Activity and Cross-Frequency Interaction of Resting-State Electroencephalographic Oscillations in Patients with Alzheimer’s Disease. *Front. Aging Neurosci.* **9**, 243 (2017).
144. *Neuroscience*. (Sinauer Associates, Sunderland, Mass, 2001).

145. Citri, A. & Malenka, R. C. Synaptic Plasticity: Multiple Forms, Functions, and Mechanisms. *Neuropsychopharmacology* **33**, 18–41 (2008).
146. Rotenberg, A., Mayford, M., Hawkins, R. D., Kandel, E. R. & Muller, R. U. Mice Expressing Activated CaMKII Lack Low Frequency LTP and Do Not Form Stable Place Cells in the CA1 Region of the Hippocampus. *Cell* **87**, 1351–1361 (1996).
147. Kentros, C. *et al.* Abolition of Long-Term Stability of New Hippocampal Place Cell Maps by NMDA Receptor Blockade. *Science* **280**, 2121–2126 (1998).
148. Barry, J. M. *et al.* Inhibition of Protein Kinase M $\zeta$  Disrupts the Stable Spatial Discharge of Hippocampal Place Cells in a Familiar Environment. *J. Neurosci.* **32**, 13753–13762 (2012).
149. Schoenenberger, P., O’Neill, J. & Csicsvari, J. Activity-dependent plasticity of hippocampal place maps. *Nat. Commun.* **7**, 11824 (2016).
150. Knierim, J. J. Synaptic Plasticity and Place Cell Formation. in *Encyclopedia of Neuroscience* 735–740 (Elsevier, 2009). doi:10.1016/B978-008045046-9.00830-5.
151. Derdikman, D. & Moser, E. I. A Manifold of Spatial Maps in the Brain. in *Space, Time and Number in the Brain* 41–57 (Elsevier, 2011). doi:10.1016/B978-0-12-385948-8.00004-9.
152. Ashby, D. M. *et al.* LTD is involved in the formation and maintenance of rat hippocampal CA1 place-cell fields. *Nat. Commun.* **12**, 100 (2021).
153. Sun, L. *et al.* Inhibition of protein phosphatase 2A- and protein phosphatase 1-induced tau hyperphosphorylation and impairment of spatial memory retention in rats. *Neuroscience* **118**, 1175–1182 (2003).
154. Ge, Y. *et al.* Hippocampal long-term depression is required for the consolidation of spatial memory. *Proc. Natl. Acad. Sci.* **107**, 16697–16702 (2010).
155. Blackman, A. V., Abrahamsson, T., Costa, R. P., Lalanne, T. & Sjöström, P. J. Target-cell-specific short-term plasticity in local circuits. *Front. Synaptic Neurosci.* **5**, (2013).
156. Tsodyks, tMisha, Uziel, A. & Markram, H. Synchrony Generation in Recurrent Networks with Frequency-Dependent Synapses. *J. Neurosci.* **20**, RC50–RC50 (2000).

157. Deng, P.-Y. & Klyachko, V. A. The diverse functions of short-term plasticity components in synaptic computations. *Commun. Integr. Biol.* **4**, 543–548 (2011).
158. Shouval, H., H. Wang, S. S. & M. Wittenberg, G. Spike timing dependent plasticity: a consequence of more fundamental learning rules. *Front. Comput. Neurosci.* (2010) doi:10.3389/fncom.2010.00019.
159. Rahman, N. A. & Yusoff, N. Modulated spike-time dependent plasticity (STDP)-based learning for spiking neural network (SNN): A review. *Neurocomputing* **618**, 129170 (2025).
160. Caporale, N. & Dan, Y. Spike Timing–Dependent Plasticity: A Hebbian Learning Rule. *Annu. Rev. Neurosci.* **31**, 25–46 (2008).
161. Turrigiano, G. G. The Self-Tuning Neuron: Synaptic Scaling of Excitatory Synapses. *Cell* **135**, 422–435 (2008).
162. Davis, G. W. HOMEOSTATIC CONTROL OF NEURAL ACTIVITY: From Phenomenology to Molecular Design. *Annu. Rev. Neurosci.* **29**, 307–323 (2006).
163. Elger, C. E., Helmstaedter, C. & Kurthen, M. Chronic epilepsy and cognition. *Lancet Neurol.* **3**, 663–672 (2004).
164. Berg, A. T. *et al.* Special education needs of children with newly diagnosed epilepsy. *Dev. Med. Child Neurol.* **47**, 749 (2005).
165. Austin, J. K. *et al.* Recurrent Seizures and Behavior Problems in Children with First Recognized Seizures: A Prospective Study. *Epilepsia* **43**, 1564–1573 (2002).
166. Ostrom, K. J. *et al.* Not Only a Matter of Epilepsy: Early Problems of Cognition and Behavior in Children With “Epilepsy Only”—A Prospective, Longitudinal, Controlled Study Starting at Diagnosis. *Pediatrics* **112**, 1338–1344 (2003).
167. Keezer, M. R., Sisodiya, S. M. & Sander, J. W. Comorbidities of epilepsy: current concepts and future perspectives. *Lancet Neurol.* **15**, 106–115 (2016).
168. Hermann, B. P. *et al.* Neurobehavioural comorbidities of epilepsy: towards a network-based precision taxonomy. *Nat. Rev. Neurol.* **17**, 731–746 (2021).

169. Oyegbile, T. O. *et al.* The nature and course of neuropsychological morbidity in chronic temporal lobe epilepsy. *Neurology* **62**, 1736–1742 (2004).
170. Rayner, G., Jackson, G. D. & Wilson, S. J. Mechanisms of memory impairment in epilepsy depend on age at disease onset. *Neurology* **87**, 1642–1649 (2016).
171. Gauffin, H. *et al.* Similar Profile and Magnitude of Cognitive Impairments in Focal and Generalized Epilepsy: A Pilot Study. *Front. Neurol.* **12**, 746381 (2022).
172. Chauvière, L. *et al.* Early Deficits in Spatial Memory and Theta Rhythm in Experimental Temporal Lobe Epilepsy. *J. Neurosci.* **29**, 5402–5410 (2009).
173. Karnam, H. B. *et al.* Early life seizures cause long-standing impairment of the hippocampal map. *Exp. Neurol.* **217**, 378–387 (2009).
174. Liu, X. *et al.* Seizure-Induced Changes in Place Cell Physiology: Relationship to Spatial Memory. *J. Neurosci.* **23**, 11505–11515 (2003).
175. Ewell, L. A., Fischer, K. B., Leibold, C., Leutgeb, S. & Leutgeb, J. K. The impact of pathological high-frequency oscillations on hippocampal network activity in rats with chronic epilepsy. *eLife* **8**, e42148 (2019).
176. Brun, V. H. *et al.* Impaired Spatial Representation in CA1 after Lesion of Direct Input from Entorhinal Cortex. *Neuron* **57**, 290–302 (2008).
177. Davoudi, H. & Foster, D. J. Acute silencing of hippocampal CA3 reveals a dominant role in place field responses. *Nat. Neurosci.* **22**, 337–342 (2019).
178. Tyler, A. L. *et al.* Functional Network Changes in Hippocampal CA1 after Status Epilepticus Predict Spatial Memory Deficits in Rats. *J. Neurosci.* **32**, 11365–11376 (2012).
179. Yu, J. Y. & Frank, L. M. Hippocampal–cortical interaction in decision making. *Neurobiol. Learn. Mem.* **117**, 34–41 (2015).
180. Nash, M. I., Hodges, C. B., Muncy, N. M. & Kirwan, C. B. Pattern separation beyond the hippocampus: A HIGH-RESOLUTION WHOLE-BRAIN investigation of mnemonic discrimination in healthy adults. *Hippocampus* **31**, 408–421 (2021).
181. Bakker, A. *et al.* Reduction of Hippocampal Hyperactivity Improves Cognition in Amnesic Mild Cognitive Impairment. *Neuron* **74**, 467–474 (2012).

182. Brock Kirwan, C. *et al.* Pattern separation deficits following damage to the hippocampus. *Neuropsychologia* **50**, 2408–2414 (2012).
183. Yassa, M. A. *et al.* High-resolution structural and functional MRI of hippocampal CA3 and dentate gyrus in patients with amnesic Mild Cognitive Impairment. *NeuroImage* **51**, 1242–1252 (2010).
184. Bui, A. D. *et al.* Dentate gyrus mossy cells control spontaneous convulsive seizures and spatial memory. *Science* **359**, 787–790 (2018).
185. Bernhardt, B. C., Hong, S., Bernasconi, A. & Bernasconi, N. Magnetic resonance imaging pattern learning in temporal lobe epilepsy: Classification and prognostics. *Ann. Neurol.* **77**, 436–446 (2015).
186. Yilmazer-Hanke, D. M. *et al.* Subregional Pathology of the Amygdala Complex and Entorhinal Region in Surgical Specimens From Patients With Pharmacoresistant Temporal Lobe Epilepsy. *J. Neuropathol. Exp. Neurol.* **59**, 907–920 (2000).
187. Bothwell, S. *et al.* Neuronal Hypertrophy in the Neocortex of Patients with Temporal Lobe Epilepsy. *J. Neurosci.* **21**, 4789–4800 (2001).
188. Blanc, F. *et al.* Investigation of widespread neocortical pathology associated with hippocampal sclerosis in epilepsy: A postmortem study: Cortical Pathology in Hippocampal Sclerosis. *Epilepsia* **52**, 10–21 (2011).
189. Sinjab, B., Martinian, L., Sisodiya, S. M. & Thom, M. Regional thalamic neuropathology in patients with hippocampal sclerosis and epilepsy: A postmortem study. *Epilepsia* **54**, 2125–2133 (2013).
190. Tai, X. Y. *et al.* Review: Neurodegenerative processes in temporal lobe epilepsy with hippocampal sclerosis: Clinical, pathological and neuroimaging evidence. *Neuropathol. Appl. Neurobiol.* **44**, 70–90 (2018).
191. Cendes, F. *et al.* MRI volumetric measurement of amygdala and hippocampus in temporal lobe epilepsy. *Neurology* **43**, 719–719 (1993).
192. Bernasconi, N. *et al.* Entorhinal cortex atrophy in epilepsy patients exhibiting normal hippocampal volumes. *Neurology* **56**, 1335–1339 (2001).
193. Bernasconi, N. *et al.* Mesial temporal damage in temporal lobe epilepsy: a volumetric MRI study of the hippocampus, amygdala and parahippocampal region. *Brain* **126**, 462–469 (2003).

194. Bernhardt, B. C., Bonilha, L. & Gross, D. W. Network analysis for a network disorder: The emerging role of graph theory in the study of epilepsy. *Epilepsy Behav.* **50**, 162–170 (2015).
195. Bernhardt, B. C. *et al.* Longitudinal and cross-sectional analysis of atrophy in pharmaco-resistant temporal lobe epilepsy. *Neurology* **72**, 1747–1754 (2009).
196. Bernhardt, B. C., Kim, H. & Bernasconi, N. Patterns of subregional mesiotemporal disease progression in temporal lobe epilepsy. *Neurology* **81**, 1840–1847 (2013).
197. Coan, A. C., Appenzeller, S., Bonilha, L., Li, L. M. & Cendes, F. Seizure frequency and lateralization affect progression of atrophy in temporal lobe epilepsy. *Neurology* **73**, 834–842 (2009).
198. Concha, L., Beaulieu, C. & Gross, D. W. Bilateral limbic diffusion abnormalities in unilateral temporal lobe epilepsy. *Ann. Neurol.* **57**, 188–196 (2005).
199. Yogarajah, M. & Duncan, J. S. Diffusion-based magnetic resonance imaging and tractography in epilepsy. *Epilepsia* **49**, 189–200 (2008).
200. Bonilha, L. *et al.* Extrahippocampal gray matter loss and hippocampal deafferentation in patients with temporal lobe epilepsy. *Epilepsia* **51**, 519–528 (2010).
201. Hermann, B. *et al.* Network, clinical and sociodemographic features of cognitive phenotypes in temporal lobe epilepsy. *NeuroImage Clin.* **27**, 102341 (2020).
202. Bernhardt, B. C. *et al.* Mapping limbic network organization in temporal lobe epilepsy using morphometric correlations: Insights on the relation between mesiotemporal connectivity and cortical atrophy. *NeuroImage* **42**, 515–524 (2008).
203. Mueller, S. G. *et al.* Widespread neocortical abnormalities in temporal lobe epilepsy with and without mesial sclerosis. *NeuroImage* **46**, 353–359 (2009).
204. Mueller, S. G. *et al.* Involvement of the thalamocortical network in TLE with and without mesiotemporal sclerosis. *Epilepsia* **51**, 1436–1445 (2010).
205. Bettus, G. *et al.* Role of resting state functional connectivity MRI in presurgical investigation of mesial temporal lobe epilepsy. *J. Neurol. Neurosurg. Psychiatry* **81**, 1147–1154 (2010).

206. Pereira, F. R. *et al.* Asymmetrical hippocampal connectivity in mesial temporal lobe epilepsy: evidence from resting state fMRI. *BMC Neurosci.* **11**, 66 (2010).
207. Zhang, C. *et al.* Characteristics of Resting-State Functional Connectivity in Intractable Unilateral Temporal Lobe Epilepsy Patients with Impaired Executive Control Function. *Front. Hum. Neurosci.* **11**, 609 (2017).
208. Zhang, Z. *et al.* Altered spontaneous neuronal activity of the default-mode network in mesial temporal lobe epilepsy. *Brain Res.* **1323**, 152–160 (2010).
209. Zhang, C. *et al.* Impaired prefrontal cortex-thalamus pathway in intractable temporal lobe epilepsy with aberrant executive control function: MRI evidence. *Clin. Neurophysiol.* **130**, 484–490 (2019).
210. Liao, W. *et al.* Default mode network abnormalities in mesial temporal lobe epilepsy: A study combining fMRI and DTI. *Hum. Brain Mapp.* **32**, 883–895 (2011).
211. Pittau, F., Grova, C., Moeller, F., Dubeau, F. & Gotman, J. Patterns of altered functional connectivity in mesial temporal lobe epilepsy. *Epilepsia* **53**, 1013–1023 (2012).
212. Haneef, Z. *et al.* Functional connectivity of hippocampal networks in temporal lobe epilepsy. *Epilepsia* **55**, 137–145 (2014).
213. Bettus, G. *et al.* Decreased basal fMRI functional connectivity in epileptogenic networks and contralateral compensatory mechanisms. *Hum. Brain Mapp.* **30**, 1580–1591 (2009).
214. Morgan, V. L., Rogers, B. P., Sonmezturk, H. H., Gore, J. C. & Abou-Khalil, B. Cross hippocampal influence in mesial temporal lobe epilepsy measured with high temporal resolution functional magnetic resonance imaging: Cross Hippocampal fMRI Influence in mTLE. *Epilepsia* **52**, 1741–1749 (2011).
215. Bai, X. *et al.* Resting functional connectivity between the hemispheres in childhood absence epilepsy. *Neurology* **76**, 1960–1967 (2011).
216. Luo, C. *et al.* Resting state basal ganglia network in idiopathic generalized epilepsy. *Hum. Brain Mapp.* **33**, 1279–1294 (2012).
217. Masterton, R. A., Carney, P. W. & Jackson, G. D. Cortical and thalamic resting-state functional connectivity is altered in childhood absence epilepsy. *Epilepsy Res.* **99**, 327–334 (2012).

218. McGill, M. L. *et al.* Default mode network abnormalities in idiopathic generalized epilepsy. *Epilepsy Behav.* **23**, 353–359 (2012).
219. Yang, T. *et al.* Altered resting-state connectivity during interictal generalized spike-wave discharges in drug-naïve childhood absence epilepsy. *Hum. Brain Mapp.* **34**, 1761–1767 (2013).
220. Van Diessen, E. *et al.* Brain Network Organization in Focal Epilepsy: A Systematic Review and Meta-Analysis. *PLoS ONE* **9**, e114606 (2014).
221. Vlooswijk, M. C. G. *et al.* Loss of network efficiency associated with cognitive decline in chronic epilepsy. *Neurology* **77**, 938–944 (2011).
222. Vaessen, M. J. *et al.* White Matter Network Abnormalities Are Associated with Cognitive Decline in Chronic Epilepsy. *Cereb. Cortex* **22**, 2139–2147 (2012).
223. Gauffin, H. *et al.* Impaired language function in generalized epilepsy: Inadequate suppression of the default mode network. *Epilepsy Behav.* **28**, 26–35 (2013).
224. Hampson, M., Driesen, N. R., Skudlarski, P., Gore, J. C. & Constable, R. T. Brain Connectivity Related to Working Memory Performance. *J. Neurosci.* **26**, 13338–13343 (2006).
225. Kelly, A. M. C., Uddin, L. Q., Biswal, B. B., Castellanos, F. X. & Milham, M. P. Competition between functional brain networks mediates behavioral variability. *NeuroImage* **39**, 527–537 (2008).
226. Bernhardt, B. C., Chen, Z., He, Y., Evans, A. C. & Bernasconi, N. Graph-Theoretical Analysis Reveals Disrupted Small-World Organization of Cortical Thickness Correlation Networks in Temporal Lobe Epilepsy. *Cereb. Cortex* **21**, 2147–2157 (2011).
227. Rayner, G., Tailby, C., Jackson, G. & Wilson, S. Looking beyond lesions for causes of neuropsychological impairment in epilepsy. *Neurology* **92**, (2019).
228. Bender, A. C., Luikart, B. W. & Lenck-Santini, P.-P. Cognitive Deficits Associated with Nav1.1 Alterations: Involvement of Neuronal Firing Dynamics and Oscillations. *PLOS ONE* **11**, e0151538 (2016).
229. Kleen, J. K., Scott, R. C., Holmes, G. L. & Lenck-Santini, P. P. Hippocampal interictal spikes disrupt cognition in rats. *Ann. Neurol.* **67**, 250–257 (2010).

230. Kleen, J. K. *et al.* Hippocampal interictal epileptiform activity disrupts cognition in humans. *Neurology* **81**, 18–24 (2013).
231. Suárez, L. M. *et al.* Systemic Injection of Kainic Acid Differently Affects LTP Magnitude Depending on its Epileptogenic Efficiency. *PLoS ONE* **7**, e48128 (2012).
232. Lenz, M., Ben Shimon, M., Deller, T., Vlachos, A. & Maggio, N. Pilocarpine-Induced Status Epilepticus Is Associated with Changes in the Actin-Modulating Protein Synaptopodin and Alterations in Long-Term Potentiation in the Mouse Hippocampus. *Neural Plast.* **2017**, 1–7 (2017).
233. Lynch, M., Sayin, Ü., Bownds, J., Janumpalli, S. & Sutula, T. Long-term consequences of early postnatal seizures on hippocampal learning and plasticity. *Eur. J. Neurosci.* **12**, 2252–2264 (2000).
234. Hernan, A. E. *et al.* Focal epileptiform activity in the prefrontal cortex is associated with long-term attention and sociability deficits. *Neurobiol. Dis.* **63**, 25–34 (2014).
235. Agosta, F. *et al.* Resting state fMRI in Alzheimer’s disease: beyond the default mode network. *Neurobiol. Aging* **33**, 1564–1578 (2012).
236. Wang, Y. *et al.* Altered Default Mode Network Connectivity in Older Adults with Cognitive Complaints and Amnesic Mild Cognitive Impairment. *J. Alzheimers Dis.* **35**, 751–760 (2013).
237. Dickerson, B. C. *et al.* Increased hippocampal activation in mild cognitive impairment compared to normal aging and AD. *Neurology* **65**, 404–411 (2005).
238. Celone, K. A. *et al.* Alterations in Memory Networks in Mild Cognitive Impairment and Alzheimer’s Disease: An Independent Component Analysis. *J. Neurosci.* **26**, 10222–10231 (2006).
239. Hämäläinen, A. *et al.* Increased fMRI responses during encoding in mild cognitive impairment. *Neurobiol. Aging* **28**, 1889–1903 (2007).
240. Busche, M. A. *et al.* Clusters of Hyperactive Neurons Near Amyloid Plaques in a Mouse Model of Alzheimer’s Disease. *Science* **321**, 1686–1689 (2008).
241. Minkeviciene, R. *et al.* Amyloid  $\beta$ -Induced Neuronal Hyperexcitability Triggers Progressive Epilepsy. *J. Neurosci.* **29**, 3453–3462 (2009).

242. Šišková, Z. *et al.* Dendritic Structural Degeneration Is Functionally Linked to Cellular Hyperexcitability in a Mouse Model of Alzheimer's Disease. *Neuron* **84**, 1023–1033 (2014).
243. Tijms, B. M. *et al.* Alzheimer's disease: connecting findings from graph theoretical studies of brain networks. *Neurobiol. Aging* **34**, 2023–2036 (2013).
244. Brier, M. R. *et al.* Functional connectivity and graph theory in preclinical Alzheimer's disease. *Neurobiol. Aging* **35**, 757–768 (2014).
245. Dai, Z. *et al.* Disrupted structural and functional brain networks in Alzheimer's disease. *Neurobiol. Aging* **75**, 71–82 (2019).
246. Salat, D. H. *et al.* White matter pathology isolates the hippocampal formation in Alzheimer's disease. *Neurobiol. Aging* **31**, 244–256 (2010).
247. Sexton, C. E. *et al.* MRI correlates of episodic memory in Alzheimer's disease, mild cognitive impairment, and healthy aging. *Psychiatry Res. Neuroimaging* **184**, 57–62 (2010).
248. Binnewijzend, M. A. A. *et al.* Brain network alterations in Alzheimer's disease measured by Eigenvector centrality in fMRI are related to cognition and CSF biomarkers. *Hum. Brain Mapp.* **35**, 2383–2393 (2014).
249. De Flores, R. *et al.* Medial Temporal Lobe Networks in Alzheimer's Disease: Structural and Molecular Vulnerabilities. *J. Neurosci.* **42**, 2131–2141 (2022).
250. Lorenzini, L. *et al.* Eigenvector centrality dynamics are related to Alzheimer's disease pathological changes in non-demented individuals. *Brain Commun.* **5**, fcad088 (2023).
251. Skouras, S. *et al.* Mechanisms of functional compensation, delineated by eigenvector centrality mapping, across the pathophysiological continuum of Alzheimer's disease. *NeuroImage Clin.* **22**, 101777 (2019).
252. Ingala, S. *et al.* Amyloid-driven disruption of default mode network connectivity in cognitively healthy individuals. *Brain Commun.* **3**, fcab201 (2021).
253. Greicius, M. D., Srivastava, G., Reiss, A. L. & Menon, V. Default-mode network activity distinguishes Alzheimer's disease from healthy aging: Evidence from functional MRI. *Proc. Natl. Acad. Sci.* **101**, 4637–4642 (2004).

254. Buckner, R. L. *et al.* Molecular, Structural, and Functional Characterization of Alzheimer's Disease: Evidence for a Relationship between Default Activity, Amyloid, and Memory. *J. Neurosci.* **25**, 7709–7717 (2005).
255. Buckner, R. L., Andrews-Hanna, J. R. & Schacter, D. L. The Brain's Default Network: Anatomy, Function, and Relevance to Disease. *Ann. N. Y. Acad. Sci.* **1124**, 1–38 (2008).
256. Binnewijzend, M. A. A. *et al.* Resting-state fMRI changes in Alzheimer's disease and mild cognitive impairment. *Neurobiol. Aging* **33**, 2018–2028 (2012).
257. Jones, D. T. *et al.* Cascading network failure across the Alzheimer's disease spectrum. *Brain* **139**, 547–562 (2016).
258. Small, S. A., Perera, G. M., DeLapaz, R., Mayeux, R. & Stern, Y. Differential regional dysfunction of the hippocampal formation among elderly with memory decline and Alzheimer's disease. *Ann. Neurol.* **45**, 466–472 (1999).
259. Golby, A. Memory encoding in Alzheimer's disease: an fMRI study of explicit and implicit memory. *Brain* **128**, 773–787 (2005).
260. Pariente, J. *et al.* Alzheimer's patients engage an alternative network during a memory task. *Ann. Neurol.* **58**, 870–879 (2005).
261. Rombouts, S. A. R. B., Barkhof, F., Goekoop, R., Stam, C. J. & Scheltens, P. Altered resting state networks in mild cognitive impairment and mild Alzheimer's disease: An fMRI study. *Hum. Brain Mapp.* **26**, 231–239 (2005).
262. Sperling, R. A. *et al.* Functional Alterations in Memory Networks in Early Alzheimer's Disease. *NeuroMolecular Med.* **12**, 27–43 (2010).
263. Schwindt, G. C. & Black, S. E. Functional imaging studies of episodic memory in Alzheimer's disease: a quantitative meta-analysis. *NeuroImage* **45**, 181–190 (2009).
264. Trinchese, F. *et al.* Progressive age-related development of Alzheimer-like pathology in APP/PS1 mice. *Ann. Neurol.* **55**, 801–814 (2004).
265. Cayzac, S. *et al.* Altered hippocampal information coding and network synchrony in APP-PS1 mice. *Neurobiol. Aging* **36**, 3200–3213 (2015).

266. Zhou, H. *et al.* Disruption of hippocampal neuronal circuit function depends upon behavioral state in the APP/PS1 mouse model of Alzheimer's disease. *Sci. Rep.* **12**, 21022 (2022).
267. Zhao, R., Fowler, S. W., Chiang, A. C. A., Ji, D. & Jankowsky, J. L. Impairments in experience-dependent scaling and stability of hippocampal place fields limit spatial learning in a mouse model of Alzheimer's disease: Impaired Place Field Scaling and Stability in App Mice. *Hippocampus* **24**, 963–978 (2014).
268. Goutagny, R. *et al.* Alterations in hippocampal network oscillations and theta–gamma coupling arise before AB overproduction in a mouse model of Alzheimer's disease. *Eur. J. Neurosci.* **37**, 1896–1902 (2013).
269. Mehak, S. F., Shivakumar, A. B., Kumari, S., Muralidharan, B. & Gangadharan, G. Theta and gamma oscillatory dynamics in mouse models of Alzheimer's disease: A path to prospective therapeutic intervention. *Neurosci. Biobehav. Rev.* **136**, 104628 (2022).
270. Van Den Berg, M., Toen, D., Verhoye, M. & Keliris, G. A. Alterations in theta-gamma coupling and sharp wave-ripple, signs of prodromal hippocampal network impairment in the TgF344-AD rat model. *Front. Aging Neurosci.* **15**, 1081058 (2023).
271. Prabhu, P. *et al.* Abnormal gamma phase-amplitude coupling in the parahippocampal cortex is associated with network hyperexcitability in Alzheimer's disease. *Brain Commun.* **6**, fcae121 (2024).
272. Rodinskaia, D., Radinski, C. & Labuhn, J. EEG coherence as a marker of functional connectivity disruption in Alzheimer's disease. *Aging Health Res.* **2**, 100098 (2022).
273. Yan, S., Yang, X., Yang, H. & Sun, Z. Decreased coherence in the model of the dorsal visual pathway associated with Alzheimer's disease. *Sci. Rep.* **13**, 3495 (2023).
274. Hope, T. *et al.* The structure of wandering in dementia. *Int. J. Geriatr. Psychiatry* **9**, 149–155 (1994).
275. Silva, A. & Martínez, M. C. Spatial memory deficits in Alzheimer's disease and their connection to cognitive maps' formation by place cells and grid cells. *Front. Behav. Neurosci.* **16**, 1082158 (2023).

276. Dicks, E., Van Der Flier, W. M., Scheltens, P., Barkhof, F. & Tijms, B. M. Single-subject gray matter networks predict future cortical atrophy in preclinical Alzheimer's disease. *Neurobiol. Aging* **94**, 71–80 (2020).
277. Katsumi, Y. *et al.* Default mode network tau predicts future clinical decline in atypical early Alzheimer's disease. *Brain* awae327 (2024)  
doi:10.1093/brain/awae327.
278. Gothelf, D. *et al.* Neuroanatomy of fragile X syndrome is associated with aberrant behavior and the fragile X mental retardation protein (FMRP). *Ann. Neurol.* **63**, 40–51 (2008).
279. Hoeft, F. *et al.* Region-specific alterations in brain development in one- to three-year-old boys with fragile X syndrome. *Proc. Natl. Acad. Sci.* **107**, 9335–9339 (2010).
280. Lightbody, A. A. & Reiss, A. L. Gene, brain, and behavior relationships in fragile X syndrome: Evidence from neuroimaging studies. *Dev. Disabil. Res. Rev.* **15**, 343–352 (2009).
281. Hollander, E. *et al.* Striatal Volume on Magnetic Resonance Imaging and Repetitive Behaviors in Autism. *Biol. Psychiatry* **58**, 226–232 (2005).
282. Langen, M. *et al.* Changes in the Development of Striatum Are Involved in Repetitive Behavior in Autism. *Biol. Psychiatry* **76**, 405–411 (2014).
283. Qiu, T. *et al.* Two years changes in the development of caudate nucleus are involved in restricted repetitive behaviors in 2–5-year-old children with autism spectrum disorder. *Dev. Cogn. Neurosci.* **19**, 137–143 (2016).
284. Sandoval, G. M. *et al.* Neuroanatomical abnormalities in fragile X syndrome during the adolescent and young adult years. *J. Psychiatr. Res.* **107**, 138–144 (2018).
285. Dalton, K. M., Holsen, L., Abbeduto, L. & Davidson, R. J. Brain function and gaze fixation during facial-emotion processing in fragile X and autism. *Autism Res.* **1**, 231–239 (2008).
286. Comery, T. A. *et al.* Abnormal dendritic spines in fragile X knockout mice: Maturation and pruning deficits. *Proc. Natl. Acad. Sci.* **94**, 5401–5404 (1997).
287. Cruz-Martin, A., Crespo, M. & Portera-Cailliau, C. Delayed Stabilization of Dendritic Spines in Fragile X Mice. *J. Neurosci.* **30**, 7793–7803 (2010).

288. Levenega, J. *et al.* Subregion-specific dendritic spine abnormalities in the hippocampus of Fmr1 KO mice. *Neurobiol. Learn. Mem.* **95**, 467–472 (2011).
289. Hall, S. S., Jiang, H., Reiss, A. L. & Greicius, M. D. Identifying Large-Scale Brain Networks in Fragile X Syndrome. *JAMA Psychiatry* **70**, 1215 (2013).
290. Schmitt, L. M. *et al.* Altered frontal connectivity as a mechanism for executive function deficits in fragile X syndrome. *Mol. Autism* **13**, 47 (2022).
291. Li, R. *et al.* Association of Intrinsic Functional Brain Network and Longitudinal Development of Cognitive Behavioral Symptoms in Young Girls With Fragile X Syndrome. *Biol. Psychiatry* **94**, 814–822 (2023).
292. Radwan, B., Dvorak, D. & Fenton, A. A. Impaired cognitive discrimination and discoordination of coupled theta–gamma oscillations in Fmr1 knockout mice. *Neurobiol. Dis.* **88**, 125–138 (2016).
293. Schmitt, L. M. *et al.* Parallel learning and cognitive flexibility impairments between Fmr1 knockout mice and individuals with fragile X syndrome. *Front. Behav. Neurosci.* **16**, 1074682 (2023).
294. Ouardouz, M. *et al.* Disrupted Hippocampal-Prefrontal Networks in a Rat Model of Fragile X Syndrome: A Study Linking Neural Dynamics to Autism-Like Behavioral Impairments. Preprint at <https://doi.org/10.1101/2024.10.15.617900> (2024).
295. Gonçalves, J. T., Anstey, J. E., Golshani, P. & Portera-Cailliau, C. Circuit level defects in the developing neocortex of Fragile X mice. *Nat. Neurosci.* **16**, 903–909 (2013).
296. Contractor, A., Klyachko, V. A. & Portera-Cailliau, C. Altered Neuronal and Circuit Excitability in Fragile X Syndrome. *Neuron* **87**, 699–715 (2015).
297. Wilson, L. *et al.* The chronic and evolving neurological consequences of traumatic brain injury. *Lancet Neurol.* **16**, 813–825 (2017).
298. Zhang, B.-L. *et al.* Cognitive impairment after traumatic brain injury is associated with reduced long-term depression of excitatory postsynaptic potential in the rat hippocampal dentate gyrus. *Neural Regen. Res.* **13**, 1753 (2018).
299. Semple, B. D., Zamani, A., Rayner, G., Shultz, S. R. & Jones, N. C. Affective, neurocognitive and psychosocial disorders associated with traumatic brain injury and post-traumatic epilepsy. *Neurobiol. Dis.* **123**, 27–41 (2019).

300. Aravind, A., Ravula, A. R., Chandra, N. & Pfister, B. J. Behavioral Deficits in Animal Models of Blast Traumatic Brain Injury. *Front. Neurol.* **11**, 990 (2020).
301. Golub, V. M. & Reddy, D. S. Contusion brain damage in mice for modelling of post-traumatic epilepsy with contralateral hippocampus sclerosis: Comprehensive and longitudinal characterization of spontaneous seizures, neuropathology, and neuropsychiatric comorbidities. *Exp. Neurol.* **348**, 113946 (2022).
302. Ngadimon, I. W. *et al.* An Interplay Between Post-Traumatic Epilepsy and Associated Cognitive Decline: A Systematic Review. *Front. Neurol.* **13**, 827571 (2022).
303. Verellen, R. M. & Cavazos, J. E. Post-traumatic epilepsy: an overview. *Therapy* **7**, 527–531 (2010).
304. Majdan, M. *et al.* Epidemiology of traumatic brain injuries in Europe: a cross-sectional analysis. *Lancet Public Health* **1**, e76–e83 (2016).
305. Dewan, M. C. *et al.* Estimating the global incidence of traumatic brain injury. *J. Neurosurg.* **130**, 1080–1097 (2019).
306. Glushakov, A. V., Glushakova, O. Y., Doré, S., Carney, P. R. & Hayes, R. L. Animal Models of Posttraumatic Seizures and Epilepsy. *Inj. Models Cent. Nerv. Syst.* **1462**, 481–519 (2016).
307. Sharma, S., Tiarks, G., Haight, J. & Bassuk, A. G. Neuropathophysiological Mechanisms and Treatment Strategies for Post-traumatic Epilepsy. *Front. Mol. Neurosci.* **14**, 612073 (2021).
308. Golub, V. M. & Reddy, D. S. Post-Traumatic Epilepsy and Comorbidities: Advanced Models, Molecular Mechanisms, Biomarkers, and Novel Therapeutic Interventions. *Pharmacol. Rev.* **74**, 387–438 (2022).
309. Golarai, G., Greenwood, A. C., Feeney, D. M. & Connor, J. A. Physiological and Structural Evidence for Hippocampal Involvement in Persistent Seizure Susceptibility after Traumatic Brain Injury. *J. Neurosci.* **21**, 8523–8537 (2001).
310. Kharatishvili, I., Nissinen, J. P., McIntosh, T. K. & Pitkänen, A. A model of posttraumatic epilepsy induced by lateral fluid-percussion brain injury in rats. *Neuroscience* **140**, 685–697 (2006).

311. Chrzaszcz, M., Venkatesan, C., Dragisic, T., Watterson, D. M. & Wainwright, M. S. Minoxac Treatment Prevents Increased Seizure Susceptibility in a Mouse “Two-Hit” Model of Closed Skull Traumatic Brain Injury and Electroconvulsive Shock-Induced Seizures. *J. Neurotrauma* **27**, 1283–1295 (2010).
312. Hunt, R. F., Scheff, S. W. & Smith, B. N. Regionally Localized Recurrent Excitation in the Dentate Gyrus of a Cortical Contusion Model of Posttraumatic Epilepsy. *J. Neurophysiol.* **103**, 1490–1500 (2010).
313. Bolkvadze, T. & Pitkänen, A. Development of Post-Traumatic Epilepsy after Controlled Cortical Impact and Lateral Fluid-Percussion-Induced Brain Injury in the Mouse. *J. Neurotrauma* **29**, 789–812 (2012).
314. Kuśmierczak, M., Lajeunesse, F., Grand, L. & Timofeev, I. Changes in long-range connectivity and neuronal reorganization in partial cortical deafferentation model of epileptogenesis. *Neuroscience* **284**, 153–164 (2015).
315. Lillis, K. P. *et al.* Evolution of Network Synchronization during Early Epileptogenesis Parallels Synaptic Circuit Alterations. *J. Neurosci.* **35**, 9920–9934 (2015).
316. Li, L. *et al.* Topographical reorganization of brain functional connectivity during an early period of epileptogenesis. *Epilepsia* **62**, 1231–1243 (2021).
317. Cramer, S. W. *et al.* Wide-field calcium imaging reveals widespread changes in cortical functional connectivity following mild traumatic brain injury in the mouse. *Neurobiol. Dis.* **176**, 105943 (2023).
318. Rubovitch, V. *et al.* A mouse model of blast-induced mild traumatic brain injury. *Exp. Neurol.* **232**, 280–289 (2011).
319. Tweedie, D. *et al.* Changes in mouse cognition and hippocampal gene expression observed in a mild physical- and blast-traumatic brain injury. *Neurobiol. Dis.* **54**, 1–11 (2013).
320. Säljö, A., Svensson, B., Mayorga, M., Hamberger, A. & Bolouri, H. Low-Level Blasts Raise Intracranial Pressure and Impair Cognitive Function in Rats. *J. Neurotrauma* **26**, 1345–1352 (2009).
321. Säljö, A., Bolouri, H., Mayorga, M., Svensson, B. & Hamberger, A. Low-Level Blast Raises Intracranial Pressure and Impairs Cognitive Function in Rats: Prophylaxis with Processed Cereal Feed. *J. Neurotrauma* **27**, 383–389 (2010).

322. Budde, M. D. *et al.* Primary Blast Traumatic Brain Injury in the Rat: Relating Diffusion Tensor Imaging and Behavior. *Front. Neurol.* **4**, (2013).
323. Ning, Y.-L. *et al.* Chronic caffeine exposure attenuates blast-induced memory deficit in mice. *Chin. J. Traumatol.* **18**, 204–211 (2015).
324. Ping, X. & Jin, X. Transition from Initial Hypoactivity to Hyperactivity in Cortical Layer V Pyramidal Neurons after Traumatic Brain Injury *In Vivo*. *J. Neurotrauma* **33**, 354–361 (2016).
325. Koch, P. F. *et al.* Traumatic Brain Injury Preserves Firing Rates But Disrupts Laminar Oscillatory Coupling and Neuronal Entrainment in Hippocampal CA1. *eneuro* **7**, ENEURO.0495-19.2020 (2020).
326. Spellman, T. *et al.* Hippocampal–prefrontal input supports spatial encoding in working memory. *Nature* **522**, 309–314 (2015).
327. Tamura, M., Spellman, T. J., Rosen, A. M., Gogos, J. A. & Gordon, J. A. Hippocampal-prefrontal theta-gamma coupling during performance of a spatial working memory task. *Nat. Commun.* **8**, 2182 (2017).
328. Angelousi, A., Margioris, A. N. & Tsatsanis, C. ACTH Action on the Adrenals. in *Endotext* (eds. Feingold, K. R. et al.) (MDText.com, Inc., South Dartmouth (MA), 2000).
329. Paprocka, J. *et al.* Effectiveness of ACTH in Patients with Infantile Spasms. *Brain Sci.* **12**, 254 (2022).
330. Allen, M. J. & Sharma, S. Physiology, Adrenocorticotrophic Hormone (ACTH). in *StatPearls* (StatPearls Publishing, Treasure Island (FL), 2024).
331. Lightman, S. L., Birnie, M. T. & Conway-Campbell, B. L. Dynamics of ACTH and Cortisol Secretion and Implications for Disease. *Endocr. Rev.* **41**, bnaa002 (2020).
332. Scantlebury, M. H., Chun, K.-C., Ma, S.-C., Rho, J. M. & Kim, D. Y. Adrenocorticotrophic hormone protects learning and memory function in epileptic *Kcna1* -null mice. *Neurosci. Lett.* **645**, 14–18 (2017).
333. Brunson, K. L., Khan, N., Eghbal-Ahmadi, M. & Baram, T. Z. Corticotropin (ACTH) acts directly on amygdala neurons to down-regulate corticotropin-releasing hormone gene expression. *Ann. Neurol.* **49**, 304–312 (2001).

334. Filippenkov, I. B. *et al.* Synthetic Adrenocorticotropin Peptides Modulate the Expression Pattern of Immune Genes in Rat Brain following the Early Post-Stroke Period. *Genes* **14**, 1382 (2023).
335. Filippenkov, I. B. *et al.* ACTH-like Peptides Compensate Rat Brain Gene Expression Profile Disrupted by Ischemia a Day After Experimental Stroke. *Biomedicines* **12**, 2830 (2024).
336. Levitskaya, N. G. *et al.* The Neuroprotective Effects of Semax in Conditions of MPTP-Induced Lesions of the Brain Dopaminergic System. *Neurosci. Behav. Physiol.* **34**, 399–405 (2004).
337. Martins, C. A. *et al.* Neuroprotective effect of ACTH on collagenase-induced peri-intraventricular hemorrhage in newborn male rats. *Sci. Rep.* **10**, 17734 (2020).
338. Hernan, A. E., Alexander, A., Lenck-Santini, P.-P., Scott, R. C. & Holmes, G. L. Attention Deficit Associated with Early Life Interictal Spikes in a Rat Model Is Improved with ACTH. *PLoS ONE* **9**, e89812 (2014).
339. Massey, A. T., Lerner, D. K., Holmes, G. L., Scott, R. C. & Hernan, A. E. ACTH Prevents Deficits in Fear Extinction Associated with Early Life Seizures. *Front. Neurol.* **7**, (2016).
340. Berkovich, R. & Agius, M. A. Mechanisms of action of ACTH in the management of relapsing forms of multiple sclerosis. *Ther. Adv. Neurol. Disord.* **7**, 83–96 (2014).
341. Windebank, A. J., Smith, A. G. & Russell, J. W. The effect of nerve growth factor, ciliary neurotrophic factor, and ACTH analogs on cisplatin neurotoxicity in vitro. *Neurology* **44**, 488–488 (1994).
342. Van Der Zee, C. E. E. M., Van Den Buuse, M. & Gispen, W. H. Beneficial effect of an ACTH-(4-9) analog on peripheral neuropathy and blood pressure response to tyramine in streptozocin diabetic rats. *Eur. J. Pharmacol.* **177**, 211–213 (1990).
343. Moscovitz, A. E. *et al.* The Importance of Melanocortin Receptors and Their Agonists in Pulmonary Disease. *Front. Med.* **6**, 145 (2019).
344. Yeo, G. S. H. *et al.* The melanocortin pathway and energy homeostasis: From discovery to obesity therapy. *Mol. Metab.* **48**, 101206 (2021).

345. Mountjoy, K. G., Robbins, L. S., Mortrud, M. T. & Cone, R. D. The Cloning of a Family of Genes That Encode the Melanocortin Receptors. *Science* **257**, 1248–1251 (1992).
346. Roy, S., Rached, M. & Gallo-Payet, N. Differential Regulation of the Human Adrenocorticotropin Receptor [Melanocortin-2 Receptor (MC2R)] by Human MC2R Accessory Protein Isoforms  $\alpha$  and  $\beta$  in Isogenic Human Embryonic Kidney 293 Cells. *Mol. Endocrinol.* **21**, 1656–1669 (2007).
347. Desarnaud, F., Labbe, O., Eggerickx, D., Vassart, G. & Parmentier, M. Molecular cloning, functional expression and pharmacological characterization of a mouse melanocortin receptor gene. *Biochem. J.* **299**, 367–373 (1994).
348. Gantz, I. *et al.* Molecular cloning, expression, and gene localization of a fourth melanocortin receptor. *J. Biol. Chem.* **268**, 15174–15179 (1993).
349. Farooqi, I. S. *et al.* Clinical Spectrum of Obesity and Mutations in the Melanocortin 4 Receptor Gene. *N. Engl. J. Med.* **348**, 1085–1095 (2003).
350. Wintzen, M. & Gilchrest, B. A. Proopiomelanocortin, Its Derived Peptides, and the Skin. *J. Invest. Dermatol.* **106**, 3–10 (1996).
351. Yang, Y. *et al.* Molecular Determinants of Ligand Binding to the Human Melanocortin-4 Receptor. *Biochemistry* **39**, 14900–14911 (2000).
352. Tao, Y.-X. The Melanocortin-4 Receptor: Physiology, Pharmacology, and Pathophysiology. *Endocr. Rev.* **31**, 506–543 (2010).
353. Zhou, Y. *et al.* Aged Brains Express Less Melanocortin Receptors, Which Correlates with Age-Related Decline of Cognitive Functions. *Molecules* **26**, 6266 (2021).
354. Daniels, Z. S., Nick, T. G., Liu, C., Casedy, A. & Glauser, T. A. Obesity is a common comorbidity for pediatric patients with untreated, newly diagnosed epilepsy. *Neurology* **73**, 658–664 (2009).
355. Sheth, R. D., Goulden, K. J. & Ronen, G. M. Aggression in Children Treated with Clobazam for Epilepsy: *Clin. Neuropharmacol.* **17**, 332–337 (1994).
356. Spaccapelo, L. *et al.* Melanocortin MC4 receptor agonists counteract late inflammatory and apoptotic responses and improve neuronal functionality after cerebral ischemia. *Eur. J. Pharmacol.* **670**, 479–486 (2011).

357. Giuliani, D. *et al.* Melanocortins protect against progression of Alzheimer's disease in triple-transgenic mice by targeting multiple pathophysiological pathways. *Neurobiol. Aging* **35**, 537–547 (2014).
358. Shen, Y. *et al.* Stimulation of the Hippocampal POMC/MC4R Circuit Alleviates Synaptic Plasticity Impairment in an Alzheimer's Disease Model. *Cell Rep.* **17**, 1819–1831 (2016).
359. Ma, K. & McLaurin, J.  $\alpha$ -Melanocyte Stimulating Hormone Prevents GABAergic Neuronal Loss and Improves Cognitive Function in Alzheimer's Disease. *J. Neurosci.* **34**, 6736–6745 (2014).
360. Forslin Aronsson, Å. *et al.*  $\alpha$ -MSH Rescues Neurons from Excitotoxic Cell Death. *J. Mol. Neurosci.* **33**, 239–251 (2007).
361. Zhang, Y. *et al.*  $\alpha$ -Melanocyte-stimulating hormone prevents glutamate excitotoxicity in developing chicken retina via MC4R-mediated down-regulation of microRNA-194. *Sci. Rep.* **5**, 15812 (2015).
362. Shen, Y., Fu, W.-Y., Cheng, E. Y. L., Fu, A. K. Y. & Ip, N. Y. Melanocortin-4 Receptor Regulates Hippocampal Synaptic Plasticity through a Protein Kinase A-Dependent Mechanism. *J. Neurosci.* **33**, 464–472 (2013).
363. Chen, S. *et al.* Activation of melanocortin receptor 4 with RO27-3225 attenuates neuroinflammation through AMPK/JNK/p38 MAPK pathway after intracerebral hemorrhage in mice. *J. Neuroinflammation* **15**, 106 (2018).
364. Chen, S. *et al.* The MC<sub>4</sub> receptor agonist RO27-3225 inhibits NLRP1-dependent neuronal pyroptosis via the ASK1/JNK/p38 MAPK pathway in a mouse model of intracerebral haemorrhage. *Br. J. Pharmacol.* **176**, 1341–1356 (2019).
365. Mastinu, A. *et al.* Melanocortin 4 receptor stimulation improves social deficits in mice through oxytocin pathway. *Neuropharmacology* **133**, 366–374 (2018).
366. Minakova, E. *et al.* Melanotan-II reverses autistic features in a maternal immune activation mouse model of autism. *PLOS ONE* **14**, e0210389 (2019).
367. Peñagarikano, O. *et al.* Exogenous and evoked oxytocin restores social behavior in the *Cntnap2* mouse model of autism. *Sci. Transl. Med.* **7**, (2015).
368. Vasile, F., Dossi, E. & Rouach, N. Human astrocytes: structure and functions in the healthy brain. *Brain Struct. Funct.* **222**, 2017–2029 (2017).

369. Siracusa, R., Fusco, R. & Cuzzocrea, S. Astrocytes: Role and Functions in Brain Pathologies. *Front. Pharmacol.* **10**, 1114 (2019).
370. Vezzani, A. *et al.* Astrocytes in the initiation and progression of epilepsy. *Nat. Rev. Neurol.* **18**, 707–722 (2022).
371. Hubbard, J. A., Szu, J. I., Yonan, J. M. & Binder, D. K. Regulation of astrocyte glutamate transporter-1 (GLT1) and aquaporin-4 (AQP4) expression in a model of epilepsy. *Exp. Neurol.* **283**, 85–96 (2016).
372. Sumadewi, K. T., De Liyis, B. G., Linawati, N. M., Widyadharma, I. P. E. & Astawa, I. N. M. Astrocyte dysregulation as an epileptogenic factor: a systematic review. *Egypt. J. Neurol. Psychiatry Neurosurg.* **60**, 69 (2024).
373. Papadopoulos, M. C. & Verkman, A. S. Aquaporin water channels in the nervous system. *Nat. Rev. Neurosci.* **14**, 265–277 (2013).
374. Verkhratsky, A. & Nedergaard, M. Physiology of Astroglia. *Physiol. Rev.* **98**, 239–389 (2018).
375. Sofroniew, M. V. Molecular dissection of reactive astrogliosis and glial scar formation. *Trends Neurosci.* **32**, 638–647 (2009).
376. Giaume, C., Koulakoff, A., Roux, L., Holcman, D. & Rouach, N. Astroglial networks: a step further in neuroglial and gliovascular interactions. *Nat. Rev. Neurosci.* **11**, 87–99 (2010).
377. Yang, Z. & Wang, K. K. W. Glial fibrillary acidic protein: from intermediate filament assembly and gliosis to neurobiomarker. *Trends Neurosci.* **38**, 364–374 (2015).
378. Liddelow, S. A. & Barres, B. A. Reactive Astrocytes: Production, Function, and Therapeutic Potential. *Immunity* **46**, 957–967 (2017).
379. Pathak, D. & Sriram, K. Neuron-astrocyte omnidirectional signaling in neurological health and disease. *Front. Mol. Neurosci.* **16**, 1169320 (2023).
380. Araque, A. *et al.* Gliotransmitters Travel in Time and Space. *Neuron* **81**, 728–739 (2014).
381. Kimelberg, H. K. & Nedergaard, M. Functions of Astrocytes and their Potential As Therapeutic Targets. *Neurotherapeutics* **7**, 338–353 (2010).
382. De Strooper, B. & Karran, E. The Cellular Phase of Alzheimer’s Disease. *Cell* **164**, 603–615 (2016).

383. Dai, D. L., Li, M. & Lee, E. B. Human Alzheimer's disease reactive astrocytes exhibit a loss of homeostatic gene expression. *Acta Neuropathol. Commun.* **11**, 127 (2023).
384. Kamphuis, W. *et al.* GFAP Isoforms in Adult Mouse Brain with a Focus on Neurogenic Astrocytes and Reactive Astrogliosis in Mouse Models of Alzheimer Disease. *PLoS ONE* **7**, e42823 (2012).
385. Abdelhak, A. *et al.* Blood GFAP as an emerging biomarker in brain and spinal cord disorders. *Nat. Rev. Neurol.* **18**, 158–172 (2022).
386. Kim, K. Y., Shin, K. Y. & Chang, K.-A. GFAP as a Potential Biomarker for Alzheimer's Disease: A Systematic Review and Meta-Analysis. *Cells* **12**, 1309 (2023).
387. Chatterjee, P. *et al.* Plasma glial fibrillary acidic protein in autosomal dominant Alzheimer's disease: Associations with A $\beta$ -PET, neurodegeneration, and cognition. *Alzheimers Dement.* **19**, 2790–2804 (2023).
388. Leipp, F. *et al.* Glial fibrillary acidic protein in Alzheimer's disease: a narrative review. *Brain Commun.* **6**, fcae396 (2024).
389. Olabarria, M., Noristani, H. N., Verkhratsky, A. & Rodríguez, J. J. Concomitant astroglial atrophy and astrogliosis in a triple transgenic animal model of Alzheimer's disease. *Glia* **58**, 831–838 (2010).
390. Hulshof, L. A., Van Nuijs, D., Hol, E. M. & Middeldorp, J. The Role of Astrocytes in Synapse Loss in Alzheimer's Disease: A Systematic Review. *Front. Cell. Neurosci.* **16**, 899251 (2022).
391. Kulijewicz-Nawrot, M., Verkhratsky, A., Chvátal, A., Syková, E. & Rodríguez, J. J. Astrocytic cytoskeletal atrophy in the medial prefrontal cortex of a triple transgenic mouse model of Alzheimer's disease. *J. Anat.* **221**, 252–262 (2012).
392. Makitani, K., Nakagawa, S., Izumi, Y., Akaike, A. & Kume, T. Inhibitory effect of donepezil on bradykinin-induced increase in the intracellular calcium concentration in cultured cortical astrocytes. *J. Pharmacol. Sci.* **134**, 37–44 (2017).
393. Shah, D. *et al.* Astrocyte calcium dysfunction causes early network hyperactivity in Alzheimer's disease. *Cell Rep.* **40**, 111280 (2022).

394. Andersen, J. V. *et al.* Hippocampal disruptions of synaptic and astrocyte metabolism are primary events of early amyloid pathology in the 5xFAD mouse model of Alzheimer's disease. *Cell Death Dis.* **12**, 954 (2021).
395. Weiss, B. E. *et al.* Loss of signaling fidelity between astrocyte endfeet and adjacent cerebral arterioles in an amyloid mouse model of Alzheimer's disease. Preprint at <https://doi.org/10.1101/2025.01.24.634584> (2025).
396. Wasilewski, D. *et al.* Reactive Astrocytes Contribute to Alzheimer's Disease-Related Neurotoxicity and Synaptotoxicity in a Neuron-Astrocyte Co-culture Assay. *Front. Cell. Neurosci.* **15**, 739411 (2022).
397. Vincent, A. J., Gasperini, R., Foa, L. & Small, D. H. Astrocytes in Alzheimer's Disease: Emerging Roles in Calcium Dysregulation and Synaptic Plasticity. *J. Alzheimers Dis.* **22**, 699–714 (2010).
398. Takahashi, K. *et al.* Restored glial glutamate transporter EAAT2 function as a potential therapeutic approach for Alzheimer's disease. *J. Exp. Med.* **212**, 319–332 (2015).
399. Pajarillo, E., Rizor, A., Lee, J., Aschner, M. & Lee, E. The role of astrocytic glutamate transporters GLT-1 and GLAST in neurological disorders: Potential targets for neurotherapeutics. *Neuropharmacology* **161**, 107559 (2019).
400. Brymer, K. J. *et al.* Asymmetric dysregulation of glutamate dynamics across the synaptic cleft in a mouse model of Alzheimer's disease. *Acta Neuropathol. Commun.* **11**, 27 (2023).
401. Mookherjee, P. *et al.* GLT-1 Loss Accelerates Cognitive Deficit Onset in an Alzheimer's Disease Animal Model. *J. Alzheimers Dis.* **26**, 447–455 (2011).
402. Gao, J. *et al.* GLT-1 Knockdown Inhibits Ceftriaxone-Mediated Improvements on Cognitive Deficits, and GLT-1 and xCT Expression and Activity in APP/PS1 AD Mice. *Front. Aging Neurosci.* **12**, 580772 (2020).
403. Andersen, J. V. *et al.* Glutamate metabolism and recycling at the excitatory synapse in health and neurodegeneration. *Neuropharmacology* **196**, 108719 (2021).
404. Fatemi, S. H., Folsom, T. D., Reutiman, T. J. & Lee, S. Expression of astrocytic markers aquaporin 4 and connexin 43 is altered in brains of subjects with autism. *Synapse* **62**, 501–507 (2008).

405. Kajiwara, Y. *et al.* GJA1 (connexin43) is a key regulator of Alzheimer's disease pathogenesis. *Acta Neuropathol. Commun.* **6**, 144 (2018).
406. Xu, Z. *et al.* Deletion of aquaporin-4 in APP/PS1 mice exacerbates brain A $\beta$  accumulation and memory deficits. *Mol. Neurodegener.* **10**, 58 (2015).
407. Dong, R. *et al.* Connexin 43 gap junction-mediated astrocytic network reconstruction attenuates isoflurane-induced cognitive dysfunction in mice. *J. Neuroinflammation* **19**, 64 (2022).
408. Alvarez, J. I., Katayama, T. & Prat, A. Glial influence on the blood brain barrier. *Glia* **61**, 1939–1958 (2013).
409. Oksanen, M. *et al.* Astrocyte alterations in neurodegenerative pathologies and their modeling in human induced pluripotent stem cell platforms. *Cell. Mol. Life Sci.* **76**, 2739–2760 (2019).
410. Liddelow, S. A. *et al.* Neurotoxic reactive astrocytes are induced by activated microglia. *Nature* **541**, 481–487 (2017).
411. Yun, S. P. *et al.* Block of A1 astrocyte conversion by microglia is neuroprotective in models of Parkinson's disease. *Nat. Med.* **24**, 931–938 (2018).
412. Zhang, Y. *et al.* Interaction Between the Glymphatic System and  $\alpha$ -Synuclein in Parkinson's Disease. *Mol. Neurobiol.* **60**, 2209–2222 (2023).
413. Lapshina, K. V. & Ekimova, I. V. Aquaporin-4 and Parkinson's Disease. *Int. J. Mol. Sci.* **25**, 1672 (2024).
414. Chai, H. *et al.* Neural Circuit-Specialized Astrocytes: Transcriptomic, Proteomic, Morphological, and Functional Evidence. *Neuron* **95**, 531-549.e9 (2017).
415. Batiuk, M. Y. *et al.* Identification of region-specific astrocyte subtypes at single cell resolution. *Nat. Commun.* **11**, 1220 (2020).
416. Lin, L.-F. H., Doherty, D. H., Lile, J. D., Bektesh, S. & Collins, F. GDNF: a Glial Cell Line-Derived Neurotrophic Factor for Midbrain Dopaminergic Neurons. *Science* **260**, 1130–1132 (1993).
417. Williams, M. R. *et al.* Neuropathological changes in the nucleus basalis in schizophrenia. *Eur. Arch. Psychiatry Clin. Neurosci.* **263**, 485–495 (2013).

418. Wang, C., Aleksic, B. & Ozaki, N. Glia-related genes and their contribution to schizophrenia. *Psychiatry Clin. Neurosci.* **69**, 448–461 (2015).
419. Katsel, P. *et al.* Astrocyte and Glutamate Markers in the Superficial, Deep, and White Matter Layers of the Anterior Cingulate Gyrus in Schizophrenia. *Neuropsychopharmacology* **36**, 1171–1177 (2011).
420. Toker, L., Mancarci, B. O., Tripathy, S. & Pavlidis, P. Transcriptomic Evidence for Alterations in Astrocytes and Parvalbumin Interneurons in Subjects With Bipolar Disorder and Schizophrenia. *Biol. Psychiatry* **84**, 787–796 (2018).
421. Wu, Y.-F., Sytwu, H.-K. & Lung, F.-W. Polymorphisms in the Human Aquaporin 4 Gene Are Associated With Schizophrenia in the Southern Chinese Han Population: A Case–Control Study. *Front. Psychiatry* **11**, 596 (2020).
422. Zhang, F. *et al.* Blood–Brain Barrier Disruption in Schizophrenia: Insights, Mechanisms, and Future Directions. *Int. J. Mol. Sci.* **26**, 873 (2025).
423. Hu, W., MacDonald, M. L., Elswick, D. E. & Sweet, R. A. The glutamate hypothesis of schizophrenia: evidence from human brain tissue studies. *Ann. N. Y. Acad. Sci.* **1338**, 38–57 (2015).
424. Rimmele, T. S. *et al.* Neuronal Loss of the Glutamate Transporter GLT-1 Promotes Excitotoxic Injury in the Hippocampus. *Front. Cell. Neurosci.* **15**, 788262 (2021).
425. Karlsson, R.-M. *et al.* Assessment of Glutamate Transporter GLAST (EAAT1)-Deficient Mice for Phenotypes Relevant to the Negative and Executive/Cognitive Symptoms of Schizophrenia. *Neuropsychopharmacology* **34**, 1578–1589 (2009).
426. Matos, M. *et al.* Deletion of Adenosine A2A Receptors From Astrocytes Disrupts Glutamate Homeostasis Leading to Psychomotor and Cognitive Impairment: Relevance to Schizophrenia. *Biol. Psychiatry* **78**, 763–774 (2015).
427. Binder, D. K. & Steinhäuser, C. Functional changes in astroglial cells in epilepsy. *Glia* **54**, 358–368 (2006).
428. Barker-Haliski, M. & White, H. S. Glutamatergic Mechanisms Associated with Seizures and Epilepsy. *Cold Spring Harb. Perspect. Med.* **5**, a022863 (2015).

429. Bedner, P. *et al.* Astrocyte uncoupling as a cause of human temporal lobe epilepsy. *Brain* **138**, 1208–1222 (2015).
430. Wilcox, J. M. *et al.* Altered synaptic glutamate homeostasis contributes to cognitive decline in young APP/PSEN1 mice. *Neurobiol. Dis.* **158**, 105486 (2021).
431. Chen, T.-S., Huang, T.-H., Lai, M.-C. & Huang, C.-W. The Role of Glutamate Receptors in Epilepsy. *Biomedicines* **11**, 783 (2023).
432. Heuser, K. *et al.* Variants of the genes encoding AQP4 and Kir4.1 are associated with subgroups of patients with temporal lobe epilepsy. *Epilepsy Res.* **88**, 55–64 (2010).
433. Szu, J. I., Chaturvedi, S., Patel, D. D. & Binder, D. K. Aquaporin-4 Dysregulation in a Controlled Cortical Impact Injury Model of Posttraumatic Epilepsy. *Neuroscience* **428**, 140–153 (2020).
434. Lu, D. C., Zador, Z., Yao, J., Fazlollahi, F. & Manley, G. T. Aquaporin-4 Reduces Post-Traumatic Seizure Susceptibility by Promoting Astrocytic Glial Scar Formation in Mice. *J. Neurotrauma* **38**, 1193–1201 (2021).
435. Rostami, F., Jaafari Suha, A., Janahmadi, M. & Hosseinmardi, N. Aquaporin-4 inhibition attenuates Pentylentetrazole-induced behavioral seizures and cognitive impairments in kindled rats. *Physiol. Behav.* **278**, 114521 (2024).
436. Deshpande, T. *et al.* Constitutive deletion of astrocytic connexins aggravates kainate-induced epilepsy. *Glia* **68**, 2136–2147 (2020).
437. Walrave, L., Vinken, M., Leybaert, L. & Smolders, I. Astrocytic Connexin43 Channels as Candidate Targets in Epilepsy Treatment. *Biomolecules* **10**, 1578 (2020).
438. Bedner, P. & Steinhäuser, C. Role of Impaired Astrocyte Gap Junction Coupling in Epileptogenesis. *Cells* **12**, 1669 (2023).
439. Caruso, C., Carniglia, L., Durand, D., Scimonelli, T. N. & Lasaga, M. Astrocytes: new targets of melanocortin 4 receptor actions. *J. Mol. Endocrinol.* **51**, R33–R50 (2013).
440. Caruso, C. *et al.* Activation of Melanocortin 4 Receptors Reduces the Inflammatory Response and Prevents Apoptosis Induced by Lipopolysaccharide and Interferon- $\gamma$  in Astrocytes. *Endocrinology* **148**, 4918–4926 (2007).

441. Caruso, C. *et al.* Melanocortin 4 receptor activation induces brain-derived neurotrophic factor expression in rat astrocytes through cyclic AMP – Protein kinase A pathway. *Mol. Cell. Endocrinol.* **348**, 47–54 (2012).
442. Caruso, C. *et al.*  $\alpha$ -Melanocyte-stimulating hormone modulates lipopolysaccharide plus interferon- $\gamma$ -induced tumor necrosis factor- $\alpha$  expression but not tumor necrosis factor- $\alpha$  receptor expression in cultured hypothalamic neurons. *J. Neuroimmunol.* **227**, 52–59 (2010).
443. Kamermans, A. *et al.* Setmelanotide, a Novel, Selective Melanocortin Receptor-4 Agonist Exerts Anti-inflammatory Actions in Astrocytes and Promotes an Anti-inflammatory Macrophage Phenotype. *Front. Immunol.* **10**, 2312 (2019).
444. Lisak, R. & Benjamins, J. Melanocortins, Melanocortin Receptors and Multiple Sclerosis. *Brain Sci.* **7**, 104 (2017).
445. Seibenhener, M. L. & Wooten, M. C. Use of the Open Field Maze to measure locomotor and anxiety-like behavior in mice. *J. Vis. Exp. JoVE* e52434 (2015) doi:10.3791/52434.
446. Tatem, K. S. *et al.* Behavioral and locomotor measurements using an open field activity monitoring system for skeletal muscle diseases. *J. Vis. Exp. JoVE* 51785 (2014) doi:10.3791/51785.
447. Faul, F., Erdfelder, E., Lang, A.-G. & Buchner, A. G\*Power 3: A flexible statistical power analysis program for the social, behavioral, and biomedical sciences. *Behav. Res. Methods* **39**, 175–191 (2007).
448. Khalife, M. R. *et al.* Melanocortin 4 Receptor-Dependent Mechanism of ACTH in Preventing Anxiety-Like Behaviors and Normalizing Astrocyte Proteins after Early Life Seizures. *eNeuro* **12**, ENEURO.0564-24.2025 (2025).
449. Fisher, R. S. *et al.* ILAE Official Report: A practical clinical definition of epilepsy. *Epilepsia* **55**, 475–482 (2014).
450. Beghi, E. The Epidemiology of Epilepsy. *Neuroepidemiology* **54**, 185–191 (2020).
451. Ettinger, A. B. *et al.* Symptoms of depression and anxiety in pediatric epilepsy patients. *Epilepsia* **39**, 595–599 (1998).

452. LaGrant, B., Marquis, B. O., Berg, A. T. & Grinspan, Z. M. Depression and anxiety in children with epilepsy and other chronic health conditions: National estimates of prevalence and risk factors. *Epilepsy Behav. EB* **103**, 106828 (2020).
453. Lodhi, S. & Agrawal, N. Neurocognitive problems in epilepsy. *Adv. Psychiatr. Treat.* **18**, 232–240 (2012).
454. Ahmed, G. K., Darwish, A. M., Khalifa, H. & Haridy, N. A. Relationship between Attention Deficit Hyperactivity Disorder and epilepsy: a literature review. *Egypt. J. Neurol. Psychiatry Neurosurg.* **58**, 52 (2022).
455. Sayed, N. M., Aldin, M. T. K., Ali, S. E. & Hendi, A. E. Cognitive functions and epilepsy-related characteristics in patients with generalized tonic–clonic epilepsy: a cross-sectional study. *Middle East Curr. Psychiatry* **30**, 15 (2023).
456. Valeta, T. Psychosocial Impact of Epilepsy. in *The Epilepsy Book: A Companion for Patients: Optimizing Diagnosis and Treatment* (ed. Valeta, T.) 161–166 (Springer International Publishing, Cham, 2017). doi:10.1007/978-3-319-61679-7\_23.
457. Charuvani, A., Ouvrier, R. A., Procopis, P. G., Antony, J. H. & Fagan, E. R. ACTH treatment in intractable seizures of childhood. *Brain Dev.* **14**, 102–106 (1992).
458. Kivity, S. *et al.* Long-term Cognitive Outcomes of a Cohort of Children with Cryptogenic Infantile Spasms Treated with High-dose Adrenocorticotrophic Hormone. *Epilepsia* **45**, 255–262 (2004).
459. Okumura, A. *et al.* ACTH therapy for generalized seizures other than spasms. *Seizure - Eur. J. Epilepsy* **15**, 469–475 (2006).
460. Darke, K. *et al.* Developmental and epilepsy outcomes at age 4 years in the UKISS trial comparing hormonal treatments to vigabatrin for infantile spasms: a multi-centre randomised trial. *Arch. Dis. Child.* **95**, 382–386 (2010).
461. Novoselova, T. V. *et al.* ACTH signalling and adrenal development: lessons from mouse models. (2019) doi:10.1530/EC-19-0190.
462. Brabec, J. L., Ouardouz, M., Mahoney, J. M., Scott, R. C. & Hernan, A. E. Differential regulation of gene expression pathways with dexamethasone and ACTH after early life seizures. *Neurobiol. Dis.* **174**, 105873 (2022).

463. Yang, Y. Structure, function and regulation of the melanocortin receptors. *Eur. J. Pharmacol.* **660**, 125–130 (2011).
464. Cai, M. & Hruby, V. J. The Melanocortin Receptor System: A Target for Multiple Degenerative Diseases. <http://www.eurekaselect.com> **17**, (2016).
465. Binder, D. K. & Steinhäuser, C. Astrocytes and Epilepsy. *Neurochem. Res.* **46**, 2687–2695 (2021).
466. Jia, Y.-F. *et al.* Astrocytic Glutamate Transporter 1 (GLT1) Deficiency Reduces Anxiety- and Depression-Like Behaviors in Mice. *Front. Behav. Neurosci.* **14**, 57 (2020).
467. Jia, Y.-F., Wininger, K., Peyton, L., Ho, A. M.-C. & Choi, D.-S. Astrocytic glutamate transporter 1 (GLT1) deficient mice exhibit repetitive behaviors. *Behav. Brain Res.* **396**, 112906 (2021).
468. Itoh, N. *et al.* Estrogen receptor beta in astrocytes modulates cognitive function in mid-age female mice. *Nat. Commun.* **14**, 6044 (2023).
469. Zhu, Y. *et al.* Ablation of NF1 function in neurons induces abnormal development of cerebral cortex and reactive gliosis in the brain. *Genes Dev.* **15**, 859–876 (2001).
470. Zheng, R. *et al.* Deficiency of the RII $\beta$  subunit of PKA affects locomotor activity and energy homeostasis in distinct neuronal populations. *Proc. Natl. Acad. Sci.* **110**, (2013).
471. Ruggiero, R. N. *et al.* Dysfunctional hippocampal-prefrontal network underlies a multidimensional neuropsychiatric phenotype following early-life seizure. *eLife* **12**, RP90997 (2024).
472. Karnam, H. B., Zhao, Q., Shatskikh, T. & Holmes, G. L. Effect of age on cognitive sequelae following early life seizures in rats. *Epilepsy Res.* **85**, 221–230 (2009).
473. Holmes, G. L., Gairsa, J., Chevassus-Au-Louis, N. & Ben-Ari, Y. Consequences of neonatal seizures in the rat: Morphological and behavioral effects. *Ann. Neurol.* **44**, 845–857 (1998).
474. Holmes, G. L., Sarkisian, M., Ben-Ari, Y. & Chevassus-Au-Louis, N. Mossy fiber sprouting after recurrent seizures during early development in rats. *J. Comp. Neurol.* **404**, 537–553 (1999).

475. Holmes, G. L. *et al.* Alterations in sociability and functional brain connectivity caused by early-life seizures are prevented by bumetanide. *Neurobiol. Dis.* **77**, 204–219 (2015).
476. De Rogalski Landrot, I., Minokoshi, M., Silveira, D. C., Ho Cha, B. & Holmes, G. L. Recurrent neonatal seizures: relationship of pathology to the electroencephalogram and cognition. *Dev. Brain Res.* **129**, 27–38 (2001).
477. McCabe, B. K. *et al.* Reduced Neurogenesis after Neonatal Seizures. *J. Neurosci.* **21**, 2094–2103 (2001).
478. Isaeva, E., Isaev, D., Savrasova, A., Khazipov, R. & Holmes, G. L. Recurrent neonatal seizures result in long-term increases in neuronal network excitability in the rat neocortex. *Eur. J. Neurosci.* **31**, 1446–1455 (2010).
479. Luo, L. *et al.* Optimizing Nervous System-Specific Gene Targeting with Cre Driver Lines: Prevalence of Germline Recombination and Influencing Factors. *Neuron* **106**, 37-65.e5 (2020).
480. Jensen-Willett, S. *et al.* The Effect of Early-Life Seizures on Cognitive and Motor Development: A Case Series. *Pediatr. Phys. Ther.* **34**, 425–431 (2022).
481. Singh, H. *et al.* Learning Deficits and Attenuated Adaptive Stress Response After Early-Life Seizures in Zebrafish. *Front. Neurosci.* **16**, 869671 (2022).
482. Wikberg, J. E. S. Melanocortin receptors: perspectives for novel drugs. *Eur. J. Pharmacol.* **375**, 295–310 (1999).
483. Chen, R., Xue, G. & Hölscher, C. The role of the TNF $\alpha$ -mediated astrocyte signaling pathway in epilepsy. *Acta Epileptol.* **3**, 24 (2021).
484. Çarçak, N., Onat, F. & Sitnikova, E. Astrocytes as a target for therapeutic strategies in epilepsy: current insights. *Front. Mol. Neurosci.* **16**, 1183775 (2023).
485. Kang, N., Xu, J., Xu, Q., Nedergaard, M. & Kang, J. Astrocytic Glutamate Release-Induced Transient Depolarization and Epileptiform Discharges in Hippocampal CA1 Pyramidal Neurons. *J. Neurophysiol.* **94**, 4121–4130 (2005).
486. Tian, G.-F. *et al.* An astrocytic basis of epilepsy. *Nat. Med.* **11**, 973–981 (2005).

487. Koyama, Y. Functional alterations of astrocytes in mental disorders: pharmacological significance as a drug target. *Front. Cell. Neurosci.* **9**, (2015).
488. Kaul, D., Schwab, S. G., Mechawar, N., Ooi, L. & Matosin, N. Alterations in Astrocytic Regulation of Excitation and Inhibition by Stress Exposure and in Severe Psychopathology. *J. Neurosci.* **42**, 6823–6834 (2022).
489. Escalada, P., Ezkurdia, A., Ramírez, M. J. & Solas, M. Essential Role of Astrocytes in Learning and Memory. *Int. J. Mol. Sci.* **25**, 1899 (2024).
490. Adamsky, A. *et al.* Astrocytic Activation Generates De Novo Neuronal Potentiation and Memory Enhancement. *Cell* **174**, 59-71.e14 (2018).
491. Bohmbach, K. & Henneberger, C. Activity-induced reactivity of astrocytes impairs cognition. *PLoS Biol.* **22**, e3002712 (2024).
492. Wang, Y. *et al.* Inhibition of activated astrocyte ameliorates lipopolysaccharide- induced depressive-like behaviors. *J. Affect. Disord.* **242**, 52–59 (2019).
493. Liu, D. *et al.* Melanocortin MC4 receptor agonists alleviate brain damage in abdominal compartment syndrome in the rat. *Neuropeptides* **49**, 55–61 (2015).
494. Paco, S., Hummel, M., Plá, V., Sumoy, L. & Aguado, F. Cyclic AMP signaling restricts activation and promotes maturation and antioxidant defenses in astrocytes. *BMC Genomics* **17**, 304 (2016).
495. Zhou, Z., Ikegaya, Y. & Koyama, R. The Astrocytic cAMP Pathway in Health and Disease. *Int. J. Mol. Sci.* **20**, 779 (2019).
496. Freeman, M. R., Beckmann, S. L. & Sueoka, N. Regulation of the S100 protein and GFAP genes is mediated by two common mechanisms in RT4 neuro-glial cell lines. *Exp. Cell Res.* **182**, 370–383 (1989).
497. Segovia, J., Lawless, G. M., Tillakaratne, N. J. K., Brenner, M. & Tobin, A. J. Cyclic AMP Decreases the Expression of a Neuronal Marker (GAD<sub>67</sub>) and Increases the Expression of an Astroglial Marker (GFAP) in C6 Cells. *J. Neurochem.* **63**, 1218–1225 (1994).
498. Cebolla, B., Fernandez-Perez, A., Perea, G., Araque, A. & Vallejo, M. DREAM Mediates cAMP-Dependent, Ca<sup>2+</sup>-Induced Stimulation of GFAP Gene Expression and Regulates Cortical Astroglialogenesis. *J. Neurosci.* **28**, 6703–6713 (2008).

499. Song, Y. & Gunnarson, E. Potassium Dependent Regulation of Astrocyte Water Permeability Is Mediated by cAMP Signaling. *PLoS ONE* **7**, e34936 (2012).
500. Kitchen, P. *et al.* Targeting Aquaporin-4 Subcellular Localization to Treat Central Nervous System Edema. *Cell* **181**, 784-799.e19 (2020).
501. Hernan, A., Mahoney, J., Curry, W., Mawe, S. & Scott, R. Distributed dynamic coding for spatial working memory in hippocampal-prefrontal networks. Preprint at <https://doi.org/10.1101/630673> (2019).
502. Park, S.-P. & Kwon, S.-H. Cognitive Effects of Antiepileptic Drugs. *J. Clin. Neurol.* **4**, 99 (2008).
503. Khalife, M. R. *et al.* Melanocortin 4 Receptor-Dependent Mechanism of ACTH in Preventing Anxiety-Like Behaviors and Normalizing Astrocyte Proteins After Early Life Seizures. Preprint at <https://doi.org/10.1101/2024.10.09.617457> (2024).
504. Lasaga, M., Debeljuk, L., Durand, D., Scimonelli, T. N. & Caruso, C. Role of  $\alpha$ -melanocyte stimulating hormone and melanocortin 4 receptor in brain inflammation. *Peptides* **29**, 1825–1835 (2008).
505. Giustino, T. F. & Maren, S. The Role of the Medial Prefrontal Cortex in the Conditioning and Extinction of Fear. *Front. Behav. Neurosci.* **9**, (2015).
506. Holmes, A. & Wellman, C. L. Stress-induced prefrontal reorganization and executive dysfunction in rodents. *Neurosci. Biobehav. Rev.* **33**, 773–783 (2009).
507. Norrholm, S. D. *et al.* Fear Extinction in Traumatized Civilians with Posttraumatic Stress Disorder: Relation to Symptom Severity. *Biol. Psychiatry* **69**, 556–563 (2011).
508. Holland, F. H., Ganguly, P., Potter, D. N., Chartoff, E. H. & Brenhouse, H. C. Early life stress disrupts social behavior and prefrontal cortex parvalbumin interneurons at an earlier time-point in females than in males. *Neurosci. Lett.* **566**, 131–136 (2014).
509. Szczepanski, S. M. & Knight, R. T. Insights into Human Behavior from Lesions to the Prefrontal Cortex. *Neuron* **83**, 1002–1018 (2014).
510. Arnsten, A. F. T. Stress weakens prefrontal networks: molecular insults to higher cognition. *Nat. Neurosci.* **18**, 1376–1385 (2015).

511. Rosen, J. B. & Schulkin, J. Hyperexcitability: From Normal Fear to Pathological Anxiety and Trauma. *Front. Syst. Neurosci.* **16**, 727054 (2022).
512. Orsini, C. A. & Maren, S. Neural and cellular mechanisms of fear and extinction memory formation. *Neurosci. Biobehav. Rev.* **36**, 1773–1802 (2012).
513. Likhtik, E., Stujenske, J. M., Topiwala, M., Harris, A. Z. & Gordon, J. A. Prefrontal entrainment of amygdala activity signals safety in learned fear and innate anxiety. *Nat. Neurosci.* **17**, 106–113 (2014).
514. Quirk, G. J. & Mueller, D. Neural Mechanisms of Extinction Learning and Retrieval. *Neuropsychopharmacology* **33**, 56–72 (2008).
515. Miller, E. K. The prefrontal cortex and cognitive control. *Nat. Rev. Neurosci.* **1**, 59–65 (2000).
516. Quirk, G. J., Russo, G. K., Barron, J. L. & Lebron, K. The Role of Ventromedial Prefrontal Cortex in the Recovery of Extinguished Fear. *J. Neurosci.* **20**, 6225–6231 (2000).
517. Laurent, V., Marchand, A. R. & Westbrook, R. F. The basolateral amygdala is necessary for learning but not relearning extinction of context conditioned fear. *Learn. Mem.* **15**, 304–314 (2008).
518. Courtin, J. *et al.* Prefrontal parvalbumin interneurons shape neuronal activity to drive fear expression. *Nature* **505**, 92–96 (2014).
519. Sharpe, M. J. & Killcross, S. The prelimbic cortex uses higher-order cues to modulate both the acquisition and expression of conditioned fear. *Front. Syst. Neurosci.* **8**, (2015).
520. Herry, C. & Garcia, R. Prefrontal Cortex Long-Term Potentiation, But Not Long-Term Depression, Is Associated with the Maintenance of Extinction of Learned Fear in Mice. *J. Neurosci.* **22**, 577–583 (2002).
521. Kellett, J. & Kokkinidis, L. Extinction deficit and fear reinstatement after electrical stimulation of the amygdala: implications for kindling-associated fear and anxiety. *Neuroscience* **127**, 277–287 (2004).
522. Hernan, A. E. *et al.* Environmental enrichment normalizes hippocampal timing coding in a malformed hippocampus. *PLOS ONE* **13**, e0191488 (2018).

523. Pillow, J. W. *et al.* Spatio-temporal correlations and visual signalling in a complete neuronal population. *Nature* **454**, 995–999 (2008).
524. Park, I. M., Meister, M. L. R., Huk, A. C. & Pillow, J. W. Encoding and decoding in parietal cortex during sensorimotor decision-making. *Nat. Neurosci.* **17**, 1395–1403 (2014).
525. Ferguson, K. A. & Cardin, J. A. Mechanisms underlying gain modulation in the cortex. *Nat. Rev. Neurosci.* **21**, 80–92 (2020).
526. Gansel, K. S. Neural synchrony in cortical networks: mechanisms and implications for neural information processing and coding. *Front. Integr. Neurosci.* **16**, 900715 (2022).
527. Murray, J. D. *et al.* Stable population coding for working memory coexists with heterogeneous neural dynamics in prefrontal cortex. *Proc. Natl. Acad. Sci.* **114**, 394–399 (2017).
528. Liu, Y., Brincat, S. L., Miller, E. K. & Hasselmo, M. E. A Geometric Characterization of Population Coding in the Prefrontal Cortex and Hippocampus during a Paired-Associate Learning Task. *J. Cogn. Neurosci.* **32**, 1455–1465 (2020).
529. Kupferschmidt, D. A. *et al.* Prefrontal Interneurons: Populations, Pathways, and Plasticity Supporting Typical and Disordered Cognition in Rodent Models. *J. Neurosci.* **42**, 8468–8476 (2022).
530. Nakajima, M. Neuronal identity and cognitive control dynamics in the PFC. *Semin. Cell Dev. Biol.* **129**, 14–21 (2022).
531. Ahmed, G. K., Elbeh, K., Elserogy, Y. & Mostafa, S. Effect of long-term administration of clonazepam, carbamazepine, and valproate on cognitive, psychological, and personality changes in adult epilepsy: a case–control study. *Middle East Curr. Psychiatry* **28**, 81 (2021).
532. Xu, P., Chen, A., Li, Y., Xing, X. & Lu, H. Medial prefrontal cortex in neurological diseases. *Physiol. Genomics* **51**, 432–442 (2019).
533. Ghasemi, M., Navidhamidi, M., Rezaei, F., Azizikia, A. & Mehranfard, N. Anxiety and hippocampal neuronal activity: Relationship and potential mechanisms. *Cogn. Affect. Behav. Neurosci.* **22**, 431–449 (2022).
534. Sakurai, Y. *et al.* Diverse synchrony of firing reflects diverse cell-assembly coding in the prefrontal cortex. *J. Physiol.-Paris* **107**, 459–470 (2013).

535. Muller, T. H. *et al.* Distributional reinforcement learning in prefrontal cortex. *Nat. Neurosci.* **27**, 403–408 (2024).
536. Mainen, Z. F. & Sejnowski, T. J. Reliability of Spike Timing in Neocortical Neurons. *Science* **268**, 1503–1506 (1995).
537. Mininni, C. J., Caiafa, C. F., Zanutto, B. S., Tseng, K. Y. & Lew, S. E. Efficient enhancement of information in the prefrontal cortex during the presence of reward predicting stimuli. *PLOS ONE* **12**, e0188579 (2017).
538. Engel, A. K. & Fries, P. Beta-band oscillations — signalling the status quo? *Curr. Opin. Neurobiol.* **20**, 156–165 (2010).
539. Spitzer, B. & Haegens, S. Beyond the Status Quo: A Role for Beta Oscillations in Endogenous Content (Re)Activation. *eneuro* **4**, ENEURO.0170-17.2017 (2017).
540. Schmidt, R. *et al.* Beta Oscillations in Working Memory, Executive Control of Movement and Thought, and Sensorimotor Function. *J. Neurosci.* **39**, 8231–8238 (2019).
541. Little, S. & Brown, P. The functional role of beta oscillations in Parkinson’s disease. *Parkinsonism Relat. Disord.* **20**, S44–S48 (2014).
542. Sporn, S., Hein, T. & Herrojo Ruiz, M. Alterations in the amplitude and burst rate of beta oscillations impair reward-dependent motor learning in anxiety. *eLife* **9**, e50654 (2020).
543. Szatmáry, B. & Izhikevich, E. M. Spike-Timing Theory of Working Memory. *PLoS Comput. Biol.* **6**, e1000879 (2010).
544. Srivastava, K. H. *et al.* Motor control by precisely timed spike patterns. *Proc. Natl. Acad. Sci.* **114**, 1171–1176 (2017).
545. Waschke, L. *et al.* Single-neuron spiking variability in hippocampus dynamically tracks sensory content during memory formation in humans. *Nat. Commun.* **16**, 236 (2025).
546. Harris, K. D. & Mrsic-Flogel, T. D. Cortical connectivity and sensory coding. *Nature* **503**, 51–58 (2013).

547. Andrade-Talavera, Y., Fisahn, A. & Rodríguez-Moreno, A. Timing to be precise? An overview of spike timing-dependent plasticity, brain rhythmicity, and glial cells interplay within neuronal circuits. *Mol. Psychiatry* **28**, 2177–2188 (2023).
548. Newman, M. E. J. Analysis of weighted networks. *Phys. Rev. E* **70**, 056131 (2004).
549. Bassett, D. S. & Bullmore, E. Small-World Brain Networks. *The Neuroscientist* **12**, 512–523 (2006).
550. Shimono, M. & Beggs, J. M. Functional Clusters, Hubs, and Communities in the Cortical Microconnectome. *Cereb. Cortex* **25**, 3743–3757 (2015).
551. Cohen, J. R. & D’Esposito, M. The Segregation and Integration of Distinct Brain Networks and Their Relationship to Cognition. *J. Neurosci.* **36**, 12083–12094 (2016).
552. Massullo, C. *et al.* Decreased brain network global efficiency after attachment memories retrieval in individuals with unresolved/disorganized attachment-related state of mind. *Sci. Rep.* **12**, 4725 (2022).

## Appendix A

### IACUC Approval



Institutional Animal Care and Use Committee  
1600 Rockland Road  
Wilmington, DE 19803  
p (302) 651-6826 f (302)-651-6881  
[IACUC@nemours.org](mailto:IACUC@nemours.org)

#### MEMORANDUM

---

**DATE:** November 19, 2021

**TO:** Amanda Hernan, PhD

**FROM:** Paul T. Fawcett, PhD, Chair

**SUBJECT:** **RSP21-42555-001 Mechanisms for Improving Cognitive Outcome in Pediatric Epilepsy with ACTH**

**Amendment:** Add support personnel  
Dr. Rodney Scott, Mohamed Rabieh Khalife, Haley Holm, Pravin Wagley, and Mohamed Ouardouz

The Institutional Animal Care and Use Committee (IACUC) have reviewed the submitted amendment on the above referenced protocol, and the following decision has been made:

**Action: Approved**

**Date of Action: November 19, 2021**

Please submit your Biosafety Classification form electronically to the Alfred I. duPont Hospital for Children Institutional Biosafety Committee via the link:

<http://www.nemours.org/pediatric-research/approval/biosafety-committee.html>

Please note that the study cannot begin until the Office of Regulatory Compliance in Research Administration has received all approvals.

Please maintain this approval with your project records. A tally of the number of animals approved and the number ordered for the project will be maintained in the Life Science Center. If changes occur in your protocol or if you require more animals than approved, and amendment to your protocol will need to be submitted for consideration

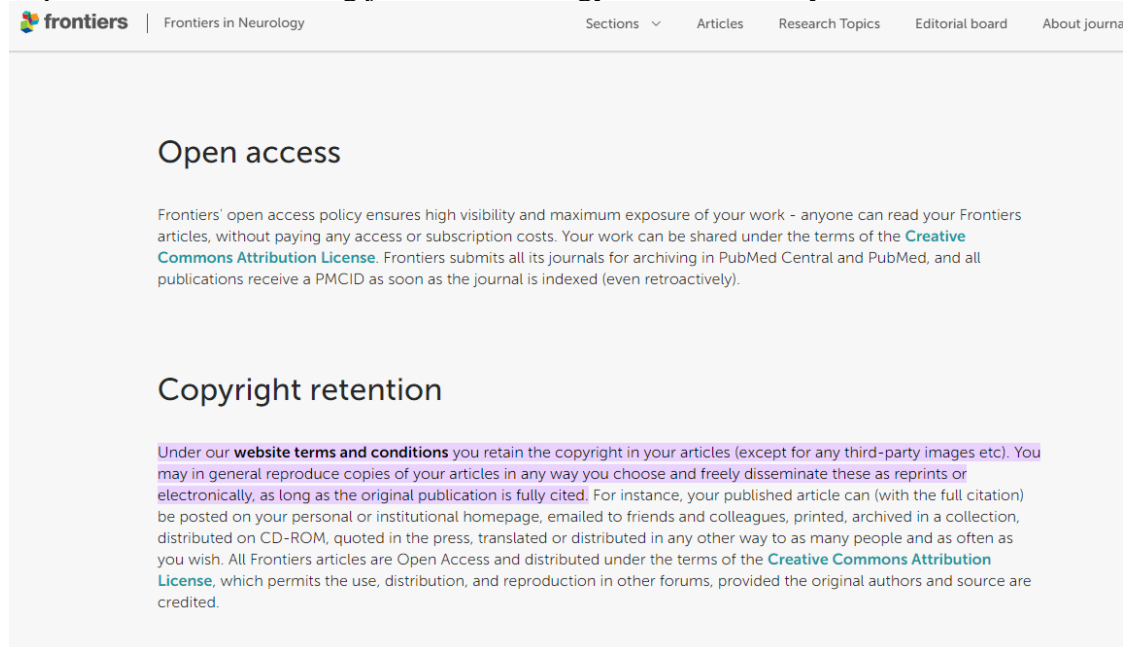
If you have any questions regarding this memorandum, please contact Paul T. Fawcett, Ph.D. at x6776 or email: [pfawcett@nemours.org](mailto:pfawcett@nemours.org).

## Appendix B

### PERMISSIONS

**Chapter 2** is partially adopted and modified from a published article in Frontiers in Neurology Journal – Open Access <sup>38</sup>

<https://www.frontiersin.org/journals/neurology/for-authors/why-submit>



The screenshot shows the Frontiers website page for authors. The header includes the Frontiers logo, 'Frontiers in Neurology', and navigation links for 'Sections', 'Articles', 'Research Topics', 'Editorial board', and 'About journals'. The main content is divided into two sections: 'Open access' and 'Copyright retention'. The 'Open access' section states that Frontiers' policy ensures high visibility and maximum exposure of work, with all articles being Open Access and distributed under the Creative Commons Attribution License. The 'Copyright retention' section states that authors retain copyright in their articles (except for third-party images) and can reproduce copies in various ways, provided the original authors and source are credited.

**Chapter 3** is fully adopted from a published article in eNeuro journal – Open Access 448.

<https://www.eneuro.org/content/general-information#policies>

#### Policy on Copyright and Funder Compliance

It is essential that the authors retain the copyright for any prepublished material submitted to *eNeuro*, and that they are willing and able to relinquish to *eNeuro* any licenses that *eNeuro* requires for publication of accepted manuscripts. Copyright of all material published in *eNeuro* remains with the authors. The authors grant the Society for Neuroscience a license to publish their work. Immediately upon publication, the work becomes available for the public to copy, distribute, or display under the [Creative Commons Attribution 4.0 International \(CC BY 4.0\) license](#). Per the terms of the license, it is not necessary to obtain permission or pay a fee to reuse this material, provided the authors receive proper acknowledgment.